Studies of Neurotropism and Endonuclease Targeting of Varicella Zoster Virus Using a Cultured Human Neuron System

by

Betty W. Wu

B.S, University of California Davis, 2013

Submitted to the Graduate Faculty of the

School of Medicine in partial fulfillment

of the requirements for the degree of

Doctor of Philosophy

University of Pittsburgh

2022

UNIVERSITY OF PITTSBURGH

SCHOOL OF MEDICINE

This dissertation was presented

by

Betty W. Wu

It was defended on

May 26, 2022

and approved by

Neal A. DeLuca PhD, Professor, Department of Microbiology and Molecular Genetics

Leah C. Byrne PhD, Assistant Professor, Department of Ophthalmology

Saumendra N. Sarkar PhD, Associate Professor, Department of Microbiology and Molecular Genetics

Fred L. Homa PhD, Professor, Department of Microbiology and Molecular Genetics

Kathryn M. Albers PhD, Professor, Department of Neurobiology

Dissertation Director: Paul R. Kinchington PhD, Professor, Department of Ophthalmology

Studies of Neurotropism and Endonuclease Targeting of Varicella Zoster Virus Using a Cultured Human Neuron System

Betty W. Wu, PhD

University of Pittsburgh, 2022

The alphaherpesvirus varicella zoster virus (VZV) causes varicella (chickenpox) after primary infection, and herpes zoster (shingles) during reactivation from latency in sensory ganglia. Its 125kb dsDNA genome encodes several transactivators, some of which are virion-incorporated and facilitate initiation of lytic infections. Two abundant virion-associated transactivators are encoded by ORFs 10 and 62, homologs of HSV VP16 and ICP4, respectively. VP16 is essential for virion formation and promotes immediate early gene transcription, facilitating exit from latency. However, ORF10 is dispensable in cell culture, though it is important for skin infections; its role in neurons is unknown. VZV virions also contain abundant IE62 (ICP4 is a minor HSV virion component). We hypothesized ORF10 protein may have overlapping transactivation functions with virion IE62 upon infection, perhaps in cell type-specific roles. To test this, recombinant viruses deleted for ORF10 with and without an ORF62 mutation preventing IE62 virion incorporation were evaluated for epithelial and neuronal spread in culture. VZV lacking one or both virion transactivators were successfully isolated in epithelial cells and replicated similarly to wild type. VZV lacking virion IE62 was slightly impaired for epithelial replication, but severely impaired in human neurons, indicating a neuron-specific role. Unexpectedly, when ORF10 was subsequently deleted, neuronal growth was restored. Partially purified virion analyses suggested ORF10 deletion causes novel compensatory mechanisms to still incorporate virion IE62 for efficient neuronal spread, despite continued presence of the ORF62 mutation that normally prevents virion accumulation.

The second part of this thesis addresses the targeting of the essential duplicated ORF62/71 genes by AAV vector-delivered CRISPR/Cas9, to effectively limit VZV replication and spread in epithelial and neuronal cultures. We show that a single treatment with ORF62-targeting Cas9 AAV effectively reduced VZV progeny virus in multiple epithelial cell types and lytically infected neurons. In targeting latent and reactivating infections, these constructs greatly reduced production of infectious virus from reactivation, though not latent genome loads. Taken together, our results support a novel important role of virion IE62 in neuronal infections, and the potential of AAV-delivered genome editing tools as an antiviral strategy to limit VZV epithelial and neuron growth, reducing the reactivated viral burden.

Table of Contents

Acknowledgements xiv

1.0 Introduction 1

1.1 General Virology 1

1.1.1 Classification 1

1.1.2 Genome 3

1.1.3 Virion Structure 5

1.1.3.1 Transactivators 9

1.1.4 Lytic Replication 12

1.1.5 Latency and Reactivation 16

1.1.6 Challenges in the Laboratory and VZV Model Systems 18

1.2 Clinical Disease 21

1.2.1 Pathogenesis and Varicella Disease 21

1.2.2 Herpes Zoster 22

1.2.2.1 Vaccines, Antiviral Therapeutics, and Pain Management 23

2.0 Specific Aims and Rationale 27

2.1 Aim 1: Define the role of two virion-associated transactivators in driving neuronal infection, dissemination, and establishment of latency. 28

2.2 Aim 2: Inhibit VZV replication and silence the latent genome using CRISPR/Cas9. 28

3.0 VZV genome targeting for inactivation using CRISPR/Cas9 30

3.1 Project Summary 30

3.2 Importance 31

3.3 Introduction 32

3.4 Materials and Methods 35

3.4.1 Cells and Viruses 35

3.4.2 CRISPR/Cas9 Plasmid and gRNA Design 36

3.4.3 Preparation of AAV 37

3.4.4 Quantification of Viral Genomes 38

3.4.5 Generation of Recombinant VZV 39

3.4.6 Virus Derivation and Growth Curves 42

3.4.7 Neuron Cultures 43

3.4.8 Fluorescent Microscopy 45

3.4.9 Flow Cytometry and Statistical Analyses 45

3.5 Results 46

3.5.1 Characterization of VZV-Specific gRNAs for *in-vitro* Specificity 46

3.5.2 AAV Serotypes for Delivery to VZV-permissive Epithelial Cells and Human Stem Cell-derived Neurons 49

3.5.3 AAV-62-1gR-saCas9 Reduces VZV Lytic Replication in Epithelial Cells 52

3.5.4 AAV-62-1gR-saCas9 Reduces VZV Lytic Replication in hESC-Derived Human Neuron Cultures 56

3.5.5 AAV-62-1gR-saCas9 Reduces VZV Replication Following Reactivation in Model Latently Infected Neuron Cultures 60

3.6 Discussion 65

4.0 Roles of ORFs 10 and 62 proteins in Neuronal Replication 71

4.1 Project Summary 71

4.2 Importance 72

4.3 Introduction 73

4.4 Materials and Methods 77

4.4.1 Cells 77

4.4.2 VZV 77

4.4.3 Generation of recombinant VZV BACs 78

4.4.4 Southern Blotting 80

4.4.5 Growth Curve Analyses 81

4.4.6 Antibodies 82

4.4.7 Immunoblotting 83

4.4.8 Virion Purification 84

4.4.9 Neuron Cultures 84

4.4.10 Microscopy 86

4.4.11 Preparation of Viral Nucleocapsid DNA 87

4.4.12 Statistics and Sequencing Analyses 88

4.5 Results 88

4.5.1 Development of recombinant VZV that lack trans activators from ORFs 10 and 62 in virions 88

4.5.2 VZV lacking virion ORF10 and/or IE62 trans activator proteins replicate in epithelial cell models 96

4.5.3 Replication of VZV lacking virion trans activator proteins in hESC-derived neuron cultures. 101

4.5.4 Virion analyses suggest an ORF10 deletion-dependent compensatory mechanism to packaged virion IE62 that is independent of the accumulation of IE62 in the cytoplasm. 108

4.6 Discussion 113

4.7 Role of ORFs 10-12 in VZV replication 120

5.0 Summary and Future Perspectives 125

Bibliography 133

List of Tables

Table 1 gRNA Oligos 37

Table 2 Primers for Quantification of AAVs. 39

Table 3 Primer Design for VZV DR-62gmut BAC Recombineering. 42

Table 4 Primer design for VZV BAC Recombineering. 80

Table 5 Primer Design for Southern Blot 81

List of Figures

Figure 1 Phylogenetic tree of human herpesviruses. 2

Figure 2 VZV genome structure, with major and minor isoforms. 4

Figure 3 Generalized schematic of a VZV virion. 6

Figure 4 VZV transcriptional cascade. 15

Figure 5 Design and dimensions of compartmentalized microfludic neuron devices. 20

Figure 6 A preliminary study to evaluate ORF62- and ORF63-targeting gRNAs in pX601 to prevent gene expression. 48

Figure 7 A preliminary study of AAV serotypes able to deliver to epithelial cells and neurons. 51

Figure 8 AAV-62-1gR-saCas9 reduces VZV productive infection in infected epithelial cells. 54

Figure 9 VZV DR-62gmut grows similarly to WT VZV. 56

Figure 10 Pretreatment with AAV-62-1gR-saCas9 knockdown of VZV lytic replication in exogenously in-fected human neuron cultures. 59

Figure 11 AAV-62-1gR-saCas9 treatment of latently infected neurons reduces VZV progeny and spread following reactivation induction. 63

Figure 12 Enlargement of figure 7b 64

Figure 13 Enlargement of figure 11a 64

Figure 14 Recombinant VZV Constructs. 90

Figure 15 Southern blot analyses of VZV set B to show that ORF62 reduplicates ORF71 in virus infected cells. 93

Figure 16 IE62 cellular localization in VZV-infected cells are strictly nuclear in the presence of the 62-S686A mutation. 95

Figure 17 IE62 localization in Set A VZV-infected cells are strictly nuclear in the presence of the 62-S686A mutation. 96

Figure 18 Growth rate comparisons of set B VZV in human epithelial ARPE-19 cells..... 98

Figure 19 Growth of set A VZV in human epithelial ARPE-19 cells. 100

Figure 20 (a-b) Lytic infection and spread of Set B recombinant VZV in hESC-derived human neuron cultures..... 103

Figure 20 (c-d) Lytic infection and spread of Set B recombinant VZV in hESC-derived human neuron cultures..... 104

Figure 21 Infection of neurons by VZV via the axonal route in compartmentalized chamber neuron cultures..... 107

Figure 22 Immunoblotting of relevant tegument proteins in purified VZV virion preparations..... 111

Figure 23 (a-b) Full time course of Lytic infection and spread of recombinant VZV in embryonic stem cell-derived human neuron cultures imaged by repetitive live cell microscopy at the same points. 112

Figure 23 (c) Full time course of Lytic infection and spread of recombinant VZV in embryonic stem cell-derived human neuron cultures imaged by repetitive live cell microscopy at the same points. 113

Figure 24 Growth rate comparisons of Δ10, 11, 12, Δ10-11, Δ11-12, and Δ10-12 VZV mutants in ARPE-19 cells..... 122

Figure 25 Time course of lytic infection and spread of recombinant VZV in hESC-derived neuron cultures imaged by live cell microscopy..... 124

Acknowledgements

I would like to express my gratitude to my mentors. Firstly, my thesis advisor, Paul (Kip) R. Kinchington, PhD, for his support throughout my studies. His enthusiasm of the subject and encouragement of me to "think outside the box" has propelled my continued dedication to research. Outside of research, Kip has also been incredibly supportive of my personal endeavors, giving me good advice and supporting my work-life balance. I would also like to thank my thesis committee members, Neal Deluca, PhD, Leah Byrne, PhD, Saumendra Sarkar, PhD, Kathryn Albers, PhD, and Fred Homa, PhD, who have spent countless hours over the years listening to my concerns and having thoughtful conversations about my projects. Thank you all for believing in me and for providing excellent advice through the years. I would like to thank Robert Shanks, PhD, and Kira Lathrop, MAMS, for their roles as additional mentors in the department. Finally, I would like to mention my previous mentors from high school (Ray Hill, PhD), college (Sarah Perrault, PhD, Larry Morand, PhD, Douglas Nelson, PhD, and Andrew Groover, PhD), and beyond (John Wills, PhD), who have all played critical roles in my academic development and made me the scientist I am today. Without any of these mentors, this dissertation would not have been possible.

I would like to extend my gratitude to past and present members of the Ophthalmology research group, especially members of the Kinchington, Shanks, and Campbell research labs, who shared the lab space and made working here a pleasure. Special thanks to my colleagues Michael Yee, MS, Benjamin Warner, PhD, Lillian Laemmle, PhD, Joseph Flot, Kate Carroll, PhD, Dana Previte, PhD, Nicholas Stella, and Kathleen Yates, for having scientific discussions with me and also being my friends. I will miss our lunch and boba tea excursions.

Finally, I would like to acknowledge my biological and chosen family, who have been with me throughout this journey. Special thanks to Jean Wu, DDS, for always supporting my choices and looking out for me. Also, Mildred Wu Green, Rita Zhang, and Philip Wu, MA, for making me the person I am today. Thanks to Timothy Kleck, PharmD, for believing in me when I didn't even believe in myself, and to Benni Vargas, soon-to-be PhD, Nikki Niam, PhD, Sharon Wei, MS, Runa Miah, Hazel Aragon, Stephanie Martin, Douglas May, MD, Youngmin Chu, MD, Truc Tran, MD, Sharon Jia, MD, and Eren Chu, PhD, for encouraging me to pursue my dreams and never give up.

1.0 Introduction

1.1 General Virology

1.1.1 Classification

Herpesviruses are a group of large double-stranded DNA viruses that have a characteristic structure by electron microscopy, notably including a unique structure known as the tegument, between the capsid and the envelope. A general feature of the herpesviruses is that they can have two types of infectious processes--a lytic productive infection, in which most of the viral genes are expressed and made into proteins that ultimately yield amplified progeny virions; and a persistent infection, in which the genome is maintained in a mostly chromatinized and non-productive form. By this route, infection in the respective hosts can be renewed at a later time to reinfect other hosts.

The order *Herpesvirales* describes three families of viruses: *Herpesviridae* (viruses infecting mammals, birds, and reptiles), *Alloherpesviridae* (fish and amphibians), and *Malacoherpesviridae* (bivalves) [1]. Of the *Herpesviridae* family infecting humans there are nine: herpes simplex virus 1 (HSV-1), herpes simplex virus 2 (HSV-2), human cytomegalovirus (HCMV), varicella-zoster virus (VZV), Epstein-Barr virus (EBV), human herpesvirus 6A (HHV-6A), human herpesvirus 6B (HHV-6B), human herpesvirus 7 (HHV-7), and Kaposi's sarcoma-associated herpesvirus (HHV-8). Their approximate evolutionary relationships are shown in Fig 1 [2].

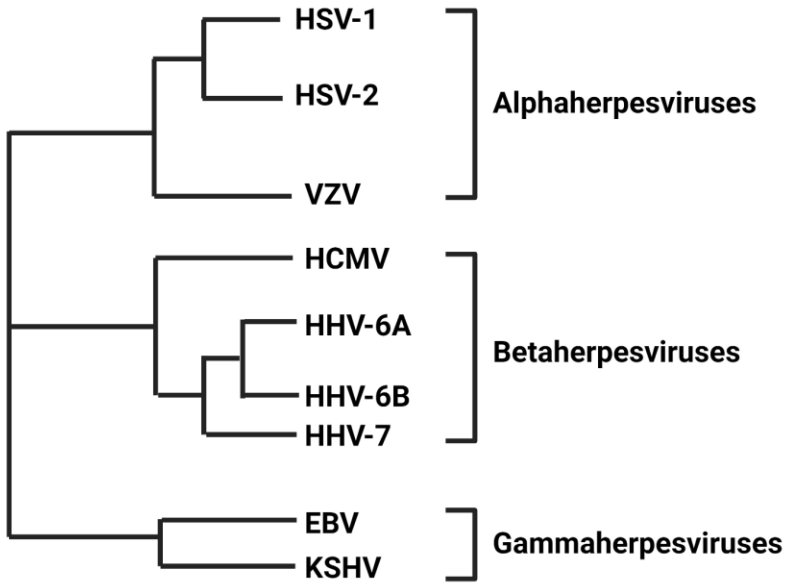

Figure 1 Phylogenetic tree of human herpesviruses. Based on data from [2]. Image was made using Biorender.com

Mammalian and Avian *Herpesviridae* members share about 44 conserved genes, mostly encoding proteins that replicate the genome or have structural functions. All of these viruses encode some of their own DNA replication factors as well as some nucleotide metabolism enzymes, and all Herpesviruses replicate their genome within the nucleus. A productive infection usually kills the host cell, and but the virus can remain in the host in a lifelong latency state, with the host cell type depending on the virus [3]. Our work focuses on varicella-zoster virus, which is one of the Alphaherpesvirus subfamily. Alphaherpesviruses have relatively fast reproductive cycles, and can show a variable host range. They have characteristic gene arrangements that differentiate them from the beta- and gammaherpesvirus members, which have more limited and restricted host range. VZV shares close gene homology with those of the herpes simplex viruses, but it is classified as being closer to non-human viruses such as pseudorabies virus (PRV) and Marek's disease virus (MDV). Its closest relationship is to the simian varicella virus (SVV) [4]. Here, we will focus primarily on the various aspects of human VZV biology.

1.1.2 Genome

At 125 kilobases, the VZV genome is actually one of the smallest among herpesviruses [5]. In the virus, the double-stranded DNA genome is predominantly linear and non-chromatinized, but upon initial infection, it may circularize after release from capsids into the cell nuclei and become associated with host intrinsic factors and chromatin components. While not determined for VZV, recent studies with HSV have suggested that circularization may not occur as early into productive infection as once was thought [6]. The VZV genome consists of a unique long (UL) region flanked by very short (88.5 bp) inverted repeat sequences known as the terminal repeat long (TRL) and internal repeat long (IRL) elements. Some 20% of the genome is a unique short (US) region, flanked by the much larger terminal repeat short (TRS) and internal repeat short (IRS) elements. The TRS and IRS regions contain diploid genes that are identical copies of each other, namely, ORFs 62/71, ORFs 63/70, and ORFs 64/69 [7]. ORFs 62-64 are located in the IRS, while ORFs 69-71 are located in the TRS. This characteristic genome structure allows for inversion and recombination of the repeats to give rise to two predominant isoforms of the genome and two minor forms (Fig 2). This contrasts with HSV, which consists of four equimolar isoforms [8]–[12]. The two VZV isoforms that predominate contain the UL in a fixed orientation with the short regions inverting at a 50:50 ratio [13]. It is thought that the fixed orientation may be due to virion packaging elements that are primarily located at the left hand end of the genome in ORF0 [14]. During latency, the DNA forms a circular episome in which the ends are covalently linked [15].

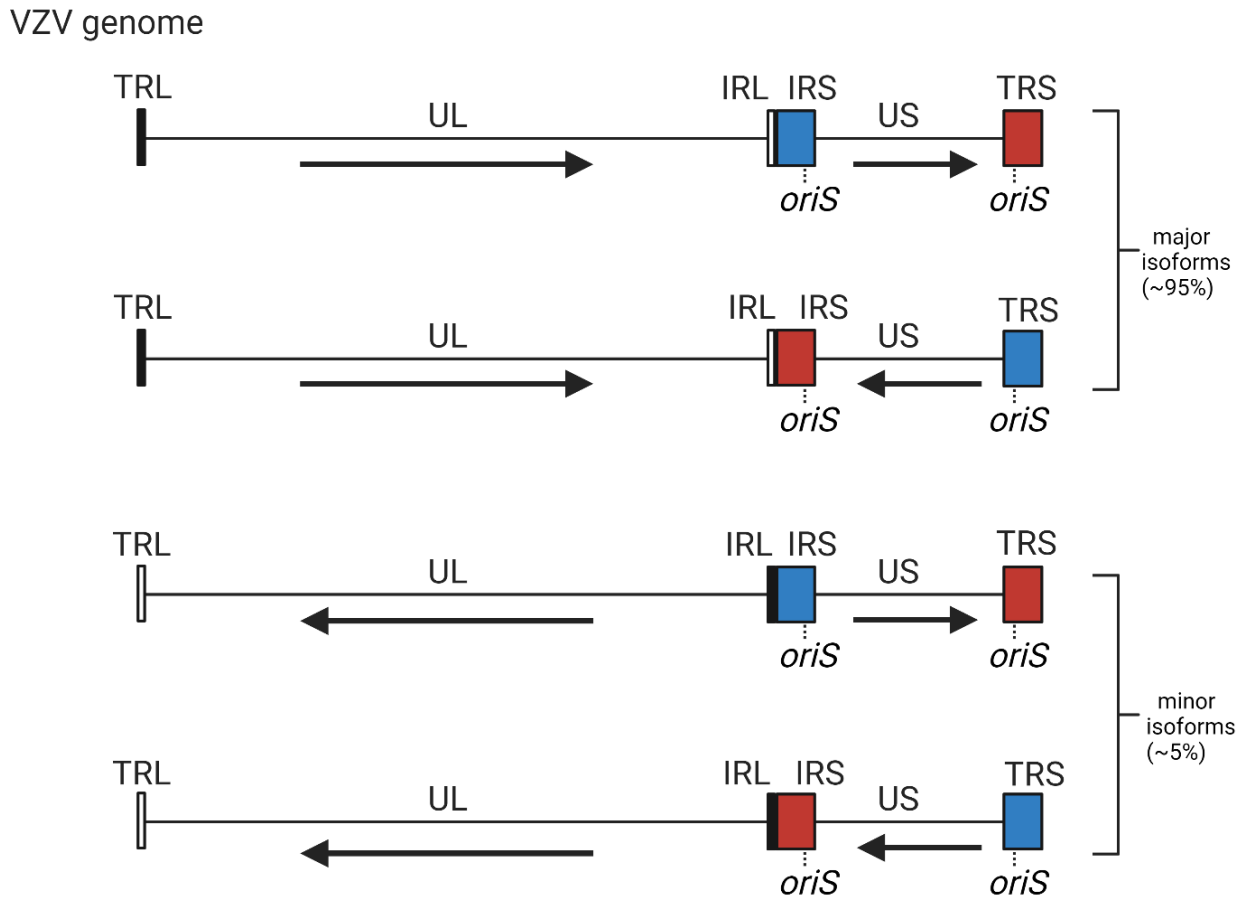

Figure 2 VZV genome structure, with major and minor isoforms. Arrow directions and different colors indicate directionality. Image was made using Biorender.com

There are at least two (duplicated) origins of replication (*oriS)* in VZV (Fig 2), which are located in the repeat regions between ORFs 62 and 63 (IRS) and 70 and 71 (TRS) [16], [17]. These are similar to two of the origins of replication in HSV, known as the *oriS* sequences. In HSV, there is also a third identified origin of replication (*oriL*) between the DNA polymerase and the ssDNA binding protein genes [18], which does not seem to be present in the UL region of VZV (between ORF28 and ORF29). However, there is some evidence for a third origin existing in VZV, since viruses deleted for both *oriS* sites can still replicate in MeWo and HELF cells [19]. In total, the VZV coding capacity is for at least 70+ unique ORFs, of which about 44 have been shown to be

essential for in-vitro spread in MeWo cells. The deletion of an additional eight genes results in moderate to severe growth defects in these cells [20]. IE62 (discussed in the following section) is an essential gene. The deletion of a number of so called “non-essential” VZV genes do, however, result is tissue-specific or cell type-specific impaired growth. Such is the case with ORF10, which is also the subject of part of this thesis (discussed in the following section) [20], [21]. Finally, there are a five or six VZV genes (S/L, 1, 2, 13, 32, and 57) that do not have an HSV homolog [21], [22]. With the exception of ORF S/L (otherwise known as ORF0), which promotes adherence of infected cells to adjacent cells and tissue [23] and contains the virion packaging elements, VZV lacking any of the other unique genes are able to fully replicate in tissue culture [24]–[28]. VZV ORF13 is known to encode a dispensable thymidylate synthase [27]. The functions of ORFs 1, 2, 32 and 57 are not known.

1.1.3 Virion Structure

Herpesviruses are defined by their virion structure, which consists of four distinct components. The capsid has a T=16 and contains the double-stranded DNA genome [29], [30]. The capsid proteins directly associate with inner tegument proteins, which then associate with outer tegument proteins, though few of the interactions in VZV are well-defined. The tegument is then surrounded by a host-derived lipid envelope containing numerous viral glycoproteins [3] (Fig 3). The VZV capsid consists of 162 capsomere units (made up of hexons and pentons) containing the major capsid protein (UL40), along with several other components (ORFs 20. 23. 33. 33.5, 41) that play roles in capsid formation and structure [31]–[34]. Packaging of the viral genome into the capsid also involves proteins that form a capsid scaffold before DNA packaging, and components that form the packaging/terminase complex (ORFs 25, 26, 30, 34, 43, 42, 45). Packaging occurs

through the portal protein (ORF54) located on one vertex of the capsid [35]. The capsids are seen as at least three distinct types in infected cells, known A-, B-, and C- capsids [36]. The A-capsids have no core structure, while B-capsids have no genome but do contain the scaffold for assembly. C-capsids contain the viral genome that no longer requires scaffolding. For VZV in cell culture, it has often been noted that there is a high abundance of empty capsids, which partly accounts for the poor infectivity of VZV.

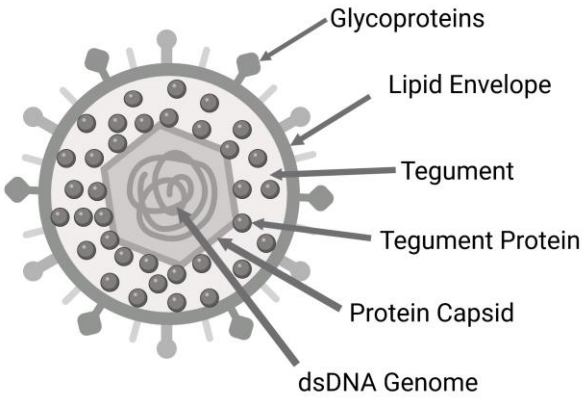

Figure 3 Generalized schematic of a VZV virion. Image was made using Biorender.com

VZV tegument proteins have been partly characterized, although many are only defined by homology to HSV, since VZV virions are difficult to purify to homogeneity. Most tegument components are of viral origin, but there may be some host proteins, as found in highly purified HSV and PRV virions. The actual number of tegument proteins in VZV is difficult to define. For HSV, it is estimated that there are 23 different viral tegument proteins and 49 host proteins are in the virion [37], [38]. Tegument proteins are located between the capsid and lipid membrane of virus particles and are generally delivered to the cytoplasm on virus entry, to adapt the host cell to infection. Some are considered “inner” tegument proteins, which are directly associated with the capsid; others are often described as “outer” tegument proteins, which are not so tightly associated

with the capsid and may dissociate upon cellular entry. The highly cell-associated nature of VZV has made it difficult to obtain large amounts of highly purified virions for mass spectroscopy, so much of the known VZV tegument protein functions are inferred from work on HSV or PRV. Inner capsid proteins are generally involved in capsid movement to the nucleus and transport in axons of neurons [39]–[43]. The suspected VZV tegument viral proteins are encoded by ORFs 3, 7, 8, 9, 10, 11, 12, 17, 21, 22, 36, 38, 44, 46, 47, 49, 53, 66, 62/71, and 64/69), some of which are essential (underlined) and others dispensable in culture [44]. Interestingly, IE62, IE4, and IE63 are from putative regulatory genes, which may be transcribed during the initial wave of gene expression upon DNA entry into the nucleus. These may then function in regulation of viral and, to some extent, host gene transcription and expression [45]–[50]. Numerous tegument proteins are suspected to play roles in suppressing the host's immune responses after VZV infection, including ORFs 47, 22, 21, 17, 10, 9, 8, 66, 64/69, 62/71, and 63 [51]–[53] (Hertzog *et al.*, in press). Of importance to this work, HSV ICP4 is also associated with the HSV virion, but is only a minor virion component. The VZV IE62 is, in contrast, highly abundant in purified virion particle preparations, as part of the tegument [22], [54]. The ORFs 9-12 gene cluster also encodes tegument components of the VZV virion, this is a conserved gene cluster found in other herpesviruses as well, and impacts viral replication of under certain conditions [38], [55]. VZV ORF 9 is the only essential VZV gene in this cluster, and encodes a structural protein that has roles in orchestrating viral particle assembly [55]–[57]. This contrasts with it homolog HSV VP22, which can be deleted in culture without affecting viral replication. VZV ORF9 also functions in immune evasion, regulating the host innate immune sensor STING (Hertzog *et al.*, in press). In contrast, VZV ORF10 is the equivalent of HSV VP16, but while VP16 is essential for assembly, ORF10 can be deleted in VZV without affecting virus growth in culture. VZV ORFs 11 and 12 are similar to

ORF10 in that they can be deleted without affecting growth in culture, but play critical roles in skin pathogenesis of VZV and in host immune evasion. There is also evidence suggesting that their HSV homologs (UL 46 and 47) regulate VP16 activity [58], [59]. Since ORF10 is homologous to VP16, it may be that ORFs 11 and 12 may also influence ORF10 expression, though studies are yet to show this. Two other tegument proteins are the VZV ORFs 47 and 66 serine/threonine protein kinases, which phosphorylate many viral and host factors and have homologs in all alphaherpesviruses [60], [61]. One target of both kinases is IE62 (see below). The ORF47 kinase has also been shown to play an important role in infection and cell-to-cell spread in human T cells and skin in SCID-hu mice, and is an important factor in forming virions: deletion mutants and VZV ORF47 kinase-dead mutants form highly aberrant virus particles [56], [62]. Finally, the tegument protein ORF7 has gained interest as it is a virulence factor involved in skin and possibly neuron infections [20], [63]. It has also been proposed to be a factor for generating an improved attenuated vaccine [64]. The remaining VZV tegument proteins remain to be well-studied with regards to their roles, but new data is constantly emerging.

The VZV envelope consists of a host-derived lipid membrane containing essential (ORFs S/L, gB, gE, gH, gL, gK) and dispensable (ORF39, gC, gI, gM, gN) viral glycoproteins [65]. It has not been completely elucidated as to which host proteins mediate receptor and viral entry into the different cell types that VZV infects during the course of pathogenesis, but studies have pointed to myelin-associated glycoprotein (MAG), insulin degrading enzyme (IDE), and mannose-6-phosphate (M6P), depending on the cell type [65]. In addition, cell surface heparin sulfate proteoglycans are also thought to play a role in virus binding of cell free VZV [66]. It is almost certain that VZV gB, gH, and gL are required for attachment, entry, and membrane fusion, as seen for the HSV equivalent proteins [67]–[71]. It has long been intriguing that VZV lacks an equivalent to the essential HSV gD

receptor-interacting protein. However, gE is critical in VZV but dispensable in HSV for culture growth, and may be the key receptor binding mediator in VZV. HSV gD is required for infection [72], [73].

1.1.3.1 Transactivators

VZV encodes for a variety of proteins that have transactivation/regulatory functions involved in viral gene expression, including those from ORFs 4, 10, 61, 62/71, and 63/70 [44], [74]. All of these correspond to known gene expression regulators in HSV, and some not only play roles in controlling mRNA expression, but also have additional post-transcriptional roles in pathogenesis, such as mRNA processing/export (IE4, [75]) and neuronal survival and anti-apoptosis (IE63, [76]). In regard to this thesis, ORF 10 protein and IE62 are abundant virion tegument components, and as such, may facilitate gene expression in the newly infected cell. However, neither virion ORF10 nor virion IE62 are essential for epithelial cell culture replication. ORF10 has been shown to be quite important for VZV growth in organized skin [55]. Until the work in this thesis was carried out, no one to our knowledge had examined the roles of these proteins in neuronal infections and inter-neuronal spread, such as occurs in reactivating ganglia prior to HZ.

ORF62 is an essential gene that encodes IE62, the homolog to ICP4. This gene is found in the short repeat regions of the genome and is thus repeated as ORF71, and is largely accepted as the major VZV transactivator f gene expression, since it transactivates most VZV genes (including itself). It greatly increases the infectivity of cell-transfected VZV DNA [48], [77]. At least one copy of the gene in its native location is absolutely needed for viral replication [48]. Even ectopic expression of just one ORF62 gene in the genome of an ORF 62/71-deleted mutant is not sufficient [48]. IE62 is structurally similar to the much better characterized ICP4 protein of HSV, one of the five HSV genes immediately transcribed upon HSV infection. ICP4 is required for the expression

of all other HSV viral gene classes that are not IE regulated [78]. IE62 is known to recruit host transcriptional machinery to viral promoters in a manner similar to ICP4 [54], [77], [79]–[81], although it is far less well studied than ICP4. However, IE62 and ICP4 share ~50% amino acid identity, concentrated in two of five regions, strongly suggesting that IE62 may have some similar roles in VZV. Indeed, HSV deleted for ICP4 but containing VZV IE62 in its place can replicate and still produce infectious virus [82]. The VZV IE62 protein is phosphorylated by both VZV encoded protein kinases, the ORF 47 and 66 viral kinases. Consequences of the phosphorylation of IE62 by ORF47 are not well-resolved. However, we do know that ORF66 kinase-mediated phosphorylation of IE62 at the S686 position adjacent to the IE62 nuclear import signal results in nuclear export and predominant cytoplasmic accumulation of this important transactivator in early to late stages of infection, where it is subsequently packaged into the tegument of virion particles [83], [84]. Previously, our lab has shown that VZV with an ORF62-S686A point mutation does not accumulate IE62 in the cytoplasm at all at any stage of infection, and does not incorporate IE62 into the virion tegument [85], [86]. Progeny virions were shown to completely lack the IE62 protein, although they were still able to replicate efficiently in epithelial cells [83], [87]. VZV lacking the ORF66 kinase did not incorporate IE62 into virions either. VZV with the 62-S686A mutation in ORF62 were only marginally impaired for growth in culture. The role of virion IE62 has not been investigated in human neurons, to our knowledge.

The other known VZV virion transactivator is encoded by ORF10. An early surprise to the field was that ORF10 is fully dispensable for VZV growth in cell culture, although it was subsequently shown that deletion of this gene results in VZV that is severely impaired when grown in organized human skin [88], [89]. ORF10 is the homolog to HSV VP16, which is known to transactivates all HSV IE genes: In VZV, transfections of ORF10 or VP16 only activate

transcription of ORF62 [74], [90]. HSV VP16 is an essential protein required for virion assembly and egress [91]. Extensive work with the VP16 in1814 mutant [92], [93], which lacks IE gene transactivation ability, and with HSV lacking the C-terminal transactivation domain of VP16 [94] has shown that the small C-terminal transactivation region of VP16 is not required for viral gene expression or replication, and high titer in1814 infection results in levels of IE gene expression that permit growth in Vero cells and even in mice eyes, despite the mutated VP16. However, low-level infections with in1814 and the C-terminal deletion VP16 result in inefficient IE gene expression and reduced replication [92], [93], [95], [96]. Complete deletion of VP16 abolishes HSV lytic replication and causes virion assembly defects, implying that the virion assembly function of VP16 is what is essential for the virus, rather than transactivation ability [97] (in VZV, critical virion assembly functions are largely attributed to the essential ORF9 and not to ORF10 [55]–[57]). Just like VP16, ORF10 is also thought to associate with host factors such as Oct1 and HCF and recruit them to bind to promotor elements called TAATGARAT motifs that promote viral IE gene transcription to promote initiating infection, especially at low multiplicities [54], [90], [98]–[101].

HSV VP16 (and we speculate that this may also apply to VZV ORF10) has apparent function in lytic/latent decisions upon neuronal infection [102], [103]. HSV in1814 does not replicate in the TG, although it does replicate in the eye [95]. A further clue came from studies of HSV distal axon infections of neurons that generally favors latency, because outer tegument transactivator proteins remain at the site of entry and are not efficiently delivered to the nucleus for IE gene expression [104]–[106]. VP16 has been shown to mediate the transition of a two-phase reactivation process seen in some neuronal models [102]. In this model, reactivation from latency proceeds in a biphasic manner. In Phase I, reactivation stimuli result in expression of genes outside

of the normal “lytic cascade” that is independent of VP16 transactivation and IE genes, and is thought to rely on cellular factors such as c-Jun N terminal kinase (JNK)-dependent histone phosphorylation for viral gene expression, despite H3K9me histone-chromatinized viral promoters [102], [107]–[109]. This gene expression may result in VP16 being made. If this associates with HCF and enters the neuron nucleus, it may initiate Phase II that involves the full viral transcriptional cascade, through VP16 transactivation of IE genes on accessible regions of the viral genome. Recent studies of single reactivation events in single neurons have strongly supported the two-phase model, using viruses that do not spread beyond the single neuron (Dochnal *et al.*, 2022 JV in press; Anna Cliffe, personal communication).

1.1.4 Lytic Replication

VZV lytic replication in both epithelial and neuronal cells involve transcription and expression of the majority of the genes in the viral genome, including transcription factors, factors that counteract the host innate response, nucleotide modifying enzymes, proteins involved in the DNA replication machinery, and structural proteins required for the assembly of new infectious particles [110], [111]. Transcription is thought to occur in a “cascade” like manner in which expression from genes can be experimentally defined as belonging to one of three kinetic phases: immediate early (IE or α), early (E or β), and late (L or γ) (Fig 4). However, there is likely a continuum and spectrum of transcription and for VZV, it has been difficult to perform the synchronized infection needed for experimental proof of which genes are made during each step, due to the highly cell-associated nature of VZV. IE gene products generally consist of gene regulatory factors and inhibitors of the intrinsic and innate immune responses, and by experimental definition, do not require *de novo* viral protein synthesis for their transcription. They are

transcribed by the host and through the actions of incoming viral tegument transactivators that recruit cellular factors to the IE gene promoters [112]–[114], or can act by the action of cellular factors alone, such as might occur during reactivation from latency, where only viral DNA preexists. The suspected IE genes in VZV include ORFs 4, 61, 62, and 63, though the speculative nature is based on homology with HSV. Interestingly, only ORF62 contains the "TAATGAARAT" sequence typically found in HSV IE promotors, though recent NGS-based long transcriptome analysis have also implicated ORF62 as more of a late transcribed gene [74], [115]. Perhaps, this is not mutually exclusive, as there is limited evidence that its HSV homolog and other IE genes in HSV might be expressed throughout infection [116], [117]. In other viruses in the varicellovirus genus, such as the closely related pseudorabies virus (a model for neuroinvasive disease in swine) and the equine herpesvirus type 1, it appears that there is only one protein made under the strict IE conditions, namely, the homolog of VZV ORF62/HSV ICP4 [118], [119]. Regardless, the putative VZV IE gene products have all been shown to have transcription regulatory activities [45], [54], [99], [100], [120]–[123]. In general, the E genes generally encode viral DNA replication machinery, nucleotide metabolizing and processing enzymes, and two virus-specific serine/threonine protein kinases that have multiple roles throughout infection. Once DNA replication is initiated, late gene transcription is then licensed through mechanisms that are poorly defined for VZV, but have been better-studied in HSV [124], [125]. Late proteins are generally structural components that compose or assemble the progeny virion particles, or proteins that mediate capsid egress across the nuclear membrane and the assembly of tegument [35]. Late genes can further be classified as leaky late (γ_1) or true late (γ_2), depending on whether genome replication increases existing expression of such genes (γ_1), or initiates expression (γ_2). The genomes are replicated and are packaged into preformed protein capsids in the nucleus and then

trafficked across the nuclear membrane (undergoing transient envelopment and de-envelopment) and processed for the addition of tegument proteins and the envelope glycoproteins in the trans-Golgi network, before egress to the cellular surface [126]–[129]. In herpesviruses, tegument acquisition to the virion is a rather complex process. Addition of some inner tegument proteins is thought to occur in the nucleus, and with the majority of outer tegument proteins added in the cytoplasm and at the trans-Golgi network [130], [131]. In VZV, these outer tegument proteins are thought to organize around key focal proteins in the cytoplasm for tegument incorporation, such as the ORF9 protein (homolog to HSV VP22, although these proteins share less than 35% homology overall). ORF9 is an abundant component of the VZV virion and known to recruit ORF66 kinase-phosphorylated (i.e. cytoplasmic forms) of IE62 [83], [85]) and the ORF47 kinase for tegument incorporation into virions [56], [57]. However, there is still much conflicting data describing at which point virions of PRV and HSV acquire certain tegument proteins, so this process is still incompletely understood. Obviously it may potentially vary depending on the virus [91], [132]–[137].

In terms of herpesviruses virion assembly and egress, there are currently multiple models to explain the process. In one model, unenveloped nucleocapsids are thought to directly exit the nucleus via nuclear pores and perinuclear enveloped nucleocapsids through a continuum of nuclear, rough endoplasmic reticulum, and Golgi membranes [138], [139]. However, the more widely accepted model is known as the envelopment-deenvelopment-reenvelopment model, in which freshly replicated viral DNA is packaged into capsids in the nucleus. These nucleocapsids then undergo a transient envelopment followed by deenevelopment through the inner and outer nuclear membranes, and associate with tegument proteins and reenevelopment in the cytoplasm, where budding of complete virions occur through the *trans* Golgi network before entering the cell

secretory pathway for egress [140]–[143]. With regards to alphaherpesvirus neuronal infections, there are also two opposing models to describe particle assembly and anterograde transport, known as the Married and Separate models [144]. The former model hypothesizes that virions are fully assembled in the soma and then trafficked down the axon in a transport vesicle, with the latter proposing that separate vesicles containing the nucleocapsids and membrane proteins are transported down axons, with final assembly of infectious virions taking place near the egress site. Clearly, further studies are needed to better understand these processes.

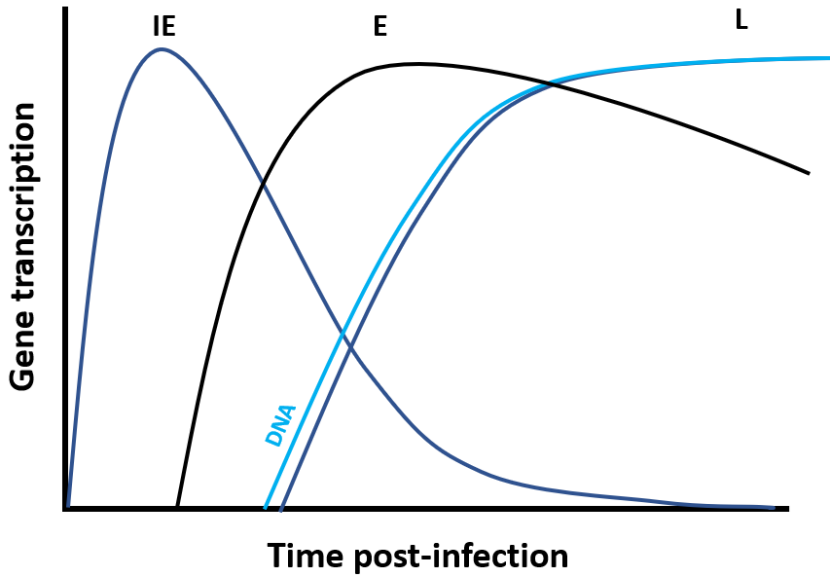

Figure 4 VZV transcriptional cascade. IE=immediate early; E=early; L=late. In temrs of the general time course for VZV infection, studies have demonstrated the presense of newly synthesized IE62 within 1h of infection, VZV replication compartment formation between 4-6h, gE and capsid protein presence by 4-9h, and the detection of virion particles by 9-12h, which completes a productive infection cycle [145].

1.1.5 Latency and Reactivation

VZV latency occurs in sensory ganglia throughout the body and may also occur in the autonomic nervous system. Virus access is thought to occur by at least two possible routes. The classical route of neuronal infection is thought to be through the axon endings of sensory neurons that infiltrate the skin and come in contact with skin lesions [21], [146]. However, there is also evidence that VZV may also gain access to sensory and other ganglia via a hematogenous route, in which cells of the systemic T cell mediated viremia can directly access the ganglia by infiltration. This has been studied in detail for the closely related SVV [147]. When virus enters neurons at the distal axon, VZV is thought to hijack host motor proteins for retrograde transport to the soma, as has been implied for VZV and shown for HSV and PRV [146], [148]. In HSV and PRV, infection at the distal axon favors latent infection, and it was speculated that this was a consequence of differential transport of some outer tegument proteins, including tegument-derived transactivators such as VP16, in reaching the nucleus to promote lytic expression [104]–[106]. However, this has not been definitively shown for HSV or VZV.

VZV latency and reactivation has, until recently, been a poorly understood aspect of infection. It is much a result of VZV being difficult to work with, in conjunction with the lack of animal models of human disease or an *in vivo* model of reactivation [146], [149], [150]. Prior to 2015, a number of studies performed on cadaveric ganglia has suggested expression from multiple regions of the latent genome in human ganglia samples. However, much of this early picture was found to be the result of post-mortem viral gene expression, as well as non-specific antibody reactivities and histological staining artifacts [151]–[155]. After 2016, more recent work applying NGS methods to cadaveric ganglia obtained after a minimal postmortem interval suggests that expression during latency is far more extremely limited, though removal of ganglia itself

introduces additional confounding factors, such as tissue trauma and hypoxia, which can signal death-induced pathways and alter results [156], [157]. These studies nevertheless revealed that latent transcription mapped to two genomic regions, ORF63, which was consistent with some earlier studies, and a new region that mapped antisense to VZV ORF61, which was termed VZV latency-associated transcript (VLT). Discovery of VLT, as well as recent advances in developing in-vitro model systems to study various aspects of latency and reactivation, were critical to our modern understanding of VZV latency and reactivation.

The location of VLT is conserved with all alphaherpesviruses as well as other related viruses such as HSV, PRV, and BHV. The implication is that VLT/LAT has a conserved function, perhaps regulating the pro-lytic ORF61 protein (the HSV ICP0 equivalent [156]). ORF61 possesses E3 ubiquitin ligase activity, which targets host factors such as promyelocytic leukemia (PML) bodies and other ND10 complex components for degradation [158]–[161]. Since the latent VZV genome is thought to be circularized and chromatinized and associate strongly with PML proteins in nuclear bodies (PML ND10s) upon entering the nucleus [145], [158], these ND10 bodies play a role in regulating transcription via protein sequestration and promotion of stress pathways, so the lytic/latent decision likely depends on the balance between these various factors [162], [163]. More recent work in 2020 revealed that VLT belongs to a group of differentially spliced transcripts, some of which are also expressed both during lytic and latent infection [157]. Importantly, these studies uncovered the existence of a VLT-ORF63 fusion transcript during reactivation, as well as an encoded VLT-ORF63 fusion protein. These were induced in stem cell-derived neurons after JNK activated stress, and the protein possessed transcriptional enhancing activity, leading to the speculation that the fusion transcript may act as an initiator of broad viral

gene expression during the reactivation process, much like during the animation phase in HSV [157], [164].

Exact mechanisms and events that occur as VZV latency transitions to reactivation are unknown. In HSV-1, the reactivation process was proposed to occur as a two-stage process, as hinted at earlier, in which expression of the leaky late gene VP16 in phase 1 is a decision point [102], [106], [165], [166]. It has been proposed that exit from latency initiates with "phase I," where stimulus-driven chromatin changes result in transient derepression of expression and the synthesis of some viral proteins outside of the classic α-β-γ lytic cascade. This stage, termed "animation," may reenter latency; however, if the VP16 made enters the nucleus, it can then stimulate the initiation of a "phase II" in which it drives expression of IE genes and the full α-β-γ regulated cascade [102], [167]. Study of HSV-1 VP16 reporter viruses in mice have supported the role of VP16 [102], [103], [106]. In VZV, it is likely that VZV ORF10 and virion IE62 may act together, perhaps in overlapping roles, in deciding the outcome of VZV infection of neurons [55]. This speculation drove the studies detailed in Chapter 4. Once reactivation occurs, it is known that VZV first undergoes intraganglionic neuron-to-neuron spread, followed by travel down microtubes in the axons in an anterograde fashion, in order to infect epithelial cells in that associated dermatome [146].

1.1.6 Challenges in the Laboratory and VZV Model Systems

VZV is relatively difficult to work with, and coupled with the lack of a fully permissive animal model, VZV studies have constantly lagged behind those of HSV [146], [149]. Although VZV and HSV share considerable gene homology, they differ in key aspects of pathogenesis and tissue tropism in humans. Obtaining high titer cell-free VZV continues to be a challenge, since

VZV replicates in only a few human cell lines. These include melanoma MeWo melanoma cells, retinal pigment epithelial ARPE-19, hTert RPE cells, human foreskin fibroblast HFF cells, and lung-derived diploid fibroblast MRC5 cells. VZV also replicates in some human neuron cultures. VZV remains highly cell-associated *in-vitro*, incompletely budding at the plasma membrane surface of infected cells [168]. Numerous particles form that are empty and not infectious. Lysing infected cells to produce cell-free VZV results in envelope damage that greatly decreases infectivity. Infections in the lab are thus frequently initiated with previously infected cells containing cell-associated virus, maintained as cell-associated stocks in liquid nitrogen. In addition, VZV is highly human-specific, much more so than HSV, so animal models of infection disease and persistence are not generally available. Guinea pigs have indicated some promise in modeling enteric VZV infections as well as establishment of (but not reactivation from) latency [169]–[171], but there is little disease or signs of infection, latency and reactivation. Immunocompromised SCID-hu mice xenografted with human fetal skin, thymus, or ganglionic tissues have also advanced our understanding of VZV lytic infection in these tissues [172]–[175]. Laboratory rats have been developed to study pain behaviors induced by VZV infection that reflect VZV association with postherpetic neuralgia [176], but the animal is not permissive for VZV replication and reflects an abortive infection [177], [178]. To model VZV latency and reactivation *in vitro*, our lab and that of others have developed human embryonic stem-cell- (hESC) or induced pluripotent stem cell (iPSC)-derived neuron platforms [179]–[183]. In many of these systems, differentiated neurons are made from iPSC or hESC lines using an intermediate co-culture step [181] or other pre-direction step [184] to direct differentiation to neurospheres and neural lineages. These are then dissected and differentiated into neurons with a mixed CNS/PNS phenotype and used for subsequent infection experiments after differentiation [181]. Such neuron cultures are

heterogenous and generally similar in distribution to a culture of primary ganglia, with our cultures typically consisting of 95% βIII tubulin (neuron marker) positive with 10-20% of the neurons expressing peripheral sensory markers brn3a and peripherin [182]. Using these neurons, we and others further developed a two-compartment microfluidic system that can separate axons from soma for modeling distal axonal infections, with the help of a nerve growth factor (NGF) gradient and differential hydrostatic pressures between culture chambers (Fig. 5) [179], [182], [185].

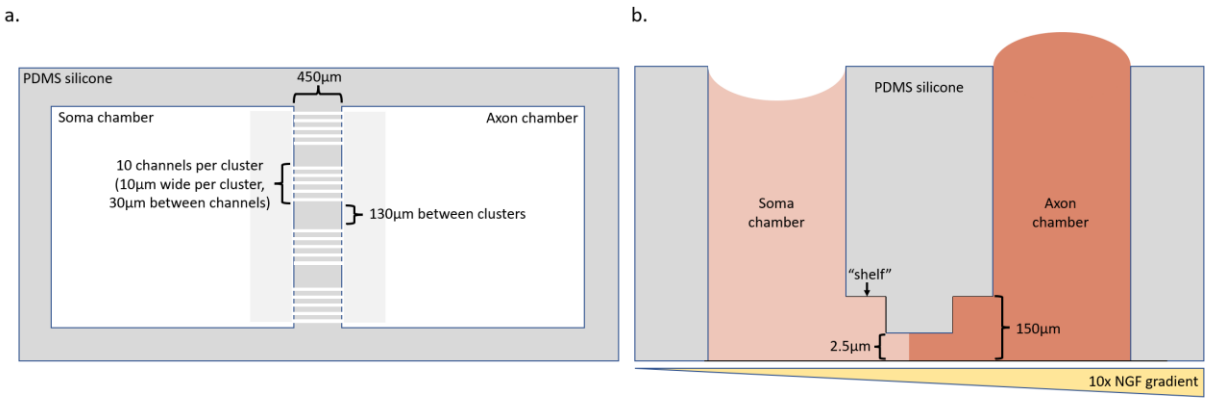

Figure 5 Design and dimensions of compartmentalized microfludic neuron devices. (a) shows a top-down view of the platform, with dimensions of each channel (10 mm), distance between channels (30 mm), distance between channel clusters (130 mm), and length of channels from chamber to chamber (450 mm). The lighter gray boxes on either side of the channels represent the 150 mm "shelf" shown in (b), where neurospheres are seeded underneath for optimally close access to the actual channels. (b) shows a transverse cross-section of a device with the differential media levels to achieve a hydrostatic pressure gradient, and differential concentrations of NGF on each side, to promote directional axonal growth.

The generation of mutant VZV via classical homologous recombination in DNA fragment and virus DNA-transfected cells and using cellular complementation has long proved to be extremely difficult for VZV due to the challenges just described. A major hurdle was purifying recombinant virus from parent without a very strong selection process, as the classic approach of homologous recombination followed by plaque picking to generate HSV mutants does not work in VZV. Progeny viruses are cell-associated and each plaque does not represent one infectious

virus particle [3]. As such, VZV greatly benefited from the development of isogenic recombination systems, initially using overlapping 25-45Kb cosmids (which relies on all four cosmids recombining properly in the cell) [27], [186], [187]. This was then followed by bacterial artificial chromosomes (BACs) containing the whole VZV genome [188]. The latter is used in our lab and can be manipulated by recombineering methods that exploit λRed-mediated recombination. The BAC system is more straightforward, compared to the previously used overlapping cosmid system [27], [186], [188]–[190]. In the BAC-based system, manipulations can relatively easily be made and propagated in bacteria, with extracted BAC DNA readily obtainable for transfection of VZV-permissive human cell lines to obtain virus. These viruses can then be used to initiate subsequent infections in a variety of models.

1.2 Clinical Disease

1.2.1 Pathogenesis and Varicella Disease

VZV is the causative agent of varicella (chickenpox) and herpes zoster (shingles). During initial infection, aerosolized droplets of viral particles from shed skin with lesions are breathed in and from there, VZV replicates in the local mucosal epithelial tissue until it gains access to lymphoid tissue via the tonsillar crypts in Waldeyer's ring [191], [192]. Infection of dendritic cells, other immune cells, and in particular, CD4+ skin-homing T cells (including VZV-mediated reprogramming of infected T cells to become skin-homing) results in a T cell viremia, allowing VZV to home to the base of the highly vascularized hair follicles [175], [193]. Subsequent infection of the adjacent skin cells eventually causes the widespread varicella rash. During viremia

or from infection of the sensory neurons that innervate skin, VZV also gains access to sensory ganglia throughout the body [146]. Lifelong latent infection is maintained in these ganglia, with later reactivation events from one or more ganglia leading to intra-ganglionic spread, trafficking down the axons of multiple neurons in an anterograde fashion, and initiating lytic infection and formation of the characteristic zosteriform rash on multiple sites of the associated cutaneous dermatome [194], [195].

Prior to the varicella vaccine, 80% of children became infected with varicella by age 8 in westernized societies [196], [197]. Primary infection is followed by a 2-3 week incubation period, after which the classic symptoms of chickenpox (fever, headache, malaise, vesicular rash throughout body) can manifest [198]. Complications can include bacterial co-infections, hemorrhagic conditions, gastrointestinal infection complications, and VZV encephalitis (rare) when the virus accesses the CNS [199]. These complications arise mostly in immunocompromised individuals, or seronegative adults who were not exposed to VZV during childhood, but rather as an adult (e.g. those living in rural tropical areas) [198], [200], [201]. Pregnant persons with varicella also risk complications and a poor prognosis [202].

1.2.2 Herpes Zoster

A third of people infected with VZV will reactivate virus to develop zoster in their lifetime, with incidence increasing to 50% for those who live up to 85 years. Risk of herpes zoster is largely affected by age, with about 68% of cases occurring in people aged 50 or older, [203]–[208]. Age and zoster reactivation is largely thought to be related to natural immune senescence, since adaptive cell-mediated immunity is known to play a key role in maintaining VZV latency throughout life [209]–[213]. However, evidence suggests that subclinical asymptomatic shedding

of VZV can occur during physiological stress [214], [215], and it is thought that the balance between VZV shedding and host immune responses to these natural "booster" events contribute to the infrequency of clinical reactivation events throughout most of an individual's lifetime [216]–[220] This is consistent with studies showing that those undergoing immunosuppressive therapies have significantly increased reactivation potential in patients, and the fact that boosting immunity via vaccination or exposure to children with varicella has significantly decreased both risk of reactivation as well as disease severity in reactivated individuals [221]–[228]. Other related triggers of reactivation include physical trauma [229] as well as solar UV exposure [230]. There are many other contributing factors, such as sex, underlying disease status, and genetics [231].

Patients with herpes zoster often describe an extremely painful rash that lasts for weeks, with potential long-term complications such as bacterial infections, scarring, and eye disease (from VZV reactivation of the trigeminal ganglia). The most common is chronic pain from neuropathic damage induced by VZV replication at the ganglia, which may persist long after VZV clearance [232]–[235]. This is generally termed post herpetic neuralgia (PHN) and can be severe and debilitating for years. In more complicated cases, acute zoster neurological symptoms can include encephalitis, paresis, neurological diseases and pneumonia [205]. It is also important to note that such complications can sometimes occur even without having developed a visible rash, termed "zoster sine herpete" [236], [237].

1.2.2.1 Vaccines, Antiviral Therapeutics, and Pain Management

Unlike all other human herpesviruses, there are effective vaccines available for VZV disease. For chickenpox, the live-attenuated Varivax vaccine (approved in 1995) prevents more than 95% of cases in the United States when given as a two dose regimen, and even greatly reduces disease severity in those with breakthrough infections [238]. For zoster, the initial vaccine

formulated was Zostavax, which consists of a more concentrated version of the same attenuate virus used in Varivax, and it was given to seropositive individuals over age 60 [222]. Zostavax reduced incidence of zoster and post-herpetic neuralgia by about 2/3rds, also lowering the disease burden in vaccinated individuals who developed VZV disease. However, as this vaccine is live-attenuated, it was contraindicated in immunocompromised individuals. Efficacy also decreased from 68% to 4% over the span of eight years [239]. In 2017, a new VZV glycoprotein E-based subunit vaccine called Shingrix was approved as a two-dose regiment to reduce zoster incidence and disease burden [240], [241]. Shingrix uses a novel adjuvant called $AS01_B$, and has higher efficacy and is also safe for immunocompromised patients to receive, although there are reports of more frequent injection site reactions, fatigue, and gastrointestinal upset after receiving the vaccine, which may deter some patients from receiving both doses of the vaccine [241], [242]. Protection also seems to last longer after both doses of Shingrix, though long-term studies are still needed [243], [244]. Finally, despite the development of VZV vaccines, implementation of such technologies is not worldwide and vaccine uptake is still low when it is available, so VZV remains an important disease that affects millions of individuals throughout the world, especially in developing countries [244]–[246]. Many of these countries use such VZV vaccines selectively, largely due to financial and access reasons [247]. Even in countries such as the United States, there is room for improvement in second-dose completion of Shringrix, for example, due to reasons such as cost, fear of side effects/needles, and lack of insurance coverage [244].

In the United States, there are only a few approved antiviral treatments for VZV disease, with a need for more options. For treatment of herpes zoster, acyclovir (ACV) and its derivatives (such as valacyclovir and famciclovir) are common first-line therapies with very good safety profiles [248], [249]. These drugs are chain-terminating nucleoside analogs specific for the viral

DNA polymerase, so they act to specifically target and stop viral DNA replication, but require activation by the Viral thymidine kinase. Early treatment with these drugs clearly decrease recovery time [250]. A major issue with antiviral treatment is that the diagnosis of zoster may be delayed and occur after viral reactivation and ganglionic replication has initiated, so that damage has already started to occur by the time that antivirals are applied. There have been reported cases of ACV-resistant VZV infections [251], [252]. A second line drug is Foscarnet, a pyrophosphate analog second-line therapy for VZV infections, though it does come with considerably higher toxicity and side effects and is usually only used in ACV resistant patients with severe disease [253]. It is important to note that both these therapies target only actively replicating VZV infections, we currently do not have an approved treatment to target the latent genome.

Although a ways from being approved for use in patients, new gene-editing technologies such as CRISPR/Cas9 and Homing Endonucleases have been successfully used to target both human and animal models infected with the related HSV-1, Epstein-Barr virus (EBV), and Marek's disease virus (MDV) in the lab [254]–[257]. Notably, AAV-delivered HSV-specific endonucleases have knocked down HSV production from infected cells in culture as well as in murine trigeminal ganglia [255], [258], [259]. These therapies are still in early development, but have the theoretical potential to target both the lytic as well as latent genome of herpesviruses, making them important and promising candidates for a potential new class of antiviral therapeutics.

Treatment of pain from zoster or post-herpetic neuralgia is largely targeted towards symptom control. For zoster-associated pain (ZAP), analgesics such as acetaminophen, NSAIDs, or corticosteroids to limit inflammation can be used in combination with an antiviral. Lidocaine and capsaicin have also been used topically. In more severe cases, longer-term or surgical

intervention can also be explored [260]. Treatment of post-herpetic neuralgia is similar to treatment for zoster-associated pain, in that therapies are targeted towards symptom control and management, often without need for antivirals [261]. The pathogenesis of PHN is different from that of ZAP, though, in that the former is far harder to treat, and many PHN cases do not responds to any applied anti-pain strategy. Some of the drugs used in PHN include anticonvulsants (gabapentinoids and phenytoin), tricyclic antidepressants, and in rare cases, opioids (which are not ideal due to long-term use and dependency concerns) [262]. Nerve blocks, cryotherapy, peripheral nerve surgery, and a variety of alternative treatments can also be considered to improve quality of life in these patients [262], [263]. However, despite these diverse options, it has been documented that a significant fraction of patients still remain refractory to all these strategies [264].

2.0 Specific Aims and Rationale

Varicella-zoster virus (VZV) causes varicella (chickenpox) during childhood primary infection and zoster (shingles) after reactivation from latency, usually in older or immunocompromised adults. About one-third of infected individuals will develop zoster, resulting in debilitating disease. Following primary infection, VZV establishes latency in sensory ganglia for decades before reactivating. A major hurdle in studying VZV latency and reactivation was the lack of a reliable animal model for complete replication of this highly human-specific pathogen. Thus, mechanisms that maintain viral latency and initiate reactivation are poorly understood.

To address this, our laboratory developed a human neuron platform representing a system in which productive infection, latency, and experimental reactivation has been achieved. This provides an opportunity to explore questions regarding latency and reactivation that have previously been unanswered. Here, we propose two aims that will identify how VZV tegument proteins affect the lytic/latent decision process, and whether latent genomes can be directly targeted to prevent reactivation. Our overlying hypothesis is that virion-associated transactivators play a crucial role in establishing primary infection as well as latency and reactivation decisions during VZV neuronal infection, and that blocking such transactivators will prevent reactivation from latency. Study of this model will reveal aspects of the VZV latency and reactivation process leading to more efficient prevention of virus spread and reactivation.

2.1 Aim 1: Define the role of two virion-associated transactivators in driving neuronal infection, dissemination, and establishment of latency.

Study of the related Herpes Simplex virus (HSV-1) suggests that transactivators in the virion tegument strongly favor lytic replication; however, whether this is true for VZV is unknown. To study the contribution of VZV transactivators towards the outcome of neuronal infections and the establishment of latency, we will assess whether recombinant VZV lacking one or both key transactivators from ORFs 10 (homolog to HSV VP16) and 62 are viable and have altered productive infection in favor of latency in human neuron cultures. We hypothesized that these VZV mutants will more efficiently establish latency in neurons due to the absence of key transactivators to drive lytic replication.

2.2 Aim 2: Inhibit VZV replication and silence the latent genome using CRISPR/Cas9.

Current antiviral therapies halt VZV replication, but do not target latent genomes. Successful studies have used CRISPR/Cas9 to cleave HSV genomes, introducing the potential to render latent VZV incapable of reactivation as well. Here, we will optimize the use of AAV-packaged Cas9 to cleave VZV genomes at repeated genes and block lytic replication. These constructs will be used to reduce the potential of neuronal reactivation in latently infected cultures. We hypothesize that delivery of targeted CRISPR/Cas9 to lytic and latently infected neurons will block viral spread and reactivation.

Successful completion of these aims will provide a better understanding of molecular components involved in VZV latency and reactivation, along with a means to target both lytic and latent viral genomes, which may be applicable in developing future VZV therapeutics.

3.0 VZV genome targeting for inactivation using CRISPR/Cas9

This chapter was adapted from the published manuscript, "Antiviral Targeting of Varicella Zoster Virus Replication and Neuronal Reactivation Using CRISPR/Cas9 Cleavage of the Duplicated Open Reading Frames 62/71," authored by Betty W. Wu, Michael B. Yee, Ronald S. Goldstein, and Paul R. Kinchington [265]. It was written by BWW and PRK and edited by BWW, PRK, MBY, and RSG. All data in this section was collected, analyzed, and curated by BWW, MBY, RSG, and PRK.

3.1 Project Summary

Varicella Zoster Virus (VZV) reactivation from neuronal latency causes Herpes Zoster (HZ), a debilitating disease with incidence rising with increasing age or immune compromise that affects a third of the unvaccinated population. While HZ incidence can be reduced by vaccination, vaccine uptake by the target population is far from ideal, and antiviral treatments for HZ are often initiated too late to prevent ganglionic damage and HZ-associated pain. Here, we addressed the potential of targeting the replicating and reactivating VZV genome using Clustered Regularly Interspaced Short Palindromic Repeat-Cas9 nucleases (CRISPR/Cas9) after delivery by adeno-associated virus (AAV) vectors. After serotype optimization, we show that a single treatment with AAV serotype 2 (AAV2) expressing Staphylococcus aureus CRISPR/Cas9 (saCas9) and a guide RNA (62gR) targeting the duplicated VZV ORF62 essential gene, were highly effective in reducing VZV progeny virus in multiple epithelial cell types and in lytically infected human

embryonic stem cell (hESC)-derived neurons. In contrast, there was no reduction of a recombinant virus in which the 62gRNA targeted sequence was altered while maintaining the coding of ORF62, establishing that antiviral effects were a consequence of specific VZV genome targeting. AAV2-delivered 62gR-saCas9 treatment of latently infected neuron cultures considerably reduced the production of infectious virus from experimentally induced reactivation, although we could not detect reduced latent genome loads. Taken together, our results demonstrate the potential of AAV-delivered genome editing methods to target a duplicated essential viral gene to limit VZV production in epithelial cells and latently infected human neurons. This approach could be developed into a badly needed strategy for treatment of VZV disease and curtailing VZV spread after reactivation.

3.2 Importance

VZV human diseases remain a major public health concern, particularly herpes zoster (HZ) caused by reactivation of VZV from neuronal latent states. This common disease of the elderly and immunocompromised is frequently complicated by difficult-to-treat chronic pain. Here, we applied the use of a viral vector-delivered CRISPR/Cas9 nuclease to a duplicated VZV gene to effectively limit viral replication and spread in epithelial cells and in human reactivated differentiated neuron cultures. This lays a foundation for further development of treatments for VZV diseases using genome editing.

3.3 Introduction

Varicella-zoster virus (VZV) is the human alphaherpesvirus that causes varicella (chickenpox) during primary infection and herpes zoster (HZ; commonly called “shingles”) when the virus reactivates from the latent state, often decades after the initial infection [146]. Without immune boosting through the use of HZ vaccines, it is estimated that one-third of the population will develop HZ in their lifetimes, with incidence rising with age and declining immune status caused by natural senescence, disease, or iatrogenic causes. HZ remains a public health concern because it is often complicated by scarring, bacterial infections, and acute pain that can be debilitating. A significant fraction of HZ patients develop difficult-to-treat chronic pain states termed post-herpetic neuralgia (PHN), which can be so severe that they reduce quality-of-life. HZ may also be followed by neurological, gastrointestinal, and vascular diseases [266]–[268], as well as potentially blinding complications that develop after facial zoster [269].

HZ incidence and severity are reduced by boosting the existing VZV-specific immunity using vaccines. The first HZ licensed vaccine (used since 2005) was based on a higher dose version of the live-attenuated VZV strain used in the varicella vaccine, and it reduced HZ incidence by half and the disease burden by two-thirds [222]. However, it was contra-indicated in immunocompromised patients who could develop vaccine virus-induced disease [270], [271]. A more recent Federal Drug Administration (FDA)-approved vaccine is based on the novel AS01B adjuvant and purified VZV glycoprotein E (gE). This subunit vaccine has higher efficacy against HZ, but requires two doses, has frequent side effects or injection-site reactions and is not used worldwide [240], [272], [273]. Hence, the uptake of the HZ vaccines remains low. HZ disease can respond to antiviral treatment if it is initiated early, but current antivirals only target active viral replication. The latent state remains refractory to any known antiviral treatment [269], [274], [275].

Thus, VZV diseases still impact millions of people worldwide and there is a need for improved HZ treatments/prevention.

One of the main hurdles in developing novel VZV therapeutic strategies has been the difficulty in modeling VZV pathogenesis in animal models. VZV demonstrates high human specificity, and does not fully replicate or cause disease in rodents, compared to the modeling of infections and diseases caused by the related herpes simplex virus type 1 (HSV-1) [276]. Indeed, there is no in vivo immunocompetent model of human VZV-induced primary disease, a VZV latent state that is reactivatable, or HZ-like disease states resulting from reactivation [146], [149]. Attempts to experimentally reactivate VZV from latently infected human cadaver ganglia have also not yet been successful [155], [277]. VZV does replicate in fetal human tissues harbored in severe compromised immunodeficient (SCID) mice, which can be used to evaluate pathogenesis and antiviral studies [278]–[280], but their use can be cost-prohibitive and requires special animal-experimentation permissions. However, neuronal culture models have been developed that harbor latent VZV that can be experimentally reactivated. We previously reported neuronal cultures derived from human embryonic stem cells (hESC) that model VZV neuronal lytic replication, axonal transport, neuron-to-neuron spread, and a prolonged viral persistent state that could be experimentally reactivated by the interruption of the NGF signaling or alteration of histone/chromatin architecture [182], [183], [281]. These and similar neuronal models used by other groups [156], [173], [179], [282]–[285] have now established the means to probe the VZV latent state and investigate the potential targeting of latent and lytic replicating genomes using gene editing. Targeted CRISPR/Cas9 and specific homing meganucleases have been explored to target HSV-infected neurons and in murine neuronal models of disease and latency in vivo [255], [258], [286], as well as human cytomegalovirus (hCMV) and Epstein–Barr virus in cultured

immune-cell models [256], [257], [259]. However, gene-editing strategies have not yet been studied for antiviral targeting of VZV replication or its latent state, as far as we are aware.

In this study, the potential of gene editing to target VZV genomes as a means to prevent lytic, latent, and reactivated infections was investigated. The *Staphylococcus aureus* CRISPR/Cas9 (saCas9) system was exploited because it has a high specificity and small size, permitting efficient packaging into AAV together with guide RNA [287], [288]. VZV essential and duplicated genes present in the internal and terminal genome repeat regions were targeted, allowing for the cleaving of genomes at more than one position using a single vector. The VZV genome contains three duplicated genes in the repeated sequences bounding the short unique region, ORFs 62/71, 63/70 and 64/69 [16], [289]. Of these, ORFs 62/71 and 63/70 encode regulatory proteins [54], [77] that have been shown to be essential [48], [290]. Furthermore, ORF62 encodes IE62, the VZV ortholog of the well-characterized HSV-1 ICP4 transcriptional transactivator that is required for the expression of all HSV-1 early and late genes. The HSV-1 ICP4 activates transcription by recruiting the host-cell transcriptional machinery to the genome [291]. VZV IE62 enhances the infectivity of transfected VZV DNA [22], [77] and has a sufficient functional-conserved structure to HSV ICP4 so that it can partly replace ICP4 in the HSV genome leading to the production of an infectious virus [292], [293]. We selected AAV vectors for delivery because AAVs have been used both in animal models as well as clinical trials for neuronal delivery, with promising therapeutic delivery potential [294]–[298]. Here, we demonstrate that AAV2-packaged saCas9 targeting VZV ORFs 62/71 can greatly reduce VZV lytic replication in epithelial cells and lytic-infected human neurons, severely curtail VZV growth and damage the virus following reactivation from latency in neuron cultures.

3.4 Materials and Methods

3.4.1 Cells and Viruses

All cell lines except the NIH-registered human embryonic stem cell line Wa09 (H9) were purchased from ATCC. Cell-culture reagents were obtained from Thermo Fisher Scientific (Thermo Fisher Scientific, Waltham, PA, USA) unless otherwise noted. The Wa09 (H9) was obtained from WiCell (Madison, WI, USA) and differentiated into neurons as detailed previously [182]. Retinal-pigmented epithelial (ARPE-19) and HEK 293 cells were grown in Dulbecco's Minimal Essential Media (DMEM, #10569-010) supplemented with 10% fetal bovine serum (FBS; #S11150, R&D Systems, Minneapolis, MN, USA), 100 units/mL penicillin + 100 mg/mL streptomycin + 0.25 mg/mL amphotericin B as an antibiotics/antimycotic solution (#ABL02, Caisson, Smithfield, UT, USA). Human melanoma (MeWo) cells were maintained in Minimum Essential Media (MEM) supplemented with 10% FBS and antibiotics/antimycotic.

All infection studies used virus or viral recombinants based on the Parent of Oka (pOka) strain, a wildtype clinical isolate that was the parent of the live attenuated varicella and zoster vaccines. Cell-associated VZV were prepared as previously described [299], as infected ARPE-19 cells that were frozen after mitotic inhibition with growth media containing 0.01 mM mitomycin C (#A4452, ApexBio, Houston, TX, USA) for 3–4 h. at 37 °C. Cell-associated VZV was slow-frozen at −80 °C overnight in media containing 10% DMSO before long-term liquid-nitrogen storage. Frozen aliquots were titrated in triplicate for subsequent infections. Cell-free VZV was prepared using a previously published protocol [300], stored aliquoted in liquid nitrogen, and titrated after freezing for use in subsequent infections.

3.4.2 CRISPR/Cas9 Plasmid and gRNA Design

Three optimal gRNA target sequences with PAM motifs and guide length that were predicted to target saCas9 to each of ORF62 and ORF63 were selected using an online protocol from the Zhang lab [287] and Software (Benchling Inc., San Francisco, CA, USA). Oligonucleotides (Table 1) were synthesized by Integrated DNA Technologies (Integrated DNA Technologies INC., Coralville, IA, USA). Oligonucleotide annealing and cloning into the backbone vector pX601 (pX601-AAV-CMV::NLS-SaCas9-NLS-3xHA-bGHpA;U6::BsaI-sgRNA was a gift from Feng Zhang; Addgene plasmid # 61591; http://n2t.net/addgene:61591; RRID:Addgene_61591 accessed 01/10/2022) were performed as published online (https://media.addgene.org/cms/filer_public/6d/d8/6dd83407-3b07-47db-8adb-4fada30bde8a/zhang-lab-general-cloning-protocol-target-sequencing_1.pdf accessed 01/10/2022). Briefly, the vector was digested with BsaI and a dsDNA formed by the hybridization of the two oligonucleotides was ligated into the pX601 plasmid, where pX601 expresses saCas9 and the inserted gRNA from the same vector. A vector expressing *Streptococcus Pyogenes* CRISPR/Cas9 targeting the intergenic region between UL3 and UL4 was developed using the pX330 vector (pX330-U6-Chimeric_BB-CBh-hSpCas9 was a gift from Feng Zhang (Addgene plasmid # 42230; http://n2t.net/addgene:42230; RRID:Addgene_42230 accessed 01/10/2022), as previously described [301], [302]. Primers used for making gRNA are listed in Table 1.

Table 1 gRNA Oligos

Gene	Direction	Primer Sequence (5′ → 3′)
ORF62-1	F	CACCGCTGGTTGAAGTCCCGATACGGA
	R	AAACTCCGTATCGGGACTTCAACCAGC
ORF62-2	F	CACCGCCGGCTTTTTACCCGAGATGGA
	R	AAACTCCATCTCGGGTAAAAAGCCGGC
ORF62-3	F	CACCGCAGCGCTCTACACCCCAACGCG
	R	AAACCGCGTTGGGGTGTAGAGCGCTGC
ORF63-1	F	CACCGATACGCGGGTGCAGAAACCG
	R	AAACCGGTTTCTGCACCCGCGTATC
ORF63-2	F	CACCGAAGACGGGTTCATTGAGGCG
	R	AAACCGCCTCAATGAACCCGTCTTC
ORF63-3	F	CACCGTTGAATTTCGGGATTCCGACG
	R	AAACCGTCGGAATCCCGAAATTCAAC
UL3-4	F	CACCGGTGACGAGCGCGATCCGGC
	R	AAACGCCGGATCGCGCTCGTCACC

3.4.3 Preparation of AAV

AAV reporter vectors of different serotypes expressing the green fluorescent protein under the chicken β-actin promoter CAG were acquired from Virovek (Virovek, Hayward, CA, USA). High titer (10^{13} viral genome copies (GC) per mL) ORF62-targeting AAV2 and a pX601 vector-only control lacking gRNA, were prepared by Penn Vector Core's Gene Therapy Program (https://gtp.med.upenn.edu/ accessed 1/10/2022). Lower titer (approximately 10^{10} GC/mL) control or ORF62-targeting AAV2 for use in preliminary experiments were made by transfecting HEK293 cells with the control pX601 (with no gRNA) or ORF62-targeting plasmid (pX601+62-1 gRNA), along with plasmids expressing AAV2 replication gene (pRC2-mi342 vector) and a helper plasmid that expresses adenoviral helper proteins (pHelper; Takara, Kusatsu, Shiga, Japan) using the Xfect reagent (#631318, Takara). 6 h after transfection, media was changed to fresh DMEM with 10%

FBS and cells were further incubated at 37 °C 5% CO_2 for 72 h. Cells were then harvested into an AAV lysis buffer (50 mM Tris, 150 mM NaCl, 0.05% Tween-20, pH 8.5) and subjected to three freeze–thaw cycles. AAV were then purified using a published protocol in which a discontinuous 15%-25%-40%-60% iodixanol gradient was used. Virus at the interface between 40% and 60% iodixanol was harvested after centrifugation at 200,000× *g* for 2 h. at 18 °C [303], [304]. Samples were then concentrated into 0.001% Pluronic F68 with 200 mM NaCl in D-PBS using Amicon Ultra-15 centrifugal filters (#C7715, Millipore Sigma, Burlington, MA, USA) and spun at 3700× *g* for 20 min at 4 °C. AAV stocks were then aliquoted and stored at −80 °C until use. An aliquot of each virus produced was titered by quantifying AAV genomes using qPCR as detailed below.

3.4.4 Quantification of Viral Genomes

The pX601-based AAV vectors were quantified by SYBR qPCR as described previously [305], using PowerUp SYBR Green Master Mix (#25741, Thermo Fisher Scientific) and primers that amplified a 93 bp fragment of the saCas9 gene in all pX601 vectors (Table 2, “SaCas9”). Linearized plasmid DNA served as the standard, and all measurements were performed in triplicate. PCR conditions were 50 °C for 2 min; 95 °C hot start for 5 min; 45 cycles of: 95 °C for 15 s, 8 °C for 10 s and 72 °C for 45 s, followed by a dissociation curve analysis (95 °C for 15 s, 60 °C for 60 s, 95 °C for 15 s) to exclude the nonspecific amplification and formation of primer-dimers.

For quantification of VZV genomes, the PowerUp SYBR Green Master Mix was again used with primers that amplified a 60 bp fragment of the VZV ORF49 gene (Table 2, “ORF49 (VZV genome)”). DNA isolated from cell-free VZV-pOka of known genome copy number content was used to generate a standard curve for genome number. The qPCR conditions were 50 °C for

2 min, 95 °C hot start for 5 min; 45 cycles of: 95 °C for 15 s, 58 °C for 10 s and 72 °C for 45 s. Dissociation curve analyses from 60 to 95 °C were performed as described above.

Table 2 Primers for Quantification of AAVs. For quantification of VZV genomes, the PowerUp SYBR Green Master Mix was again used with primers that amplified a 60 bp fragment of the VZV ORF49 gene (Table 2, "ORF49 (VZV genome)"). DNA isolated from cell-free VZV-pOka of known genome copy number content was used to generate a standard curve for genome number. The qPCR conditions were 50 °C for 2 min, 95 °C hot start for 5 min; 45 cycles of: 95 °C for 15 s, 58 °C for 10 s and 72 °C for 45 s. Dissociation curve analyses from 60 to 95 °C were performed as described above.

Gene	Direction	Primer Sequence (5′ → 3′)
SaCas9	L	AGAAATACGTGGCCGAACTG
	R	TCACGTAGTCGCTGGTCTTG
ORF49 (VZV genome)	F	CGGTCGAGGAGGAATCTGTG
	R	CCGTTGCACGTAACAAGCTC

3.4.5 Generation of Recombinant VZV

VZV were generated using a modified version of an established bacterial artificial chromosome (BAC) system (pOka DX), based on the VZV parental Oka strain (pOka) containing a self-excisable mini-F replicon [188], [189]. The parent BAC (pOka DXRR 57Luc-ZeoR) was partly detailed elsewhere [306], and is corrected for two nonsynonymous coding mutations in ORFs 40 and 50 that differed from the sequence of the parental pOka strain. It also contained a firefly luciferase reporter fused in-frame to the ORF57 gene using T2A ribosome skipping motif, and is expressed from the ORF57 late promoter (PRK and MBY, manuscript in preparation). The BAC was manipulated using two-step, markerless λ-Red-mediated recombination as previously described [188], [189] in the E. coli strain GS1783 (a gift from Dr. Gregory Smith, Northwestern University, Chicago, IL, USA). The GS1783 contains a cassette of L-arabinose-inducible

expression of the ISceI homing restriction enzyme and the 42 °C heat-inducible expression of the l-Red recombination genes. All PCR amplifications for cloning and recombineering were performed using high fidelity PrimeSTAR GXL polymerase (#R050B, Takara). Final manipulated BACs were evaluated by restriction fragment length polymorphism (RFLP) analyses and BACs made into viruses were sequenced across the relevant sites of insertion and/or mutagenesis.

A VZV dual reporter BAC and virus were developed in which the fluorescent mCherry reporter gene was fused to the N-terminus and in-frame with ORF23, which encodes a minor capsid protein. This was derived by PCR-amplification from the plasmid pmCherry-kan, which contained a reversable ISceI site containing a kanamycin resistance cassette (kan^r) derived from the plasmid pEPS-kan2 (a gift from Dr Gregory Smith, Northwestern University, Chicago, IL, USA). Resolving the internal kan^r cassette by inducing a further recombination concurrent with the induction of ISceI expression resulted in BACs with restored mCherry-ORF23. The VZV derived from this BAC was termed VZV DR (dual reporter) and expressed mCherry from the ORF23 promoter and luciferase from the ORF57 promoter. Then, the ORF71 coding sequence was replaced with a PCR-amplified ampicillin resistance cassette (amp^r), selecting for gain of ampicillin resistance in addition to resistance to chloramphenicol (chm^R is directed by the replicon) and zeomycin resistance (directed by a cassette inserted downstream of the luciferase at ORF57). VZV derived from this new BAC (VZV DR-Δ71) contained two quantifiable reporters and one copy of the ORF62 gene. Evaluation of virus at passage 6 by Southern blotting confirmed that the virus contained a restored ORF71 derived from ORF62 gene (VZV-DR-Δ71: data not shown). The VZV BAC DR-Δ71 was then further subjected to a recombinatorial mutation of the ORF62 gRNA-targeted sequence region to derive VZV DR-62gmut mutant BACs and viruses. Two primers were used to amplify kan^r from pEPS-kan2 (Table 3, "gRNA region primers"). These changed eleven

base pairs of the DNA sequence of ORF62 targeted by the 62-1 gRNA, without altering the encoded ORF62 amino acids (Table 3 “Wobble base pair changes”). The PCR amplified DNA was recombined into ORF62 in the BAC VZVD71, then selecting BACs for gain of kanamycin, chloramphenicol, and zeomycin resistance. RFLP was used to identify BACs and the kan^r was reversed out of the BAC by a second recombination and the induction of ISceI expression, as detailed elsewhere [188], [189]. Sequencing across the region in the BAC and of the resulting virus after passage 6 confirmed the presence of the desired engineered mutations.

Table 3 Primer Design for VZV DR-62gmut BAC Recombineering. a = 62 gRNA region primers that were used to alter the gRNA region. Uppercase non-italic letters denote bases that match sequence to that of VZV ORF62 pOka wild-type sequence; bases in italics denote sequence that recognizes the kanamycin resistance cassette for PCR amplification. Low-ercase letters represent altered bases designed to change the 62-1 gRNA recognition site. b = Wobble base pair changes that were engineered into the gRNA recognition sequence are shown for VZV DR-62mut, while the parental wild-type sequence is shown for VZV DR. The top line in each segment shows the DNA sequence and the bottom line shows the encoded amino acids as one-letter amino acids and their residue numbers in the ORF62 protein. Lower case letters indi-cate the mutated bases engineered by the primers.

Gene	Direction	
62 gRNA region primers (5′ → 3′) a	F	GTCATGGTGGGACGGGAACATGAGATCGTTTCAATTCCCagtGTcagtGGcCTgCAgCCtGAACCCAGAAGGATGACTACGATAAGTAGG
	R	TTGTGTTAGCTCTTCGCCAACATCTTCCGTTCTGGGTTCaGGcTGcAGgCCactgACactGGGAATTGAAAGGGTAATGCCAGTGTTAC
Wobble base pair changes b	VZV DR	TCC GTA TCG GGA CTT CAA CCA G → S68 V69 S70 G71 L72 Q73 P74
	VZV DR-62gmut	agt GTc agt GGc CTg CAg CCt G → S68 V69 S70 G71 L72 Q73 P74

3.4.6 Virus Derivation and Growth Curves

The virus was generated from the BACs that were just detailed after their transfection into MeWo cells, using Lipofectamine 3000 (#L3000015, Thermo Fisher Scientific) with 2.5 ug of purified BAC DNA and 100 ng each of plasmids expressing ORF61 and ORF62 DNA under the constitutive hCMV immediate-early promoter, as detailed previously [87], [178]. Upon the appearance of fluorescent plaques, infected cultures were amplified by trypsinization and replated with uninfected ARPE-19 cells until they exhibited >80% cytopathic effect. Viruses were further amplified for a minimum of six passages to self-excise the BAC replicon elements and restore ORF71. Virus stocks were generated from ARPE-19-infected cultures showing >80% cytopathic

effect, after treating cultures with 0.01 mM mitomycin C for 3–4 h. at 37 °C prior to harvesting for cryopreservation, as detailed previously [178].

Virus growth curves were determined as detailed previously [87], [178], initiating infections in confluent 6-wells with approximately 400 pfu of virus (per 0.5×10^6 cells in a single well) from cryopreserved, pre-titered, mitomycin C-treated aliquots of infected ARPE-19 cells. All assays were performed in triplicate. At the desired times after infection, infectious virus-associated cells were quantified by trypsinizing the monolayers and then seeding serial dilutions onto ARPE-19 monolayers grown in 6 wells seeded 24 h. prior and at 80% confluency. At 4–5 dpi, the formed plaques were counted under a fluorescent microscope, and averaged from the triplicate values. Titers were normalized to the exact titer of virus at day 0 determined from the inoculate and then normalized to parental virus VZV DR.

3.4.7 Neuron Cultures

Neuron cultures were prepared using a previously published protocol [182] based on the differentiation of H9 human embryonic stem cells (hESC) cultured on feeder cells for 1–2 weeks. H9 cells were then further amplified on a feeder-free platform. This used StemFlex™ medium supplemented with StemFlex™ supplement (Thermo Fisher Scientific) and antibiotic/antimycotic. Cells were grown on 6-well dishes pre-coated with GelTrex Basement Membrane Mix (#A1413302, Thermo Fisher Scientific). Colonies were passaged either by manual dissection or using ReLeSR™ Enzyme-free cell selection and passaging reagent (Stemcell Tech., Vancouver, BC, Canada), per the manufacturer's instructions. Following either method, ROCK inhibitor Y-27632 (#S1049, Selleckchem, Houston, TX, USA) was added to the culture media for 24 h. to increase cell survival and deplete dividing cells. Neural precursor cells (NPCs) were generated

from hESC by co-culture with the PA6 mouse stromal fibroblast cell line (RIKKEN BioResource Center, Tsukuba, Ibaraki Province, Japan) as detailed previously [181], [307]. For terminal differentiation, neurospheres were added to culture dishes coated sequentially with Poly-D Lysine (PDL) and GelTrex and cultured for 14 days in a Neuron Medium (Neurogenic Medium supplemented with CultureOne (#A3320201, Thermo Fisher Scientific).

For the fluorescent monitoring of VZV infections of neurons, neurospheres were seeded on coated 12-well glass bottom plates (P12-1.5P, Cellvis, Mountainview, CA, USA) and differentiated in neuron differentiation media for at least 14 days. Infections were initiated with PBS-washed, mitomycin-C treated VZV-infected ARPE-19 cells. Medium was changed the next day and every 2–3 days after. Latent infections were initiated with cell-free virus stocks of a previously detailed recombinant VZV (VZV66GFP) that expressed ORF66 as a GFP-ORF66 fusion [83], [182] Latently infected neurons were then maintained in media containing 50 μM acyclovir (ACV, #A1915, Tokyo Chemical Industry, Tokyo, Japan) to block sporadic lytic initiation events, as previously described [183]. Latent infections were monitored for at least one week after infection in the absence of ACV by fluorescent microscopy screening to remove from consideration any cultures showing breakthrough GFP expression as a marker for productive infection. For reactivation, the media was then replaced with the same media lacking ACV and NGF, but including 50 ug/mL anti-NGF (Biolegend, 617904) and 50 ng/mL 12-O-tetradecanoylphorbol-13-acetate (TPA; #1201 Tocris Biochemicals, Bristol, UK). Reactivation was monitored for 1–2 weeks by microscopic screening for GFP expression. To quantify the reactivated virus, treated neurons were dissociated by manual dislodging and trituration, then by replating dilutions of the neurons onto confluent ARPE-19 monolayers. Foci of infection were counted 4 days later, using a fluorescent microscope.

3.4.8 Fluorescent Microscopy

Live neuronal cultures were monitored using a Nikon TI fluorescent microscope with a 10× air objective (N.A. 0.30). Imaging of fixed neuron cultures followed previous detailed procedures [182], [183]. Neurons were immunocytochemically identified by chicken anti-beta tubulin III (Novus Biologicals, Moon Township, PA, USA) in 10% heat inactivated goat serum (HIGS) in PBS. Bound antibodies were detected using secondary goat anti chicken antibodies linked to AlexaFlor-594 (#A-11042, Thermo Fisher Scientific,). Cultures were then mounted in mounting media containing 4′,6-diamidino-2-phenylindole (DAPI) to stain nuclei. Images for all samples in each experiment were captured under identical acquisition settings and processed using Metamorph software (Version 7.7, Molecular Devices, San Jose, CA, USA). VZV fluorescent foci in infected epithelial cells were imaged at 4 dpi after growth at 34 °C after fixing in 4% paraformaldehyde and washed with 1xPBS. Multiple images containing entire individual foci that did not touch any borders or other plaques were acquired under identical acquisition settings with CellSens software (Olympus, Tokyo, Japan) on an Olympus IX83 microscope with a 10× (N.A.030) air objective. Data was exported and analyzed for size using Metamorph.

3.4.9 Flow Cytometry and Statistical Analyses

Flow cytometry was used to quantify GFP-fluorescent positive HEK293 cells in the initial evaluation of the efficiency of gRNAs to target genes and block protein expression. All flow cytometry samples were collected and analyzed using a BD FACSAria cytometer (Becton, Dickenson, and Co., Franklin Lakes, NJ, USA) and FlowJo software (FlowJo, Ashland, OR, USA). Statistical analyses were performed using GraphPad Prism software (GraphPad, La Jolla, CA,

USA). Where indicated, error bars represent standard deviation (SD) or standard error of the mean (SEM) as specified in the figure legends.

3.5 Results

3.5.1 Characterization of VZV-Specific gRNAs for *in-vitro* Specificity

The goal of the studies was to assess the potential of using gene editing as an anti-viral strategy targeting VZV, not only in lytic-infected cells that are permissive for VZV, but also in reactivating neuron cultures. We recently detailed a hESC-derived neuron culture system that can host a VZV model latent state that can subsequently be reactivated [183]. Gene editing has potential to target the latent genome before reactivation. Gene editing strategies targeting HSV-1 have suggested that two sites of double stranded breaks (DSBs) are more efficient in reducing the HSV genome load and progeny virus production compared to single genome DSB sites, which can repair. The latter can still be disruptive as a consequence of errors in DNA repair that result in indels in a single-copy critical gene [286], [308]. Our gRNA-based saCas9 antiviral strategy targeted duplicated essential VZV genes. Both ORF63/70 and ORF62/71 lie in the large reiterated genomic regions bounding the short unique region. This region also contains the ORF64/69 gene pair, but this pair has been shown to be dispensable for in vitro replication in culture, and in human T cells and human fetal skin that is harbored in SCID-hu mice [290]. VZV ORF 62/71 protein functions as the major transcriptional activator (transactivator) in VZV [77], while ORF63 protein has regulatory [309] and anti-apoptotic [76] activities, and ORF63 transcription is associated with

latency [157]. One report has suggested that ORF63 is not essential for VZV culture growth [310], while others report ORF63 as absolutely required for VZV replication [290].

Three gRNA candidates for each gene were selected based on an optimal on/off-target specificity, the presence of the PAM motif, and length. The appropriate hybridized oligonucleotides were then cloned into the AAV-based pX601 backbone plasmid (Table 1) co-expressing saCas9. We then conducted a preliminary study to demonstrate that each gRNA construct was able to target the respective gene. Each pX601-based plasmid or control (pUC19 and pX330-UL 3/4) plasmid was co-transfected with corresponding CMV IE promoter-driven ORF-GFP fusion constructs into HEK293 cells. We reasoned that cleavage by the targeted saCas9 should prevent translation of the protein and reduce expression of the GFP reporter, measured by flow cytometry. Comparison of the three ORF62-specific gRNA constructs revealed that each greatly reduced the expression of GFP from the CMV-62GFP reporter as compared to control plasmid co-transfected cells (Fig 6a). A similar but slightly different protocol was then used to evaluate ORF63-targeting gRNAs, in which a single set amount of CMV-ORF63-GFP fusion (500 ng) was co-transfected with control plasmids pUC19 or pX601 containing the 62-1gRNA or the 3 different 63gRNA templates (Fig 6b). All of the 63gRNA showed a reduced level of GFP expression from both ORF63 N-terminal (GFP ORF63)- or C-terminal (ORF63 GFP)- tagged expression plasmids, when compared to the non-targeting CRISPR/Cas9 constructs. Taken together, the data suggested that all gRNAs could efficiently target the respective gene. We then selected the “62-1” ORF62-targeting construct (62-1gR-saCas9) for further development.

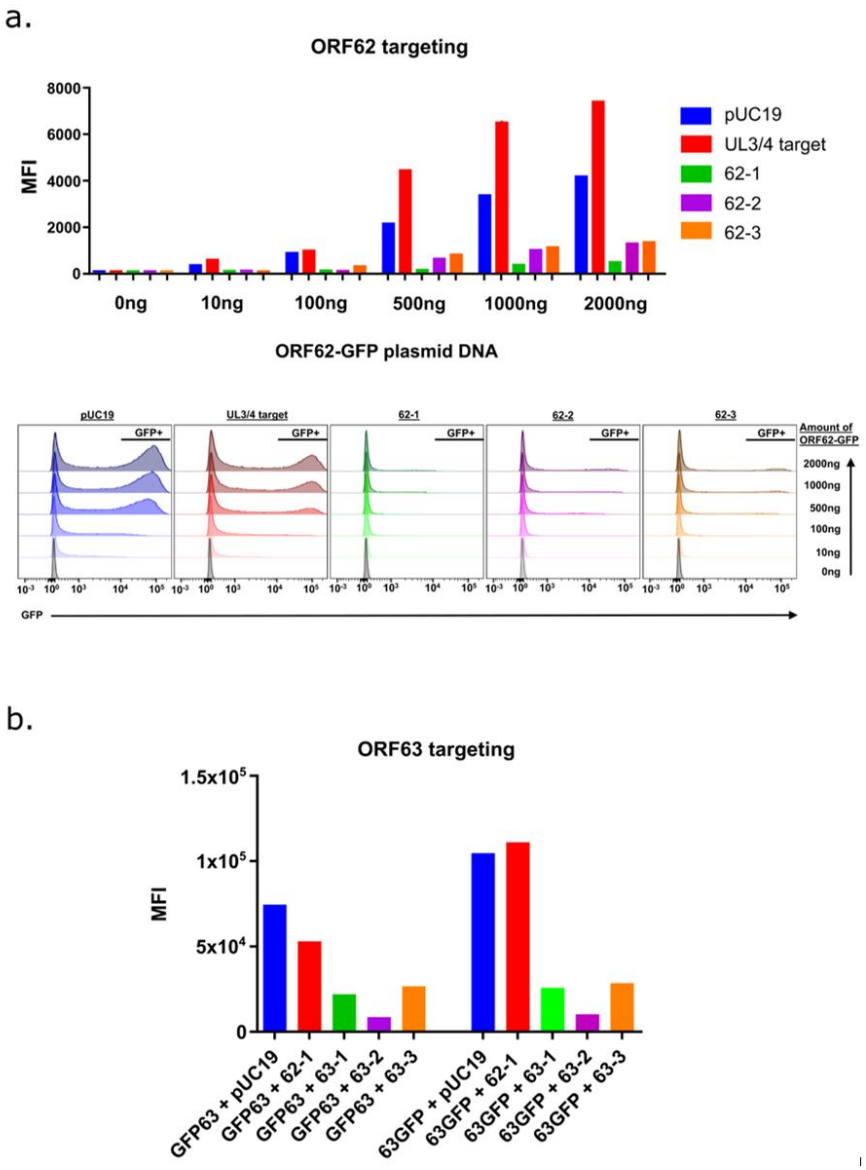

Figure 6 A preliminary study to evaluate ORF62- and ORF63-targeting gRNAs in pX601 to prevent gene expression.

(a) HEK 293 cells in 6-well plates were transfected with a range (0–2000 ng) of CMV-ORF62-GFP plasmid, along with 2 □g of plasmid pUC19; a pX330-based plasmid with a gRNA template de-rived from HSV UL3/4; or pX601 AAV plasmids containing the templates for ORF62 gRNAs 1–3, constructed as detailed in the Methods. To maintain the same level of DNA in each transfection, pUC19 was added. At 36 h post transfection, cells were harvested by trypsinization and analyzed by flow cytometry to determine the mean fluorescence intensity (MFI) for each treatment. (b) To determine the optimal gRNAs for targeting ORF63 in pX601, HEK293 cells in 6-wells were co-transfected with 500 ng of CMV-promoter-driven ORF63-GFP plasmid expressing a C-terminal tagged GFP (63GFP) or a similar plasmid-driving expression of N-terminal tagged GFP (GFP63); each with either 1500 ng of pUC19 DNA, the px601 containing the 62-1gR template, or one of three selected pX601 plasmids containing the ORF63-gR templates as detailed in Table 1. After 72 h, the cells were subject to flow cytometry and the MFI was determined using FlowJo software. The data represent the MFI of single transfections performed in parallel and were not statistically evaluated.

3.5.2 AAV Serotypes for Delivery to VZV-permissive Epithelial Cells and Human Stem Cell-derived Neurons

AAV capsid serotypes confer different tissue tropisms [311]–[314]. We considered it important to identify an AAV serotype that transduces epithelial cell lines that support VZV replication, in addition to being able to transduce hESC-derived neurons that can harbor model VZV reactivatable latent states. A preliminary study was conducted with four commercially acquired AAV neurotropic serotypes containing CAG-GFP reporters (serotypes 2, 5.2, 8.2, and 9), which have been previously exploited for murine-neuron delivery [315]. AAV 5.2 and 8.2 recombinant serotypes contain modifications of the corresponding WT serotypes that are potentially better able to escape cellular vesicles once endocytosed, avoiding lysosomal breakdown (Virovek, Hayward, CA, USA). AAV transduction with each serotype was performed at equivalent genome copy levels per cell and the transduction of MeWo and ARPE 19 cells was assessed by determining the fraction of cells showing GFP expression, using flow cytometry after 3 days incubation (Fig 7a). AAV2 appeared to be efficient in transducing both MeWo and ARPE19 cells, as GFP expression was detected in nearly 100% of the cells for both lines. Other serotypes did not result in GFP expression in the majority of cells of both lines. The ability of each serotype to transduce and express GFP in hESC-derived neurons was also confirmed. Fluorescent microscopy images (Fig 7b, enlarged in Fig 12) indicate that all four serotypes resulted in GFP expression in the hESC-derived neuron culture platform. For AAV2, the GFP intensity appeared weaker than that seen after neuron transduction with AAV5.2, but AAV5.2 appeared to transduce a lower proportion of neurons compared to AAV2. These observations are consistent with previous studies reporting the ability of AAV2 and AAV5 to transduce ARPE-19 cells [316] and murine neurons [317]. The three-dimensional nature of hESC-derived neuron cultures [182] did not permit

more accurate quantitation of neuronal transduction, but given the ability of AAV2 to efficiently transduce VZV permissive epithelial cells close to 100%, we selected AAV2 for packaging of the pX601-based vectors containing saCas9, with or without the 62-1 guide RNA.

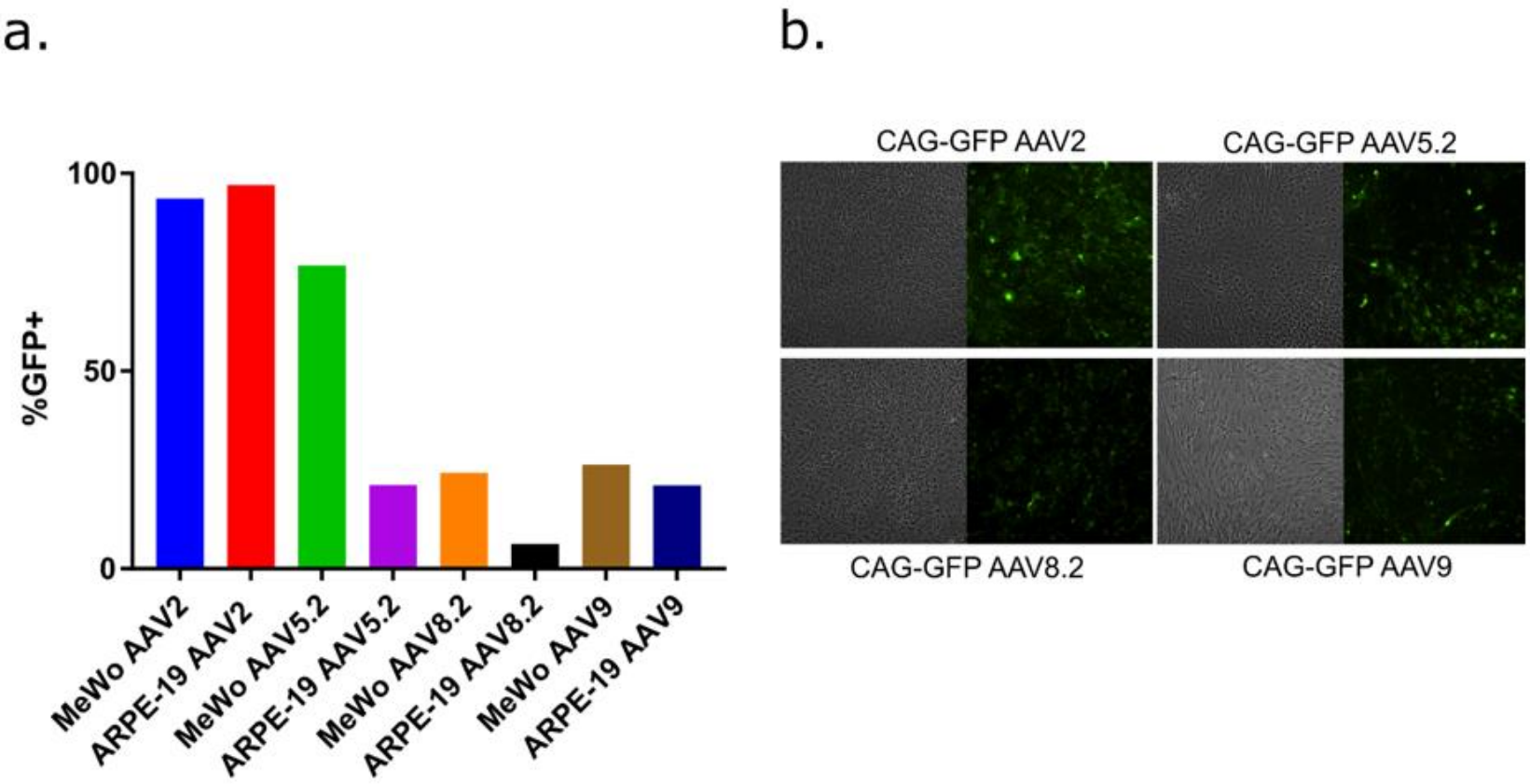

Figure 7 A preliminary study of AAV serotypes able to deliver to epithelial cells and neurons. (a) The fraction of two VZV permissive epithelial cell lines (MeWo and ARPE-19) that expressed GFP, as determined by flow cytometry, after infection with 5 µL of 1012 GC/ mL AAV per well of a 6 well plate with AAV-GFP serotypes 2, 5.2, 8.2 or 9. AAV-mediated expression was measured by flow cytometry at 3 days post transduction and is represented as a fraction of the total cell population, using gates selected by analyses of untransduced cells. Of the four serotypes evaluated on MeWo and ARPE-19 cells, AAV-2 was the most efficient at transducing both cell types to express GFP. The study represents single transductions and was not statistically evaluated. (b) To qualitatively establish the transduction of hESC-derived neurons, neurons cultured in 12-well dishes were transduced with 1.25 × 1011 GC per 12-well of each GFP-expressing AAV serotype. The AAV-mediated expression of GFP was imaged at multiple (>5) non-overlapping random positions at 6 days. Representative images are shown that reflect GFP expression in neuron cultures. Fur-ther quantification could not be determined due to the heterogeneous and three-dimensional nature of the neuron cultures.

3.5.3 AAV-62-1gR-saCas9 Reduces VZV Lytic Replication in Epithelial Cells

High-titer preparations of AAV2-packaged saCas9 with (AAV-62-1gR-saCas9) or without (AAV-saCas9) the 62-1 gRNA sequence template were obtained at more than 10^{12} GC/mL and subsequently evaluated for their ability to prophylactically reduce lytic replication in VZV-infected ARPE-19 cells. ARPE-19 were mock treated or transduced with each AAV at 10^4 GC/cell and 4 days later, cultures were infected with a low dose (500 pfu per well of a 6-well plate) of mitomycin C-treated, cell-associated VZV DR or VZV DR-Δ71 (see Methods). Southern blot analyses of DNA from VZV DR-Δ71 after 6 passages in culture established that ORF71 in the virus was restored by the reduplication of ORF62 (data not shown), as expected from similar previous mutagenic studies of ORF62 in the BAC from our group [87]. Parallel infected cultures were harvested multiple times after VZV infection and assessed for the expression of the kinetically late ORF57 promoter-expressed luciferase activity.

In ARPE-19 cells not pretreated with AAV before VZV infection, or in cells pretreated with AAV-saCas9 (no guide RNA), VZV luciferase activity reported an increase in growth of both VZV DR and VZV DR-Δ71 over time. Strikingly and in contrast, cells pretreated with 10^4 GC/cell of ORF62-targeting AAV showed a dramatic reduction in the VZV reporter activity over time as compared to untreated and AAV-saCas9 controls for both viruses. This indicated that AAV-62-1gR-saCas9 was highly effective at reducing progeny virus production (Fig 8a). The VZV derived from a BAC in which ORF71 was deleted gave very similar results to VZV DR, as expected. An assessment of viral growth visualized by mCherry expression in infected foci (Fig 8b) supported the luciferase studies, in that both focus size (Fig 8c) and the number of focus numbers at 4 dpi (Fig 8d) were vastly reduced in cells pretreated with AAV-62-1gR-saCas9, compared to controls, for both VZV DR and VZV DR-Δ71. These data indicate that the AAV-62-1gR-saCas9 blocks

lytic replication of VZV in infected epithelial cells. Furthermore, the reduction in foci numbers developing in AAV-62-1gR-saCas9 pretreated cells strongly suggests that some infected cells failed completely to initiate the productive spreading foci of infection.

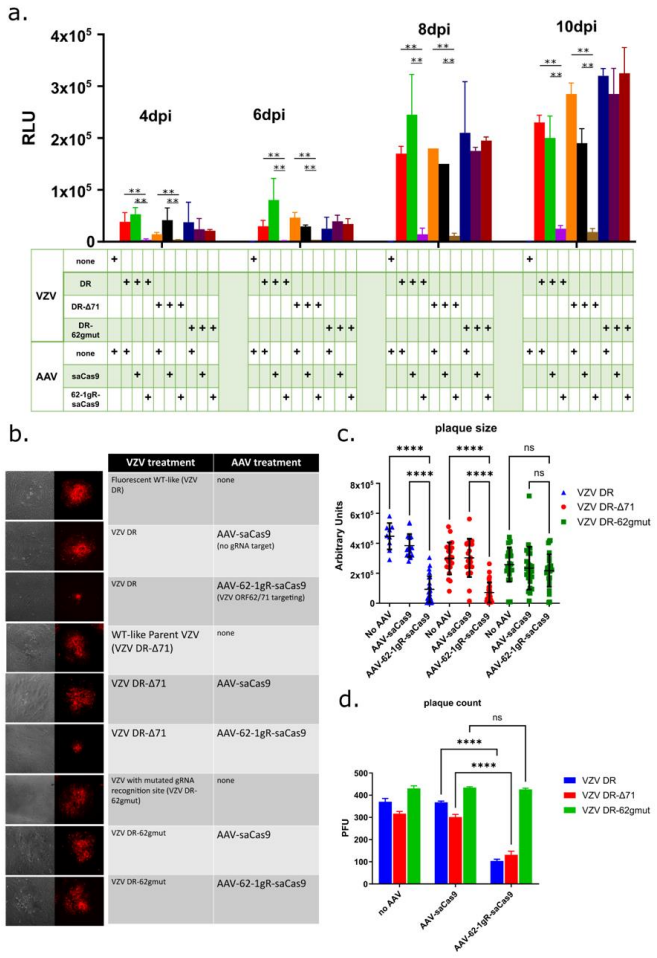

Figure 8 AAV-62-1gR-saCas9 reduces VZV productive infection in infected epithelial cells. (a) The 12-well plates of near confluent ARPE-19 cells were pre-treated with 104 GC/cell of the different AAV and at 4 days post transduction, cells were infected with 500 PFU/well of cell-associated VZV. VZV replication was measured using luciferase-reporter expression from the ORF57 gene at 4, 6, 8, and 10 days after VZV infection. Cell extracts were diluted 1000-fold prior to the assay. Significant differences between treatments, defined as $p < 0.01$ using a 2-way ANOVA with Geisser-Greenhouse's correction, are indicated by two asterisks (**). The box below the graph illustrates the components added to each condition and each condition was performed in tripli-cate. RLU = Relative Light Units (b) Representative images of infectious foci by phase-contrast imaging (first column, in gray) and by live cell fluorescence for the ORF23 promoter-driven mCherry (second column, in red) at 4 days after VZV infection in ARPE-19 cells. The boxes to the right illustrate the virus (third column) and the AAV (fourth column). (c) Quantitation of fluo-rescent focus size determined from at least 9 and less than 31 isolated, nonoverlapping foci measured for each sample condition (**= $p < 0.0001$, 1-way ANOVA with Tukey's multiple comparisons test). The average size is indicated by the horizontal bar. (d) Average visible focus counts per 6 well that were observable under 10× objective. The number of foci/well (bars repre-sent counts from triplicate wells) were clearly reduced in AAV-62-1gR-saCas9-pretreated samples infected with WT-like VZV, compared to cells infected with vectors expressing SaCas9 without guide RNA ("AAV-saCas9") (****= $p < 0.0001$, 2-way ANOVA with Tukey's multiple comparisons test). All data shown is from one of two experiments with similar results. Error bars represent STD. ns = not significant.**

The AAV-62-1gR-saCas9 was designed to specifically target VZV at the ORF62/71 gene, but a well-known issue with gene editing technologies is the possibility of off-target effects. It is conceivable that a cellular factor required for VZV replication was damaged by off-target activities that would result in similar observations to those reported above. Therefore, as an additional control, two VZV recombinants in the background of VZV DR-Δ71 were derived, in which the guide RNA target sequence was mutated at 11 bases in the codons of ORF62 (VZV DR-62gmut clones #18 and #36) that maintained the same encoded open reading frame residues for ORF62. The expectation was that the substitutions of 11 bases in the Cas9 recognition region of ORF62 would render the 62-1 gRNA no longer able to recognize and cleave at this location (Table 3). If the effect was acting though off-target activities, it would still impair the viral replication of such viruses. Growth curve analyses of the two VZV mutants after low-MOI infection of ARPE-19 monolayers indicated that the rate of luciferase expression over time was only slightly less than that of VZV DR, suggesting the silent mutation of codons might have a very minor influence on growth (Fig 9). However, testing the growth of one of these viruses (VZV DR-62gmut # 1–18) in the same conditions as those used in the experiments shown in figure 8 revealed that in AAV-62-1gR-saCas9-pretreated cells, the mutant VZV grew at rates similar to that in cells that were not AAV-pretreated or pretreated with the AAV-saCas9 control. The mutant virus did not show the dramatic reduction in luciferase activity, plaque size and plaque number as seen for the parental VZV DR and VZV DR-Δ71 viruses. These experiments strongly suggest that the reduction of VZV replication by pretreatment with AAV-62-1gR-saCas9 was a consequence of the specific targeting of VZV ORF62/71 DNA.

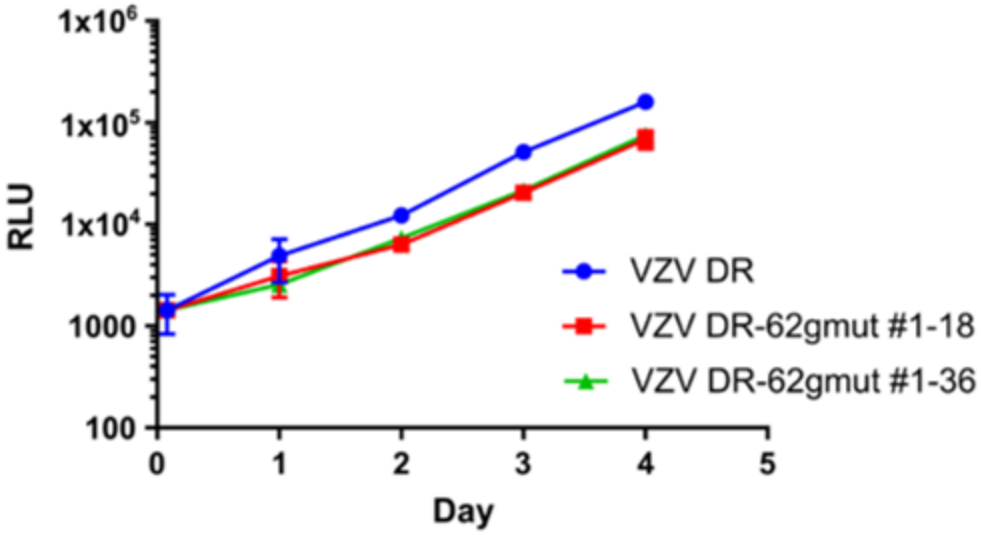

Figure 9 VZV DR-62gmut grows similarly to WT VZV. Naïve ARPE19 cells were infected with equivalent amounts of VZV-infected ARPE-19 mitomycin C treated cells, as detailed in the methods. Lucif-erase activity was measured daily. Graphs show the growth of two independently isolated clones ("#1–18" and "#1–36") of VZV DR-62gmut and VZV DR WT-like reporter virus. Each point rep-resents the average of four replicates and the data shown is representative of two independent experiments. Error bars represent STD.

3.5.4 AAV-62-1gR-saCas9 Reduces VZV Lytic Replication in hESC-Derived Human Neuron Cultures

The ability of AAV-62-1gR-saCas9 treatment to block lytic replication in hESC-derived neurons was then evaluated. We have previously shown that hESC-derived neuron cultures are able to support the spreading of productive VZV infections [22,23,81]. Neurons that were differentiated from neurospheres for 3 weeks were transduced with approximately 10^4 GC/cell of AAV or left untreated. Four days later, the cultures were infected with 500 PFU of mitotically inhibited VZV DR-infected ARPE-19 cells. Viral growth was monitored visually at the same position in the cultures by microscopy over a 10-day period, and representative live-cell images of the foci of fluorescence in the neuron cultures at day 10 post infection are shown in the first column of Fig10a. In non-AAV treated, AAV-saCas9 pre-treated and AAV-62-1gR-saCas9 pretreated

neurons infected by VZV DR-62gmut, foci of VZV infected neurons (indicated by red fluorescence) clearly developed over the 10-day incubation period (Fig 10a). However, neuron cultures treated with AAV-62-1gR-saCas9 that were infected with VZV DR or VZV DR-Δ71 developed only very small foci of red fluorescence that involved only a few neurons, far fewer than seen in the controls. This suggested the virus in this group was not able to spread and form foci as efficiently as infected neurons in wells receiving other treatments (Fig 10a). To obtain a more quantitative assessment, the infected neuron cultures at 10 dpi were dislodged, triturated, serial diluted and re-seeded onto monolayers of ARPE-19 cells. Infectious centers that formed from all non-AAV-treated or control AAV-saCas9-pretreated neurons after 5 days were approximately the same size, as were the infectious centers formed from AAV-62-1gR-saCas9 pretreated cultures infected with VZV DR-62gmut virus. However, plaques formed on ARPE-19 cells co-cultured with neurons that were infected with VZV DR or VZV DR-Δ71 after pretreatment with AAV-62-1gR-saCas9 were not only dramatically reduced in number, but at the highest concentration of neurons seeded onto ARPE-19 monolayers, only tiny foci of infection involving a few fluorescent cells were seen. No wildtype-sized plaques developed after neuron seeding on ARPE-19 under these conditions. Even taking such small foci of infection as positive, the number of infectious centers for VZV DR and VZV DR-Δ71 on neurons pretreated with AAV-62-1gR-saCas9 were more than a hundred-fold fewer compared to the non AAV-treated, mock AAV-treated, or VZV DR-62gmut-infected controls (Fig 10b). The strikingly reduced size of the plaques formed by progeny virus after AAV-62-1gR-saCas9 treatment suggested that virus produced from treated neurons was unable to replicate to wild type levels. These results strongly suggest that AAV-62-1gR-saCas9 pretreatment not only efficiently reduces the production of the progeny virus

in infected neurons but also, when virus is produced, it is damaged and severely impaired for further replication.

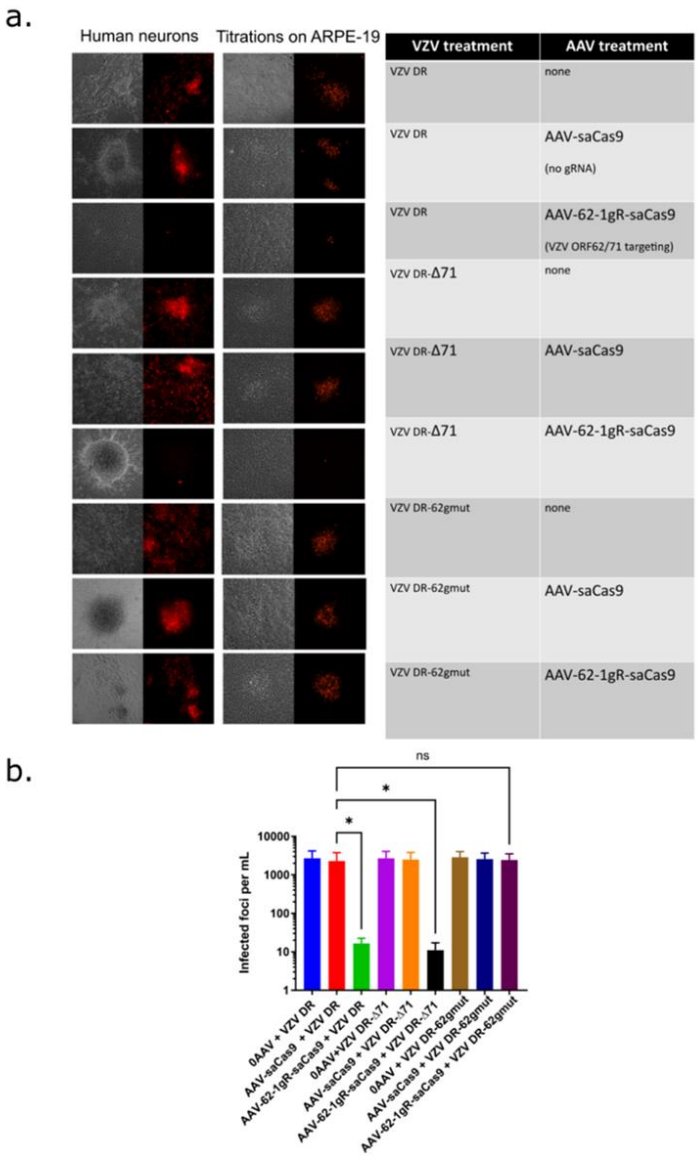

Figure 10 Pretreatment with AAV-62-1gR-saCas9 knockdown of VZV lytic replication in exogenously in-fected human neuron cultures. (a) The 12-well plates of hESC neuron cultures were transduced with 104 GC/cell of AAV-62-1gR-saCas9 constructs/well. Four days later, neurons were infected with 500 PFU of mitotically inhibited fluorescent (red)-cell associated VZV-infected cells to initiate lytic infections. Infections were subsequently monitored by fluorescence microscopy and repre-sentative images of mCherry reporter expression of infected cells and the same fields observed by phase contrast microscopy were acquired 10 days after VZV infection. (b) After imaging, duplicate infected neuron cultures were scraped, triturated, and then seeded onto confluent ARPE-19 cells to quantify the number of VZV-infected neurons by the number of infectious foci they generated. Foci were counted after 5 days. Representative images of foci formed on ARPE-19 at day 5 from virus obtained from the treated neuron cultures are shown in column 2 of Figure 5a. Data rep-resents quadruplicate measurements and significant differences between treatments depicted by asterisks (*= $p < 0.01$, ordinary one-way ANOVA with multiple comparisons; ns=not significant). Similar results were obtained in two independent experiments. Error bars depict the STD.

3.5.5 AAV-62-1gR-saCas9 Reduces VZV Replication Following Reactivation in Model Latently Infected Neuron Cultures

A goal of VZV targeting by gene editing is to reduce the capacity of latent genomes to reactivate and induce zoster disease, not only by reducing spread at the periphery, but also in the ganglia, to reduce its intra-ganglionic spread after a reactivation event has initiated. Even without complete elimination of reactivation, a reduction of lytic replication in the ganglia could potentially limit sensory damage caused by VZV reactivation. The hESC neuron cultures used here have been shown to support a latent VZV infection (defined by the prolonged absence of any indicators of productive infection and lytic gene reporter expression), which can then be experimentally reactivated (to renew lytic reporter gene expression and produce virus that spreads to other neurons) [183]. We thus explored the potential of AAV-62-1gR-saCas9 as a treatment for preventing VZV reactivation and subsequent replication. Latent infections were established by exposing neuron cultures to cell-free virus of a previously characterized recombinant VZV that expresses GFP linked to ORF66 (VZV66GFP), and then incubated in the presence of 50 uM acyclovir (ACV) to inhibit lytic replication for 7 days. Cultures were then incubated for 7 days in the absence of ACV. None of the cultures contained GFP fluorescence indicating lytic infection. Cultures containing latently infected neurons were then transduced with approximately 10^4 GC/cell AAV or mock transduced, and then incubated in media without ACV. At 7 days post AAV transduction, GFP positive cells were again not observed, indicating that the AAV transduction itself did not induce VZV reactivation. A set of cultures was reactivated by treating with a combination of NGF withdrawal, antibody-mediated NGF depletion and the addition of 50 ng/mL 12-O-tetradecanoylphorbol-13-acetate (TPA), and cultures were monitored daily for GFP

fluorescence indicating reactivation events for 7 days. After imaging, the neurons were dislodged, triturated, and seeded onto confluent ARPE-19 cells for infectious center assay (Fig 11b).

None of the neuron cultures latently infected with VZV66GFP and not subjected to reactivation stimuli expressed GFP. When such neurons were seeded on ARPE19 cells, infectious centers did not form. In contrast, the latently infected neurons receiving the reactivation stimulus developed numerous GFP-positive foci and formed multiple infectious centers when seeded onto ARPE-19 monolayers, indicating that productive reactivation had occurred (Fig 11a and Fig 13). Latently infected neurons treated with AAV-saCas9 without guide RNA before receiving the reactivation stimulus also developed multiple GFP positive plaques in the neuronal cultures and generated infectious foci on ARPE-19 cells. Importantly, in latently infected cultures pretreated with AAV-62-1gR-saCas9 prior to receiving a reactivation stimulus, there were no visible GFP positive centers of infection forming, even at 7–10 days post stimulus. Subsequent seeding of these neurons onto ARPE-19 cells did result in the formation of a few small GFP positive foci, but these were significantly fewer and considerably smaller in size (Fig 11a, second column; enlarged in Fig 13). These data indicate that reactivation events were not completely prevented and virus still formed after treatment with AAV-62-1gR-saCas9, the AAV treatment greatly reduced the number of infectious progenies after reactivation induction.

To investigate whether the reduction in the number of productively infected neurons in reactivated cultures pre-treated with AAV-62-1gR-saCas9 was due to a reduction in the number reactivating genomes or a result of reduction of viral spread to additional neurons, SYBR-based qPCR quantification of VZV genomes was performed. There was an increase of more than 10-fold in genome copies at 21 days-post VZV infection in reactivated samples with or without AAV pretreatment compared to neurons not receiving a reactivation stimulus. While AAV-62-1gR-

saCas9 pretreatment resulted in a significantly reduced level of genomes as compared to controls, levels of genomes measured were still higher than those seen in latently infected cultures not receiving any reactivation stimulus (Fig 11b,c). These data indicate that AAV-62-1gR-saCas9 pretreatment effectively reduced the viral burden after reactivation, but did not indicate if the latent genome load was reduced by the treatment. Thus, AAV-CRISPR/Cas9 strategy for targeting duplicated VZV genes is clearly an effective antiviral approach, greatly reducing the production of progeny by damaging genomes.

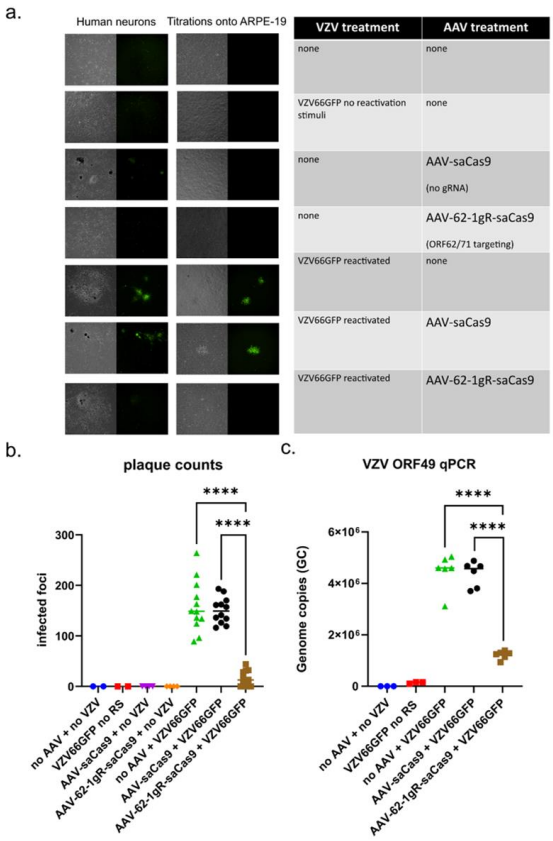

Figure 11 AAV-62-1gR-saCas9 treatment of latently infected neurons reduces VZV progeny and spread following reactivation induction. hESC-derived neurons in 12-well plates were infected with 500 PFU of cell-free virus expressing GFP (VZV ORF66 GFP) in the presence of 50 µM acyclovir (ACV) to establish latent infections. After 7 days in the presence of ACV, approximately 104 GC/cell of different AAV (or mock transduction) was added to the appropriate wells. ACV was then removed, and cultures incubated for a further 7 days. At 7-day post AAV transduction, GFP-negative neuron wells were left untreated or were stimulated to reactivate latent genomes by changing to neuron growth media lacking NGF and containing 50 □g/mL anti-NGF and 50 ng/mL TPA. Reactivation was then monitored by fluorescent microscopy and the representative images of the cultures were acquired at 7 days after the reactivation stimulus. Neurons were then scraped, triturated, and seeded onto ARPE-19 cells not treated with AAV, and infectious centers forming on ARPE-19 monolayers at 4 days from each of the experimental conditions were imaged (last two columns). (b) The number of foci forming on ARPE-19 monolayers in each 12-well plate were then counted and are shown as plaque-forming units. Each point represents the count from equal proportions of individual neuron cultures (**=p < 0.0001, ordinary one-way ANOVA with multiple comparisons). (c) DNA was extracted from 1/3 of each neuron culture treated under the different conditions, and VZV DNA was quantified using a SYBR-based qPCR using primers against a region of VZV ORF49 (Table 2). Copy number values were determined by comparison to a standard curve determined using known concentrations of VZV genomes (with a range of 101–107 genome copies). Data is representative of results from two independent experiments with similar results. RS = reactivation stimuli.**

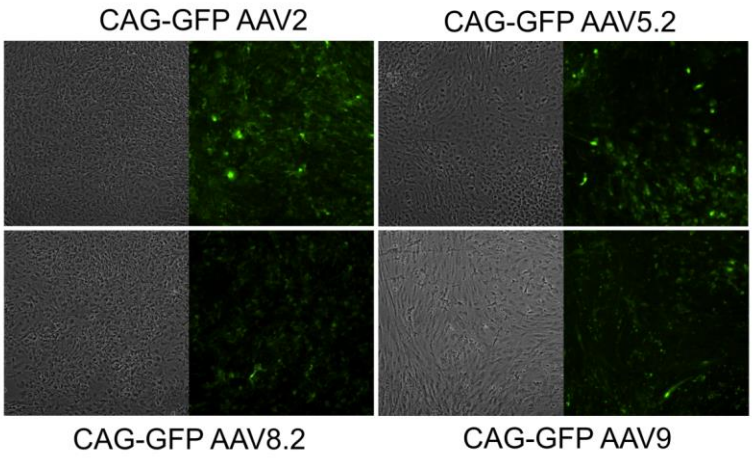

Figure 12 Enlargement of figure 7b

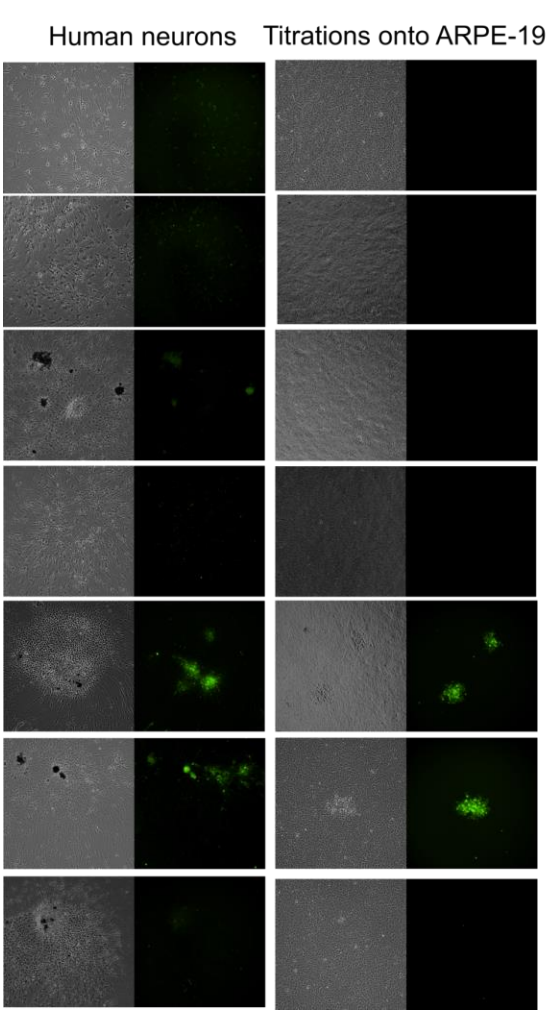

VZV treatment	AAV treatment
none	none
VZV66GFP no reactivation stimuli	none
none	AAV-saCas9 (no gRNA)
none	AAV-62-1gR-saCas9
VZV66GFP reactivated	none
VZV66GFP reactivated	AAV-saCas9
VZV66GFP reactivated	AAV-62-1gR-saCas9

Figure 13 Enlargement of figure 11a

3.6 Discussion

The goal of this study was to establish proof of principle that the CRISPR targeting of VZV genomes could be used as an antiviral strategy eventually leading to therapeutic applications. The results obtained here add to a growing body of knowledge in which several human DNA viruses (and RNA viruses with DNA genome intermediates) have been targeted by gene editing [31,33,57,82–84]. While gene editing can be performed with designer meganucleases and transcription factor-like endonucleases (TALENS), the complexity of their design and expense of their generation has made the more simple and widely available RNA-guided CRISPR/Cas technology more attractive. CRISPR/Cas also has the advantage that multiple sites on the viral genome can be targeted by increasing the number of gRNAs, rather than needing to express two or more enzymes. CRISPR-based genome editing been used to target viruses including hepatitis B virus (HBV) [322], [323], human immunodeficiency virus (HIV) [324], [325], and several herpesviruses [326] such as EBV [327], CMV [328], Kaposi's Sarcoma Virus [329], and HSV-1 [255], [258], [286]. In the case of EBV, antiviral gene editing has targeted both the viral genome [327] as well as key cellular components required for EBV replication [330]. To our knowledge, CRISPR/Cas-mediated antiviral targeting has not yet been applied to VZV, although it has been used as a research tool to generate recombinant VZV [331].

Here, we demonstrated efficient antiviral activity using AAV-delivered gRNA targeting a duplicated gene to reduce VZV replication, spread and virus production in both lytic-infected epithelial cells and hESC derived neurons. Importantly, we further showed that it dramatically reduced viral replication upon reactivation from latency in vitro. Duplicated genes were targeted because of the increase in frequency of cleavage events as well as the potential to result in the division of the genome into two segments, each incapable of replicating if both cuts occurred in

the same genome. This strategy eliminates the need for two separate vectors targeting unique region genes in order to generate dual-cleaved genomes, as performed in the study of Aubert et al., who showed that cleavage of the related HSV genome at two sites was more effective at reducing reactivation frequency than a single cleavage event [286]. Aubert et al. used two designer meganucleases to target different sites in HSV-1 that required simultaneous delivery by two different vectors and targeted duplicated genes in the repeated regions of the HSV genome. However, even with single cleavage events, error-prone DNA repair mechanisms that mutate the VZV ORF62 gene appear to reduce progeny viral replication due to the critical roles of IE62 in expression [256].

An important aspect of developing therapies from CRISPR/Cas enzymes is achieving an efficient delivery of the required gRNA and enzymes to the appropriate cell types. This is especially challenging for VZV, where the reservoir of latent viral genomes resides in ganglionic neurons throughout the peripheral nervous system. Therefore, the first steps in this project were to optimize the delivery of these molecules with a focus on human neurons. While both lentiviruses and AAV have been exploited for efficient gene delivery, current AAV vectors have the advantage in that they show little or no integration into the host genome [332]. However, the gene-packaging limits of AAV necessitate the use of smaller gene-editing enzymes, since the widely used Streptococcus pyogenes CRISPR/Cas9 is above the normal AAV packaging limit. Many smaller alternatives have recently been overviewed [333] and the Staphylococcus aureus CRISPR/Cas9 was chosen for its reported higher specificity, lower off-target activity in mouse neuroblastoma and liver cell lines [287], and the fact that it is within the packaging limits of AAV vectors [288]. Surveying four different AAV serotypes that have been shown to be neurotropic revealed that AAV2 efficiently delivered GFP to both hESC-derived neurons and two VZV-permissive

epithelial cell lines. While we only tested four serotypes, it is possible that other serotypes could be found to improve transduction or decrease the number of AAV required. We do note, however, that AAV2 is one of the most commonly used and tested serotypes used in human studies and has been applied for gene delivery to repair multiple genetic diseases, some of which are now being evaluated in clinical trials [334], [335].

Our studies show that delivering AAV-62-1gR-saCas9 decreased VZV progeny infectivity dramatically in both epithelial cells and hESC-derived neurons, compared in no AAV and no gRNA ("AAV-saCas9") controls. This was shown by the reduction of both progeny-virus plaque size and numbers. Intriguingly, VZV that survived AAV-62-1gR-saCas9 treatment generated significantly smaller plaques when seeded onto naïve VZV-permissive cells, particularly VZV derived from AAV-targeted neurons. This strongly suggests that the virus produced in AAV-62-1gR-saCas9-treated cells is damaged, most likely as a result of genome cleavage and error-prone DNA repair, resulting in indels from the activation of the dsDNA damage response. Given that ORF62 is an essential gene whose expression is required for the expression of most other VZV genes, we postulate that some of the still-replicating but impaired viruses in these plaques are damaged but still have ORF62 in frame that permits expression of an ORF62 protein with some functional mutations. The site of the gRNA target in region 1 of ORF62/71 is that which the Cas9 acted upon, because VZV with mutations in that region ("VZV DR-62gmut") showed only a minor loss of replication efficiency compared to the parental strain, but were completely resistant to pretreatment with AAV-62-1gR-saCas9. This establishes that the Cas9 did not influence VZV replication because of off-targeting of the host genome, although we cannot exclude that off-targeting effects might have also occurred that did not affect VZV replication.

One of the exciting potential applications of gene editing as an antiviral strategy is that it cannot only target productive replication of the virus, but can also damage the latent genomes and potentially prevent reactivation [326]. Treatment of latently infected and reactivated cultures of hESC derived neurons [183] with AAV-62-1gR-saCas9 resulted in greatly decreased spread of reactivation foci compared to controls. The number and size of foci that developed from reactivated neurons seeded onto ARPE-19 from AAV-62-1gR-saCas9-treated reactivated cultures also significantly decreased. Results from quantitative PCR measuring genome copies in the reactivated neurons revealed that treatment with AAV-62-1gR-saCas9 reduced replication but did not indicate a reduction of the genome load. Taken together, these results suggest that AAV-62-1gR-saCas9, in addition to reducing the viral load in lytic/productively infected cells, is an effective strategy to reduce replication in reactivated neurons. Of note, we have not yet been able to demonstrate whether latent genomes were cleaved by the targeting AAV-62-1gR-saCas9. We did not observe a loss of genome numbers in latently infected neurons after AAV-62-1gR-saCas9 treatment, but this may be a technical issue due to the very low levels of latent VZV DNA in neuronal cultures, which were insufficient to detect a significant change resulting from CRISPR/Cas9 treatment. A recent report found that gene editing of lytic HSV-1 is efficient but the editing of the chromatin-silenced latent genome required the expression of ICP0. Furthermore, ICP0 is known to alter protective chromatin, which may block the latent genome from being accessed by gene editors [320]. Similar strategies to target HSV-latent and lytic replicating genomes in an in vivo murine model of latency showed statistically significant but relatively minor reductions in the latent genome load, and also suggested relatively poor activities of CRISPR/Cas9 compared to meganuclease-mediated targeting [31,33,57,69,83]. A future possibility would be to evaluate the targeting of ORF62 by a designer meganuclease and to determine if it is more effective

than the CRISPR/Cas9 strategy. However, we feel that a better direction would be to seek improvement in targeting by expressing multiple gRNAs to additional viral targets simultaneously with the single CRISPR/Cas9 nuclease.

The results presented here demonstrate the potential of the CRISPR/Cas9 strategy to reduce both epithelial manifestations of the reactivated disease and potential damage in the ganglia that could result from ganglionic spread after a reactivation event has initiated. Of course, much remains to be worked out in translating this approach to prevent zoster and VZV disease as a therapy. A possible initial application of AAV-mediated gene editing as an antiviral strategy could be for VZV-induced retinal diseases. The retina has been a prime target for advancing AAV-mediated gene therapy strategies, and there are promising results from both animal models and human studies that AAV-mediated delivery can restore vision loss for specific inherited defects [336]. VZV replication in the retinal tissues is known to result in rare but devastating blinding diseases such as peripheral outer retinal necrosis (PORN), acute retinal necrosis (ARN) and chorioretinitis [337]. It is not uncommon for these patients to respond poorly to classic antiviral therapies, because of delayed diagnoses and/or antiviral resistance [338]. We speculate that AAV-mediated antiviral gene editing in the eye following intravitreal delivery could be an alternative treatment strategy to prevent VZV-induced retinal damage. Future work in the treatment of zoster and other VZV diseases will require additional optimization for in vivo delivery as well as the early detection of triggered VZV reactivation events in vitro, neither of which have been well-addressed for CRISPR/Cas9 therapy for other herpesviruses to date. In addition, there is a need to overcome the host antiviral immune response to AAV vectors, since clinical trials have demonstrated that this can prevent the long-term use and expression of AAV-delivered genes [339]. There remains a need for antivirals to zoster, because some studies suggest that zoster is

showing increased incidence longitudinally in populations under 50 that are not yet eligible for immunization with the zoster vaccines [340]. Nevertheless, these results serve as an important proof-of-principle of the CRISPR/Cas9 approach for treatment of a widespread and painful human disease for which there are currently few therapeutic options.

4.0 Roles of ORFs 10 and 62 proteins in Neuronal Replication

This chapter was adapted from the submitted manuscript, "Human Neuron-Specific Contribution to Varicella Zoster Virus Productive Replication by Virion-Associated Transactivator Proteins from Open Reading Frames (ORF) 62 and 10," authored by Betty W. Wu, Michael B. Yee, Kira L. Lathrop, Ronald S. Goldstein, and Paul R. Kinchington. It was written by BWW and PRK and edited by BWW, PRK, MBY, KLL, and RSG. All data in this section was collected, analyzed, and curated by BWW, MBY, KLL, RSG, and PRK.

4.1 Project Summary

The herpesvirus tegument contains premade viral (and some host) proteins that facilitate initiation of lytic infections. A well-studied example is the essential herpes simplex virus (HSV) tegument VP16, which recruits host factors to promote IE gene transcription. It may facilitate full viral exit from neuronal latency. The varicella zoster virus (VZV) ortholog of HSV VP16 (VZV ORF10) is dispensable for virus replication in cell culture. However, VZV virions contain high levels of a second transactivator, encoded by ORF62 (IE62 protein; orthologous to HSV ICP4). We postulated that the non-essential nature of ORF10 is due to overlapping functions mediated by virion IE62 (vIE62). To examine this, we developed recombinant VZV lacking one or both virion transactivators and characterized replication in epithelial cell and human neuron models of infection. VZV deleted for ORF10 replicated efficiently in epithelial cells and human embryonic

stem cell (hESC)-derived neurons at rates similar to wild-type, and initiated lytic infections of neurons after axonal infection in compartmented culture systems. A 62-S686A mutation in ORF62 abrogates IE62 distribution to the cytoplasm and its virion incorporation. Such virus is marginally growth-impaired in epithelial cell cultures, but was found to be severely impaired for replication and spread in neuronal cultures. Intriguingly, VZV deleted for ORF10 and simultaneously containing 62-S686A replicated and spread very efficiently in epithelial cells and neurons. While IE62 in this virus remained completely nuclear distributed, analyses of partially purified virions indicated that they were nevertheless associated with vIE62. We conclude that virion IE62 is important for efficient VZV growth in cultured neurons, but that co-deletion of ORF10 results in an unexpected compensatory mechanism to associate IE62 with virions, independent of IE62 cytoplasmic accumulation.

4.2 Importance

The incoming infecting virion has premade proteins that generally adapts the host cell to infection and favor initiation of viral growth. Purified VZV virions contain abundant levels of two transcription-activating proteins that were hypothesized to have overlapping functions. We tested this by making virus that were expected to lack one or both proteins in the virion. Our data indicate that the VZV lacking virion IE62 was severely impaired for replication in human neurons. However, simultaneous deletion of another virion transactivator resulted in compensatory mechanisms to still incorporate IE62 into the virion and replicate more efficiently in neurons. This work suggest that inclusion of virion IE62 or ORF10 is needed for efficient infection of neurons.

4.3 Introduction

Varicella-zoster virus (VZV) is the neurotropic alphaherpesvirus responsible for varicella (chickenpox) upon a primary infection, and herpes zoster (shingles), when virus reactivates from a neuronal latent state that was established in the host ganglia during the primary infection [146]. Zoster remains an important public health concern, affecting more than one-third of individuals in their lifetimes, with incidence increasing with age and immune decline. Zoster is frequently complicated by difficult-to-treat acute and chronic pain states, as well as other neurological and vascular sequelae [266]–[268]. While the incidence and severity of zoster can be reduced by using FDA-approved zoster vaccines to boost immunity, vaccine coverage is far from optimal in the target populations and is not used by many countries, so zoster remains a common affliction worldwide [240], [270]–[272], [341], [342]. The VZV latent state is refractory to current antivirals and most adults over age 30 years in the USA still harbor latent wild-type VZV strains with the potential to reactivate. A better understanding of factors underlying neuronal spread, latency and reactivation is still needed.

A critical component driving the typically dermatome-restricted lesions of zoster is intra-ganglionic lytic spread of virus following reactivation. Such spread results in the infection of multiple neurons of one (or a few) host ganglia that then orchestrate VZV delivery to multiple peripheral sites innervated by the reactivating ganglion [279]. While factors involved in neuron-to-neuron spread are important to identify, VZV-neuron interactions were difficult to study until recently, because the high host-specificity of VZV precluded use of most small animal models for VZV ganglionic infection [149], [285]. The closely related but distinct simian varicella virus (SVV) in natural species can be used to gain insights into VZV [343], but it is a distinct virus. Some insights developed from infection of human fetal dorsal root ganglia harbored in severe

compromised immune deficient (SCID-hu) mice [194], [279]. However, the development of human cultured human neuron platforms has made VZV-neuron interaction studies more accessible. We [182], [183] and others [157], [179] have exploited human embryonic stem cell (hESC)- or induced pluripotent (iPSC)-derived stem cells to derive neuron cultures to host productive VZV lytic neuronal infections. Indeed, they have allowed aspects of neuron-to-neuron spread to be modeled, including axon transport of virus and latent states from which experimental reactivation can be stimulated to yield renewed virus production [111], [231], [285], [344].

Here, we used the hESC-derived neuron model to explore roles of two VZV tegument proteins with the ability to actively promote viral transcription. The herpesvirus tegument is located between the DNA-containing nucleocapsid and the outer lipid-glycoprotein-studded envelope and contains some 20-30 viral (and some host) proteins that are delivered to the newly infected cell upon virus entry. They generally function to adapt the host cell to favor a productive infection and counteract innate and intrinsic cellular responses [52]. They also have roles in transport of the capsid to the nucleus [345], [346], shut-down of host transcription [347], and virus assembly and egress [348]. Tegument proteins also facilitate the transcription of the first viral genes to be expressed from the released genome in newly infected cells. A well-characterized example is HSV-1 VP16, which interacts with the host factors HCF-1, Oct1 DNA binding protein, and histone demethylases, recruiting them to specific elements in the immediate early gene promoters known as “TAATGARAT” motifs to promote IE gene transcription in the absence of de novo protein synthesis [112], [349]–[351]. VP16 is critical in the assembly of the HSV tegument [352]. While VP16 activation of IE promoters is not absolutely required for lytic infection at higher multiplicities of infection (MOI), it has more importance at lower MOI [353] and in modulating the chromatin architecture [354]. Recent studies have indicated that VP16 transactivation of IE

genes play a key role in virus reactivation from latency and the transition to full lytic replication in a two-phase reactivation process [102], [103], [106]. Specifically, VP16 mediates the transition from an unregulated temporary release of viral gene repression from the latent genome (phase I reactivation, or animation), to a classical virus-regulated (Phase II) expression pattern to produce virions [102], [103]. HSV axonal infections have been shown to favor latency [104], possibly as a consequence of the differential transport of outer tegument proteins (like VP16) and nucleocapsids after they dissemble from the nucleocapsid near the distal axon site of infection [104]–[106], [355]. The poor delivery to the neuronal nucleus may favor intrinsic default association of repressive chromatin with the genome [355]. For VZV, tegument proteins are less well-characterized than those of HSV, but data suggests some differences between the proteins in these two related viruses. VZV virions contain abundant levels of at least two known transcriptional transactivating proteins, encoded by ORF10 (HSV VP16 homolog) and the duplicated ORF62/71 genes (that encode IE62), which is the HSV ICP4 homolog [22], [54]. VZV ORF10 protein stimulates transcription of genes containing TAATGARAT elements [90], [101], [356], but is not required for growth in epithelial cell cultures [88]. However, loss of ORF10 expression greatly impairs VZV replication in organized skin grafted into SCID-hu mice [55], [88], [89], [97]). VZV IE62 is essential for VZV and shares functions with ICP4 that are sufficient for VZV IE62 to replace ICP4 in the HSV genome and lead to some virus production [292], [293]. IE62 is driven by a promoter that contains TAATGARAT elements through which ORF10 and VP16 can transactivate its transcription [54], [77]. IE62 also enhances the infectivity of transfected VZV DNA [77]. Intriguingly, VZV virions contain abundant levels of IE62 protein in the tegument (referred to hereafter as “vIE62” [54]), while HSV ICP4 is a relatively minor protein in the HSV virion tegument [357]. Virion incorporation of IE62 has been shown to require its accumulation in cytoplasmic compartments,

which is mediated by the activity of the ORF66 protein kinase [87]. ORF66 specifically targets ORF62 residue S686 adjacent to the nuclear import signal, which suppresses IE62 nuclear import and leads to its abundant cytoplasmic accumulation late in infection [83]. VZV lacking vIE62 can be generated by either deleting the ORF66 protein kinase, or by rendering S686 unable to be phosphorylated. However, both such VZV are viable in epithelial cell culture, contain IE62 protein that remains completely nuclear throughout infection, and demonstrate only marginal growth impairment in cell models.

We [83], [87], [358] have speculated that VZV lacking ORF 10 or vIE62 are viable because the two virion transactivators may have redundant functions in promoting new virus transcription upon infection. Neither virus has, to our knowledge, been examined for growth in neuron models. To examine this, recombinant VZV mutants were developed with a deleted ORF10 gene and/or with ORF62 containing the 62-S686A point mutation (that prevents vIE62 cytoplasmic accumulation and virion incorporation [83], [87]). Unexpectedly, VZV lacking both transactivators was viable, and showed near-wildtype growth, However, VZV lacking only vIE62 showed considerable growth impairment on hESC neurons that was not seen for the double mutant. The apparent restoration of growth with sequential deletion of ORF 10 in the VZV containing 62-S686A could be partially explained by an unexpected compensatory mechanism to incorporate vIE62 that was independent of the accumulation of cytoplasmic IE62, shown previously to be important for virion incorporation. Taken together, this data suggests that virion IE62 facilitates efficient neuronal infection and spread during VZV infections, but that unexpected compensatory mechanisms develop to incorporate IE62 into virions when ORF10 is also deleted, that do not require the accumulation of IE62 cytoplasmic forms in infected cells.

4.4 Materials and Methods

4.4.1 Cells

All cell lines used were commercially purchased from ATCC (Manassas, VA, USA) except the hESC line Wa09, which were acquired from WiCell (Madison, WI, USA). All culture reagents were acquired from Thermo Fisher Scientific (Waltham, MA, USA), unless otherwise stated. Human melanoma (MeWo) cells (HTB65, ATCC), Retinal pigmented epithelial ARPE-19 cells (CRL2302, ATCC), and human telomerase (hTERT) immortalized RPE (hTRPE; CRL4000, ATCC) cells were grown in Dulbecco's Minimal Essential Media (DMEM, Gibco 10569-010) supplemented with 10% fetal bovine serum (FBS, S11150, R&D Systems, Minneapolis, MN, USA) and an antibiotic/antimycotic solution (ABL02, Caisson, Smithfield, UT, USA) containing final concentrations of 100 units/mL penicillin, 100 mg/mL streptomycin and 0.25 mg/mL amphotericin B.

4.4.2 VZV

Cell-associated VZV stocks were made after mitomycin C treatment as previously described [265], [299]. Briefly, infected monolayers of ARPE-19 cells at ~70% cytopathic effect (CPE) or >90% fluorescence were incubated in media containing 0.01 mM mitomycin C (A4452, Apex Bio, Houston, TX, USA) for 3-4h at 34^{o}C. Cells were washed twice with 1x phosphate-buffered saline (PBS), trypsinized and resuspended in cell freeze media (DMEM with 20% FBS and 10% Dimethyl sulfoxide: DMSO), aliquoted and slow frozen to -80°C and then stored in liquid nitrogen. Aliquots were titrated to determine infectivity. Cell-free VZV was prepared as detailed

previously from infected ARPE19 monolayers at 1-3 days post infection [300]. Briefly, PBS washed infected ARPE-19 cells were scraped into ice cold PBS-sucrose-glutamate-serum (PSGC) buffer, lysed by rapid freeze-thaw x3 and then sonicated in an ice cooled bath sonicator (Misonix, Farmingdale, NY, USA) for 3 2min periods with 30s intervals on ice. Nuclei were removed by centrifuging at 3,000*x*g for 15min at 4°C and the supernatant combined with 1/3rd volume of Lenti-X concentrator at 4ºC (631232, Takara, Kusatsu, Shiga, Japan). The pellet obtained from centrifuging at 1,500*x*g for 45min at 4°C was resuspended into 1/50th of the initial PSGC volume at 4ºC, aliquoted and stored in liquid nitrogen. Infectious titer was determined from a thawed aliquot.

Recombinant VZV were generated using a self-excisable bacterial artificial chromosome (BAC) containing the genome of VZV parental Oka (pOka) detailed previously [188], [189] (see below), that had been corrected for two spurious mutations (Lloyd et al 2022, manuscript submitted). VZV was derived from manipulated BACs in transfected MeWo or hTRPE cells using Lipofectamine 3000 (L3000015, Thermo Fisher) as detailed previously [178], [265]. Virus was passed for at least 6 passes to allow self-excision of the BAC replicon prior to amplification for the generation of infected stocks ARPE-19 cells.

4.4.3 Generation of recombinant VZV BACs

Several recombinant viruses were generated for these studies, and their derivation is graphically represented in Figure 14. Manipulation of a VZV BAC used a two-step markerless l Red-mediated recombination method previously described [188], [189], using the bacterial strain E. coli GS1783 (a kind gift from Dr. Gregory Smith, Northwestern University, IL, USA). Parental BACs used here contained a luciferase reporter under the control of the ORF57 late gene promoter

[306]. This BAC was further manipulated to contain the fluorescent mCherry reporter gene fused to the N-terminus and in-frame with ORF23 (encoding the minor capsid protein), prepared by PCR amplification from the plasmid pmCherry-kan-in (a kind gift of Dr Greg Smith, Northwestern University, IL, USA). A second resolving recombination step removed the internal kan^r cassette and restored the ORF. Sequencing across the junction of the resulting BAC confirmed in-frame fusion of mCherry with the first methionine residue of ORF23 expressed under the native ORF23 promoter. VZV derived from this was termed VZV DR (dual reporter). All oligonucleotides were obtained from IDT (Coralville, IL, USA). The strategy to generate the S686A mutation in ORF62 was described previously [87] and used primers shown in Table 4. First a BAC was generated as recently detailed [265] that contained a deletion of the ORF71 sequence, replacing it with an ampicillin resistance cassette. Virus derived from this is termed VZV DRΔ71. Secondly the ORF62 sequence in the BAC was mutated using the primers shown in Table 4 to amplify the Kan^r cassette from pEPSkan2, recombining it into the BAC by selecting for gain of kanamycin resistance, and then by a second recombination event to remove the cassette with concurrent ISce I induction. To delete ORF10 in BACs, the entire ORF10 gene was replaced with either the kanamycin resistance cassette (kan^r; virus set B) or the turquoise 2 blue (T2B) fluorescent gene (set A viruses). Primers (table 4, ORF10 kan) were used to amplify the kan^r cassette from pEPS-kan2 [188] and colonies were selected using gain of kanamycin resistance. To replace ORF10 with a fluorescent T2B gene, the construct T2B-kan-in (containing a recombineering reversible kan^r cassette in the T2B gene) was PCR-amplified with primers (table 4) to place the gene directionally so that the T2B gene was under the ORF10 promoter. The T2B ORF was then restored by inducing recombination to reverse the internal kan^r element, coupled with concurrent L-arabinose-induced expression of the restriction enzyme ISce I to counter-select against BACs contain the kan^r gene

with the site for ISce I. Resulting BACs were then screened for loss of kan^r gene by replica plating and by RFLP. Primers used to PCR amplify the cassettes (table 4) contained 40bp of 5' sequence homologous to the site of insertion to enable direct recombination into the targeted VZV sites BAC. DNA of selected BACs were assessed by RFLP for the novel AgeI site in ORF62 mutants or for size change with ORF10 insertions. All sites of recombination were Sanger-sequenced across the insert region and relevant junctions.

Table 4 Primer design for VZV BAC Recombineering. Dir= direction. Turq =turquoise 2 blue. Kan^R= kanamycin resistance cassette. A= Uppercase letters in all rows denote bases that share sequence homology with VZV for directional recombination. Lowercase letters are mutations engineered into the primers to derive ORF62 62-S686A, with the novel inserted marker restriction site for AgeI underlined.

Gene	Dir.	Primer Sequence (5′ → 3′)
[a] **ORF62**	F	GTGTGTCCACCGGATGATCGTTTACGAACTCCGCGCAAGCGCAAGgCtCAaCC G GTC GAGAGCAGAAGCCTCCTCGACAAAGGATGACGACGATAAGTAGGG
	R	CGACGGGTGTCTCCCTAATCTTGTCGAGGAGGCTTCTGCTCTCGACCGGtTGtG cCTTGCG CTTGCGCGGAGTTCGTAAACAACCAATTAACCAATTCTGATTAG
ORF10-Turq	F	GGGAATCGCTTATTTAAACTAAAGATTTTACTCTATAAGTATGGTGAGCAAG GGCGAGGAGCTGTTCACCGGGGTGGTGC
	R	TTCGTAATTTATTTACACCCTTTACCCCAATGACGTTACATCACTTGTACAGCT CGTCCATGCCGAGAGTGATCCCGGCG
ORF10-kan^R	F	GGGAATCGCTTATTTAAACTAAAGATTTTACTCTATAAGTGCTGAGCAAAGA CCCCAACGAGAAGCGCGATCACATGGTC
	R	TTCGTAATTTATTTACACCCTTTACCCCAATGACGTTACACAACCAATTAACC AATTCTGATTAGAAAAACTCATCGAGC

4.4.4 Southern Blotting

BAC DNAs from 62-S686A-containing constructs and the corresponding virus nucleocapsid DNA extracted from infected ARPE-19 cells [359], were analyzed by Southern blotting to ensure that the ORF71 gene was replaced by reduplication of the ORF62 sequences, using a procedure similar to that detailed previously [178]. 1 μg of DNA was digested by kpn I and separated by 1% agarose gel for electrophoresis (Fig 15) and transferred to a nylon membrane

(INYC00010, Millipore Sigma, Burlington, MA, USA). The membrane was blocked using Li-cor's proprietary blocking buffer, and then probed by hybridization with biotinylated probes designed to recognize fragments containing the ORF62 and ORF71 that differ between the BAC (unrecombined) and capsid (recombined) samples. Two biotinylated probes were generated by PCR amplification using primers (Table 5) that generated 473bp (ORF62-specific) and 718bp (amp^r-specific) DNA fragments, which were labeled by incorporation of biotin conjugated nucleotides (DecaLabel kit, K0651, Thermo Fisher). Hybridization (10 ng/mL) was performed overnight at 42°C and detection via binding was assessed using fluorescent IRDye 800CW-Streptavidin (LI-COR, 926-32230). Imaging was analyzed on a LI-COR Odyssey IR in linear range and processed using Image Studio™ software. See results for further details and analysis.

Table 5 Primer Design for Southern Blot

Primer name	PCR product (probe) size (bp)	DNA fragment detection	Primer Sequence (5′ → 3′)
62-4R	473	2363bp recombined, 2367 and 2663 unrecombined	TGAGCGAACGTAATGACGAC
62-4L			CCTTCAAAGGATTGCGATTG
amp6R	718	No DNA recombined 2663 band unrecombined	ATACGGGAGGGCTTACCATC
amp6L			TTTGCCTTCCTGTTTTTGCT

4.4.5 Growth Curve Analyses

Growth analyses were initiated with titered, cryopreserved, mitomycin C-treated, and cell-associated ARPE-19 cell virus stocks, as detailed previously, with timed measurements done in triplicate [87]. For infectious center formation, confluent monolayers of ARPE-19 cells in 6-well plates were infected with 500 pfu /well of VZV and then also immediately titered. To assess the accumulation of infectious center-forming units over time (daily), infected cells were trypsinized,

serially diluted, and placed onto preformed ARPE-19 monolayers in 6-well plates. Plaques visible by brightfield or fluorescence were enumerated 4-5 days later. Growth curves by luciferase assay were done in a similar manner, except cells were rinsed once with 1xPBS before cell lysis using 250µL of 1x reporter lysis buffer (E3971, Promega, Madison, WI, USA). Samples were rapid freeze-thawed, scraped into tubes, vortexed, and remaining cell debris removed by centrifugation. Supernatants (10uL) were mixed with 100uL luciferase assay reagent (E1500, E1501 Promega) and quantified for activity at 570 nm using SpectraMax L reader with SoftMax Pro 7 software (Molecular Devices, San Jose, CA, USA). Duplicates were averaged and graphed after normalization to the day 0 titer. Statistical analyses were performed using GraphPad Prism software (GraphPad, La Jolla, CA, USA). Error bars represent standard deviation (SD) between the two readings and three triplicates per time.

4.4.6 Antibodies

Primary mouse commercial antibodies to ORF9p (HR-VZV-38), ORF10p (HR-VZV-41), IE62 (HR-VZV-23), and ORF11p (HR-VZV-07) were acquired from the Center of Proteomics at the University if Rijeka (CapRi, Rijeka, Croatia). Mouse antibody to ORF68p (gE, SC-56995) was from Santa Cruz Biotechnology (Dallas, TX, USA). Chicken antibody to βIII tubulin was acquired from Novus Biologicals (NB100-1612, Novus Biologicals, Littleton, CO, USA). Rabbit antibodies to ORF10p and ORF29p were anti peptide antibodies reported previously [360], [361]. Rabbit antibodies to ORF9 were a kind gift of Ann Arvin (Stanford University, Stanford, CA, USA). Secondary IRDye antibodies for immunoblot detection were purchased from Li-Cor to be compatible with the Li-Cor Odyssey, detected with either goat anti-mouse 680CW (926-32220), goat anti mouse 800CW (926-32210), goat anti-rabbit 680CW (926-32221), or goat anti-rabbit

800CW (926-32211). Secondary antibodies for immunofluorescence were acquired from Invitrogen (Waltham, MA, USA) and are as follows: Alexa Fluor 488 goat anti-mouse (A11029), Alexa Fluor 546 goat anti-mouse (A11030), Alexa Fluor 488 goat anti-rabbit (A11034), Alexa Fluor 546 goat anti-rabbit (A11035).

4.4.7 Immunoblotting

Immunoblotting was performed as previously described [362], with some minor changes. Extracts were prepared from sub-confluent ARPE-19 monolayers in 6-well plates that had been infected with 1000 PFU of ARPE-19-associated VZV, and harvested 72h later into PBS containing protease and phosphatase inhibitors (HALT, ThermoFisher Scientific; PhosSTOP, Roche, Basel, Switzerland). Samples were centrifuged for 1min at 12,000*x*g, 4ºC, and pellets resuspended in 100uL 1x PBS with protease inhibitors. 100uL 2x SDS PAGE lysis buffer was added, and samples were probe-sonicated for 10s, followed by heating to 95ºC for 5min. Samples were then separated by electrophoresis in commercial 4-15% polyacrylamide gels (Bio-Rad Criterion, Hercules, CA, USA), transferred overnight at 4ºC and 15V onto polyvinylidene difluoride membranes (Millipore Immobilon-FL 00010), and blocked overnight at 4ºC using Intercept blocking buffer (Li-Cor). Primary antibody stains were performed overnight at 1:500 to 1:1000 for VZV antibodies in blocking buffer diluted 1:1 with 0.2% Tween-20 in 2x PBS (PBS-T) overnight at 4ºC. Following washes with PBS-T, species-specific secondary antibodies linked to near IR dyes (Li-Cor, IRDye 680/800) were added at 1:20,000 dilution for 1h at room temperature, washed and imaged on a Li-Cor Odyssey.

4.4.8 Virion Purification

Virion purifications were performed essentially as described previously [87]. Briefly, MeWo or ARPE-19 cells were infected with cell-associated VZV and grown at 34ºC until at least 80% of cells demonstrated cytopathic effect. Cells were harvested by scraping into the media, and cells were Dounce homogenized using 20 strokes of a type B pestle. Cytoplasmic extracts remaining after centrifugation at 4150*xg* X 15 min x 4ºC. The media was centrifuged for 2 hr. at 12,000g at 4ºC and combined with cytoplasmic extracts. These were overlaid onto 5-18% Ficoll gradients, spun at 17,000*x*g for 2h at 4ºC. Diffuse light scattering bands approximately two-thirds down the tube based on previous experience [87], were harvested, concentrated by centrifugation (111,000*xg* for 1h), and resuspended overnight in 250uL Tris-EDTA. Where indicated, the Ficoll extracted virus bands were diluted 2-fold then directly overlaid onto 15-50% sucrose gradients in PBS and centrifuged similarly, resulting in a diffuse light scattering band in the center of the gradient. Protein samples were quantified for protein content using a commercial Bradford assay and analyzed by western blotting as described above. In most purifications, the approximate position of the virus band was determined by running HSV virions on parallel or even the same gradient.

4.4.9 Neuron Cultures

Neuron cultures were developed using previously published protocols [182] from Wa09 hESCs (WiCell, Madison, WI, USA), cultured by both feeder-dependent and feeder-independent methods as recently detailed [265]. Feeder-dependent methods were used to amplify cells from cryopreserved stocks, using an “hESC medium” composed of KnockOut^{TM} DMEM/F-12 medium

supplemented with GlutaMax supplement, 20% KnockOut™ serum replacement (KSR, Thermo Fisher), 1% non-essential amino acids (NEAA), 20ng/mL basic fibroblast growth factor (bFGF, Shenandoah Biotechnology, Warminster, PA, USA), 100uM 2-mercaptoethanol (2ME, ThermoFisher), and antibiotic/antimycotics. Cells were subsequently amplified in a feeder-independent culture using StemFlex™ medium supplemented with StemFlex™ and antibiotic/antimycotic. Following passage, ROCK inhibitor Y-27632 (S1049, Selleckchem, Houston, TX, USA) was added to the culture media for 24h to increase cell survival and deplete dividing cells. Differentiation to neurons was detailed previously [182], [183], by directing hESC to neurospheres using the PA6 mouse stromal fibroblast cell line (RIKKEN BioResource Center, Kyoto, Japan), and then terminally differentiating neurospheres to neurons by seeding neurospheres onto substrates that had been coated sequentially with Poly-D Lysine (PDL) and GelTrex (Thermo Fisher Scientific, A1413201). Neurons were differentiated for 14 days in Neuron Medium (Neurogenic Medium supplemented with CultureOne (A3320201, Thermo Fisher) with NGF, BDNF and NT3 as detailed previously [182], [183]. Media was changed at least every other day. Live cell microscopy of VZV neuronal infections used neurons differentiated in coated 12-well glass bottom plates (P12-1.5P, Cellvis, Mountain View, CA, USA) for at least 14 days prior to VZV infection. Infection used 200 PFU of PBS-washed mitomycin-C treated VZV infected ARPE-19 cells in neuron media, and the media was then changed at 8 hours and then every 2 days. For studies using axonal infections of neurons in compartmentalized microfluidic chambers, a previously published procedure was followed [182], [183], [265]. PDMS-based microfluidic devices were permanently bonded to glass substrates using a PE-25 plasma cleaner (Plasma Etch, Carson City, NV, USA). Chambers were then coated sequentially with PDL overnight and then GelTrex (A1413201, Thermo Fisher Scientific) under sterile conditions for 1h (ensuring channel

infiltration) before washing and addition of neurospheres to one side ("soma") of the device close to the channels. Axons were promoted to grow into the "axon" chamber using the same media containing 10-fold higher NGF concentration. The "axon" side media was maintained at a level higher than the soma side to create small hydrostatic pressure and NGF concentration gradient. Axonal projection growth through the channels was monitored using a light microscope and usually developed after 7-14 days. To infect at axons, mitotically inhibited infected cells or cell-free VZV diluted in neuron media were added to the axon side and the hydrostatic pressure gradient was reversed to be higher in the soma side to prevent the possibility of virus flow to the soma side directly. The NGF gradient was also removed. Medium in both chambers were changed every other day taking care to continually maintain the hydrostatic pressure direction.

4.4.10 Microscopy

ARPE-19 or MeWo cells were seeded in chambered 4-well Nunc Lab-Tek II slides (C6807, Sigma-Aldrich, Burlington, MA, USA) and infected 24 h later with 200PFU cell-associated VZV, followed by incubation at 37ºC for 3 days, as previously detailed [87], [178]. Cells were washed with 1x Dulbecco PBS, fixed in 4% paraformaldehyde (PFA) for 20min, permeabilized with 0.2% Triton X-100 for 5min, and blocked for at least one hour in 10% heat-inactivated goat serum (HIGS) in 1x D-PBS. Primary antibody incubation was overnight at 4ºC in PBS containing 10% HIGS. Following washing, bound antibodies were detected with a 1h incubation with Alexa Fluor-coupled secondary antibodies (specifics detailed in the legends) and nuclear staining with 4′,6-diamidino-2-phenylindole (DAPI, Thermo Fisher Scientific). Chambers were washed with PBS and mounted on coverslips using Aqua-Mount (Thermo Fisher Scientific). Images were acquired using an Olympus IX83 microscope with a 40X (N.A. 0.60) oil objective in the linear range and

processed using Olympus CellSens software and ImageJ. All comparative images were processed equally. Live-cell imaging of infected neuronal cultures in 12-well glass bottom plates used a Nikon Ti microscope with a 10x air objective (N.A. 0.30). Again, all images were imaged and processed on equal parameters. Fixed neuron cultures were processed similarly except that 1xPBS plus Ca^{2+} and Mg^{2+} was used and permeabilized with 0.5% Triton X-100 with 1% Tween-20 in PBS for 2 x 10min to maintain the fluorescence expressed by the viruses. Neurons were identified with chicken anti-beta tubulin III (Novus Biologicals, Centennial, CO, USA) in PBS-10% HIGS and after washing, bound antibodies were detected using secondary goat antibodies conjugated to AlexaFlor-594 (A-11042, Thermo Fisher Scientific). Images acquired in a given experiment were captured under identical acquisition settings and processed identically using Metamorph software (Version 7.7, Molecular Devices, San Jose, CA, USA). Axon images were acquired on the Olympus IX83 confocal microscope, using a 20x oil objective (NA 0.85) with 2x zoom. Images were analyzed using Olympus CellSens software and ImageJ.

4.4.11 Preparation of Viral Nucleocapsid DNA

Viral nucleocapsid DNA was prepared as detailed previously [359] with small modifications, from two to five 175cm^2 tissue cultures of heavily VZV infected (>90% CPE) ARPE-19 cell monolayers. Cells were dislodged by scraping into media, pelleted, and washed in PBS. Cells were resuspended in 0% glycerol "LCM" buffer and then twice extracted with the freon substitute 1,1,1,2,3,4,4,5,5,5-Decafluoropentane (94884, Sigma Aldrich). The top aqueous layer was centrifuged with a swing out rotor on discontinuous 5% glycerol-LCM, 45% glycerol-LCM gradients at 77,000*xg* 1h at 4ºC. The pellet was resuspended in TNE (1 mM Tris HCl, PH 8.0, 150mM NaCl, 1 mM EDTA) overnight at 4ºC, broken up by trituration and treated with 1%SDS

and 100 ug/mL proteinase K for 2 hr. Viral DNA was extracted using phenol-chloroform twice, ethanol-precipitated, and resuspended into TE buffer without vortexing (1 mM Tris HCl, PH 8.0, 1 mM EDTA).

4.4.12 Statistics and Sequencing Analyses

Statistical analyses were performed using GraphPad Prism software (GraphPad, La Jolla, CA, USA). Error bars represent standard deviation (SD) or standard error of the mean (SEM), as described in figure legends. Sequencing analyses and assembly were performed using the CLC Genomics Workbench platform.

4.5 Results

4.5.1 Development of recombinant VZV that lack trans activators from ORFs 10 and 62 in virions

To address the roles of the virion transactivators in infection, two sets of BACs and the corresponding VZV (set A and B) were developed independently. Initial studies examined the Set A VZV (Fig 14). For the deletion of ORF10, the entire coding sequence was replaced with mT2B. A VZV deleted for ORF10 was engineered into a VZV BAC already engineered to generate VZV that expressed mCherry as a fusion in-frame to the N terminus of ORF23, so that virus growth and spread by microscopy could be assessed by live cell microscopy [182], [183]. ORF23 encodes the homolog of HSV VP26, a minor but abundant capsid protein [363], [364]. The T2B fluorescent

reporter gene was expressed from the ORF10 promoter in the VZV [126], [182], [365], [366]. As expected from previous published data, virus was readily isolated and replicated in culture (Fig 14, "VZV mCherry-Δ10Turq.") [88], [89]. A separate BAC was used to generate VZV with ORF62 containing the 62-S686A mutation, similar to that previously detailed [87]. The BAC used contained deletion of ORF71 and a C-terminal tagging of ORF62 with eYFP, in order to track cellular localization. Virion incorporation of IE62 is blocked by the S686A mutation, which removes the target residue of ORF66 protein kinase-mediated phosphorylation that renders IE62 distribution to the cytoplasm for virion incorporation [83], [87]. This virus was called "VZV EYFP-62S686A." The latter BAC was subsequently deleted for ORF10 by replacement with T2B (Table 5 and Fig 14; to yield VZV EYFP-Δ10Turq+62S686A). We subsequently developed a second set of VZV (Set B) in which VZV had a common background (Fig 14). The parental BAC (yielding "VZV DR") contained the luciferase reporter under control of the ORF57 promoter [306], [367], as well as the mCherry-ORF23 fusion. In this BAC, ORF10 was deleted by its replacement with a kan^r cassette, yielding VZV DR-Δ10. In parallel, The BAC was deleted for ORF71, replacing it an ampicillin resistance cassette (yielding "VZV DR-Δ71"), and then the S686A mutation was introduced into ORF62 (VZV obtained from this was termed "VZV DR-62S686A"). This BAC was then modified by replacing ORF10 with the kanamycin resistance cassette to generate double mutant VZV, VZV DR-Δ10+62S686A. Two different double mutant viruses were generated independently. All BACs generated were subject to extensive RFLP analyses as well as Sanger sequencing of PCR generated fragments across the region(s) of recombination, insertion, and mutation, to verify manipulations.

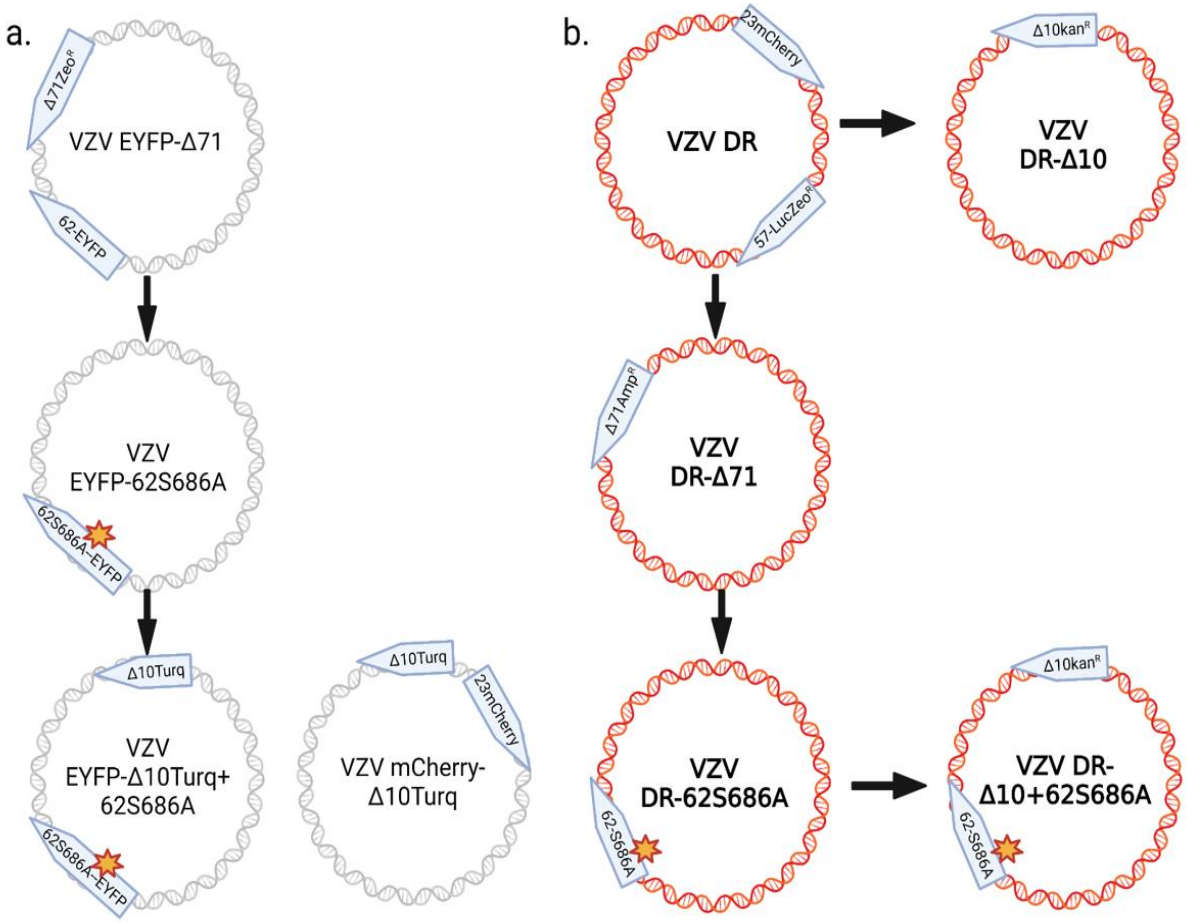

Figure 14 Recombinant VZV Constructs. Two sets of BACs and VZV (sets A and B) were developed independently to address the roles of the virion trans activators. (a) Set A constructs initiated with a parental BAC that was deleted for ORF71 by its replacement with a zeomycin resistance Cassette, and contained ORF62 C terminally tagged with a monomeric enhanced yellow fluorescent protein (EYFP), and this was used to generate VZV EYFP-D71. The BAC was then manipulated to place the ORF62 S686A mutation similar to that previously detailed [87], but yielding VZV-EYFP-62S686A. a subsequent manipulation of the BAC was made to replace ORF10 with monomeric turquoise 2 Blue gene (D10turq) to yield VZV EYFPD10turq+62S686A. A VZV deleted for just ORF10 was made in parallel in a BAC that expressed ORF23 as an mCherry -ORF fusion. The VZV EYFPD10turq+S686A was dual fluorescent for EYFP and turquoise 2 blue, and VZV mCherry-D10turq is dual fluorescent for mCherry (fused in frame to the N terminus of ORF23) and Turquoise2Blue (replacing the VZV ORF10. (b) Set B BACs were all derived from a parental BAC, yielding VZV DR, in which a previously detailed BAC that expresses ORF57 driving a luciferase gene [306]; Lloyd et al manuscript in preparation) was manipulated to also contain the mCherry-ORF23 fusion. This BAC was then manipulated to generate a BAC deleted for ORF10 (yielding "VZV DR-D10"), and a BAC deleted for ORF71 (yielding "VZV DR-D71"). The latter BAC was then modified to insert the S686A mutation into ORF62 (yielding "VZV DR-62S686A"). This was further modified to replace ORF10 with a kanamycin resistance cassette, yielding "VZV DR-D10+62S686A." All BACs in Figure 1 were characterized by extensive RFLP analyses and Sanger sequencing across the region(s) of insertion and/or mutation.

Transfecting each BAC into human melanoma (MeWo) cells resulted in the generation of viable VZV from all BACs, with viruses expressing the expected fluorescent reporters. While it was expected to find that VZV with the individual transactivators either deleted (ORF10) or prevented from being incorporated into virions (ORF62 S696A), the viability of VZV from BACs containing both 62-S686A and deletion of ORF10 was uncertain. Given that it was readily isolated from BAC transfected cells, a preliminary conclusion was that the simultaneous prevention of both transactivators from being virion incorporated was not a lethal mutation for viral replication in epithelial cells. This initially disproved a hypothesis that the two virion transactivators had complementing or overlapping functions.

The viruses containing 62-S686A mutations were generated in a BAC containing an ampicillin resistance cassette that deleted ORF71, so that only ORF62 was present for manipulation. Previous similar strategies in which the duplicated ORF63/70 gene was manipulated after deletion of ORF70 showed that the ORF70 was restored in virus by reduplication of ORF63 [178]. It was considered important to verify that the deleted ORF71 in the BAC was reduplicated by ORF62 in the virus. A Southern blot analysis was done on the BACs and on nucleocapsid DNA of each virus made that originated from BACs with ORF71 deleted (Fig 15a). Digestion of BAC and VZV DNA with kpnI was predicted to yield fragments derived from ORF62 and the position of ORF71 that were diagnostic of recombination in the BAC when probed with an ORF62/71 promoter-specific probe (4L/4R, Fig 15b). In circular BAC DNAs, the labelled DNA probe bound to two different sized products of 2367bp and 2663bp, but in VZV nucleocapsid DNAs, the ORF62 and ORF71 generate identical fragments of 2663bp that hybridize the probe. In contrast, a DNA probe derived from the ampicillin gene (6R/6L probe) hybridized only to a single DNA fragment present in the BACs that was removed in the corresponding viral nucleocapsid DNAs (Fig 15c).

PCR amplification of the ORF62 S686 region from the virus nucleocapsid DNA and Sanger sequencing revealed that the S686 was at 100% of the expected allele and contained the engineered mutations in the respective viruses where engineered. As such, we conclude that any phenotype seen for these viruses is not a consequence of a lack of the reiterated terminal and internal sequences. Further studies established that the F1 BAC replicon was also removed (data not shown).

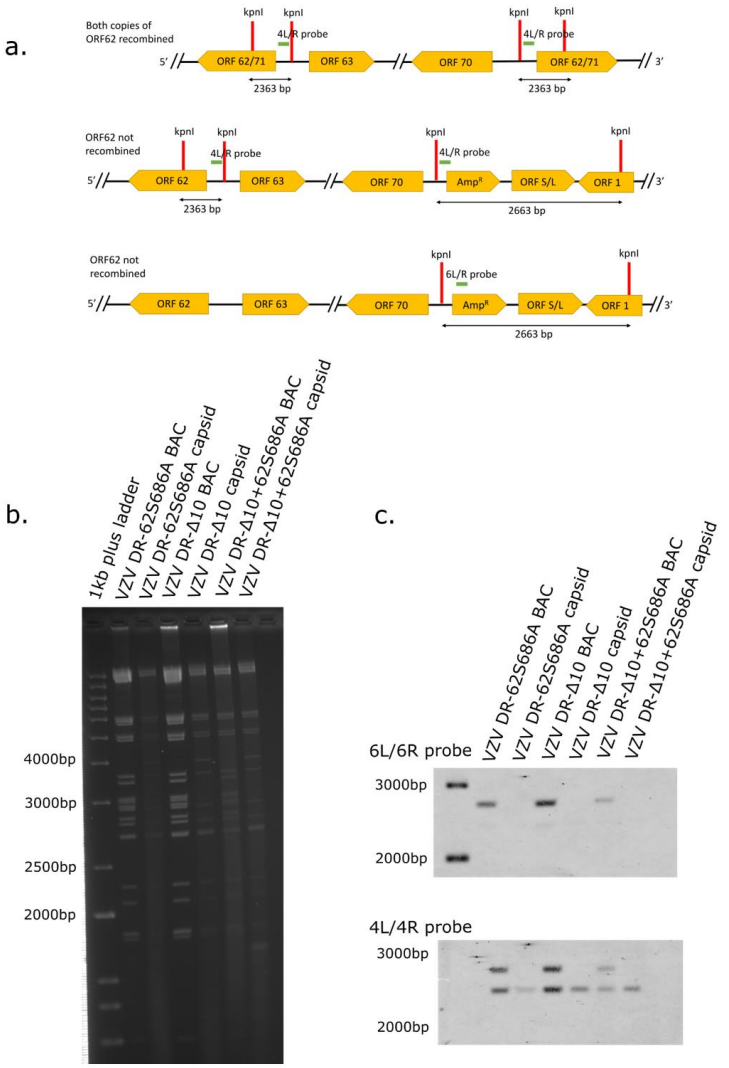

Figure 15 Southern blot analyses of VZV set B to show that ORF62 reduplicates ORF71 in virus infected cells.

(a) Diagrammatic representation of the physical map of the VZV DNA containing ORF62 and ORF71 and the size of the fragment of the VZV DNA (top line) and the BAC DNA (middle and lower line) when digested by the restriction enzyme KpnI; and the predicted fragments to which probes 4L/R and 6L/R bind. Probe 4L/R bind to a VZV specific promoter region upstream of ORF62/ORF71; Fragment 6L/R binds to a DNA fragment derived from the ampicillin resistance gene. The sizes of the fragments expected to hybridize the probes are shown below the genome representation. (b) approximately 1ug DNA derived from the BAC, or from the isolated virus DNA obtained from purified nucleocapsids (capsid) were digested kpnI and separated on a 1% Agarose gel. The image shows the ethidium bromide stained pattern, the approximate location of the key size markers for 2, 3 and 4Kbp and the fragments to which the probes bind. A 4.2Kbp fragment represents the replicon element in the VZV BACs. (c) Southern blot labelled fragments hybridizing the 6L/R probe (top) and the 4R/L probe (bottom). The 4R/4L probe binds to 1 fragment (2363bp) if ORF62 has reduplicated to replace the ORF71 deletion, but yields 2 DNA fragments when unrecombined in the BAC DNAs (2367bp and 2663bp), while 6R/6L probe binds 1 DNA fragment in the unrecombined BAC (2663bp) and n fragments in the VZV if ORF71 has been restored by the duplication of ORF62 to ORF71 (c). Virtual digests were analyzed on Benchling (last accessed Jan 2022, Retrieved from https://benchling.com).

Further studies addressed the cellular distribution of IE62 in the respective viruses, using either immunofluorescence to detect IE62 in set B viruses (Fig 16), or visualization of EYFP fused to IE62 C terminus in set A viruses (Fig 17). VZV with wild type IE62 (VZV DR, DR-Δ71, DR-Δ10) clearly showed the presence of IE62 in both nuclear and cytoplasmic forms, while viruses with the engineered S686A mutation in ORF62 produced IE62 that was completely nuclear in every infected cell, when viewed at both low (Fig 16b) and higher (Fig 16a) magnification. Importantly, we point out that VZV containing the simultaneous deletion of ORF10 with ORF62 S686A mutation showed a completely nuclear distribution of IE62, while IE62 showed a cytoplasmic distribution in the VZV deleted for ORF10. A similar analysis of set A viruses revealed similar results (Fig 17). This data establishes that mutations designed to preventing virion incorporation of both transactivators did not result in obvious effects that affected the expected IE62 distribution in these viruses.

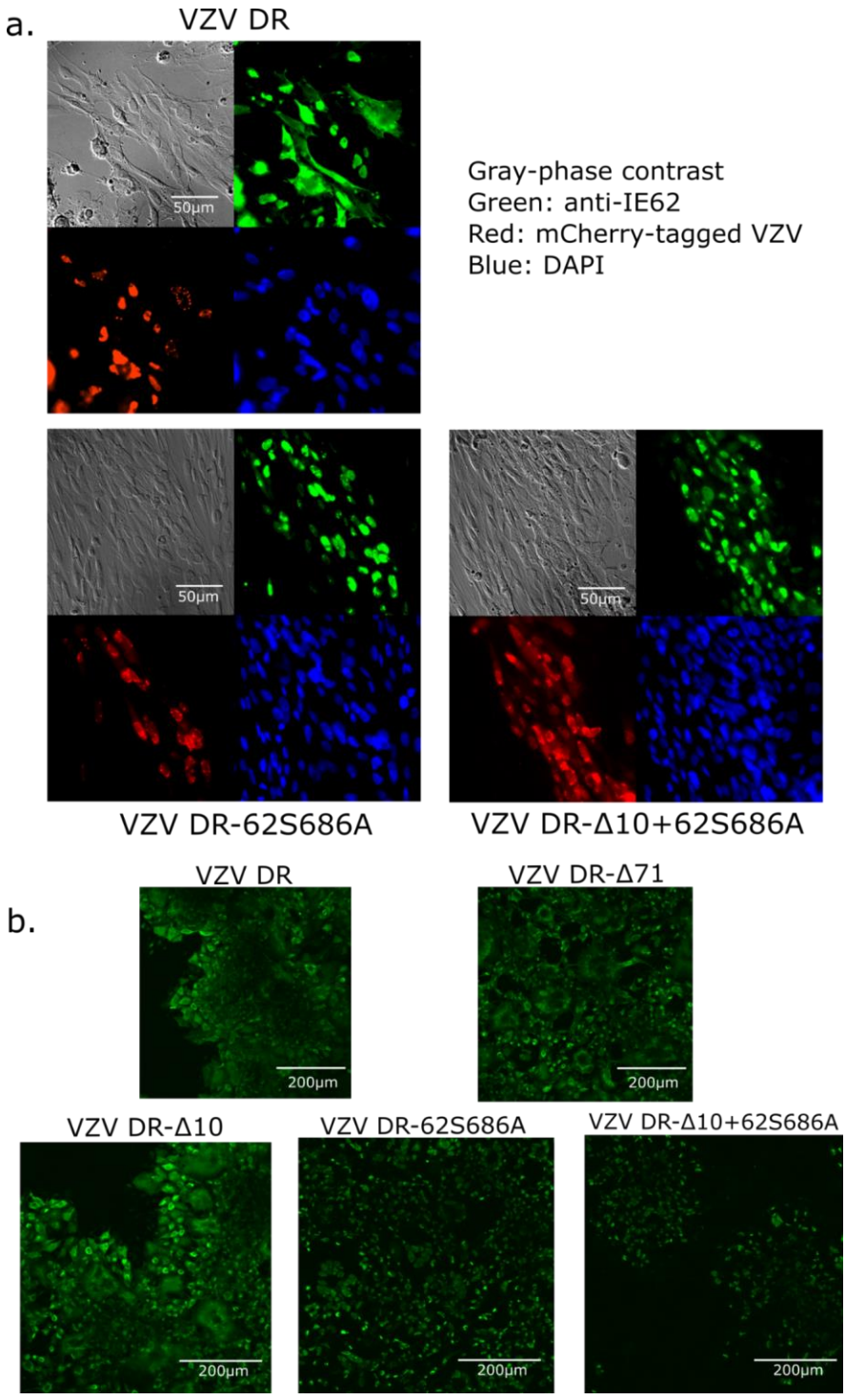

Figure 16 IE62 cellular localization in VZV-infected cells are strictly nuclear in the presence of the 62-S686A mutation. Images of VZV centers of infection on ARPE19 cells (a) and in MeWo cells (b) is for shown viruses presented for IE62 (green) after 4 days of growth of VZV DR, VZV DR-62S686A and VZV DR- Δ10+62S686A. Gray=phase-contrast, Green=anti-IE62, Red=mCherry-tagged ORF23, Blue=DAPI. Images in (a) were taken with a fluorescent microscope under a 40x oil objective. Images in (b) are taken with a confocal microscope with a 20x oil objective and 2x zoom.

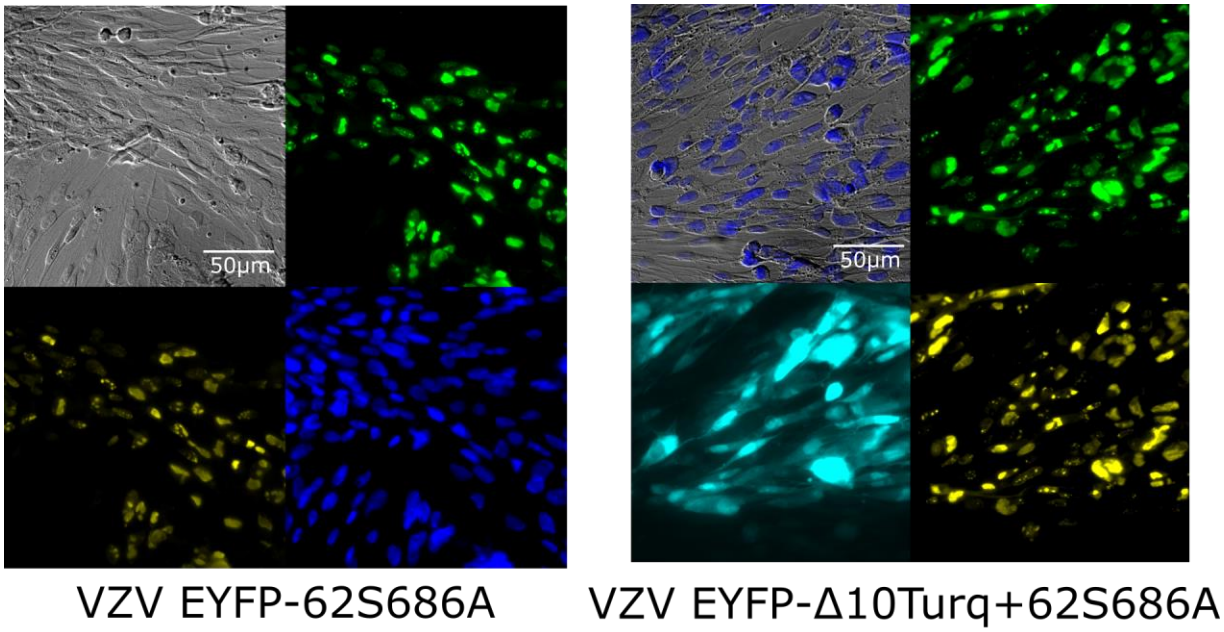

Figure 17 IE62 localization in Set A VZV-infected cells are strictly nuclear in the presence of the 62-S686A mutation. Antibodies to IE62 (green) are shown in MeWo cells infected with recombinant set A VZV containing the IE62 S686A mutation after 4 days post infection, along with the localization of the EYFP-tagged IE62 (infection with VZV EYFP-62S686A and VZV EYFP- Δ10+62S686A-infected cells). IE62 shows a predominantly nuclear distribution. Gray=phase-contrast, Green=anti-IE62, Yellow=EYFP-tagged IE62; Turquoise=Turq2 that replaces ORF10 in VZV EYFP- Δ10+62S686A-infected cells; Blue=DAPI staining of nuclei. Images in were taken with 40x oil objective.

4.5.2 VZV lacking virion ORF10 and/or IE62 trans activator proteins replicate in epithelial cell models

Given that recombinant VZV from all BACs manipulated to prevent transactivators from expression or virion incorporation were viable and showed the expected cellular distribution of IE62, we next assessed how growth was affected. Plaque sizes of the recombinant viruses were

qualitatively similar in size on ARPE-19 cell monolayers at day 5 post infection, suggesting there was not significant impairment of growth and spread. To assess lytic fitness of each virus, parallel multi-step growth curves were initiated, starting with low input (~200 pfu/well), using pre-titrated and mitomycin C treated ARPE-19 cell-associated stocks. The number of infected cells capable of initiating new foci on fresh monolayers at different times after infection were assessed. Different virus combinations were compared in parallel (Fig.18), and some growth comparisons included VZV ORF66-GFP, which was previously demonstrated to replicate robustly and at levels similar to the wild type virus POka [83]. Growth rate comparisons of VZV DR to VZV derived from VZV DRΔ71 were identical (Fig 18a), and VZV DR growth was similar to that of VZV ORF66GFP (Fig 18b). Two independently derived isolates of VZV from BAC DRΔ71 that were engineered to contain the 62-S686A mutation in ORF62 showed a marginally attenuated growth phenotype with statistically significant growth impairment at day 3 post infection, compared to VZV DR (Fig 18b). A marginal growth defect was seen previously for independently derived VZV with 62-S686A in ORF62 compared to wild type VZV [87]. The deletion of ORF10 also trended to marginally reduced growth rates, but none were significant. Importantly, the double mutant still replicated efficiently, although notably less well than the WT-like VZV66GFP.

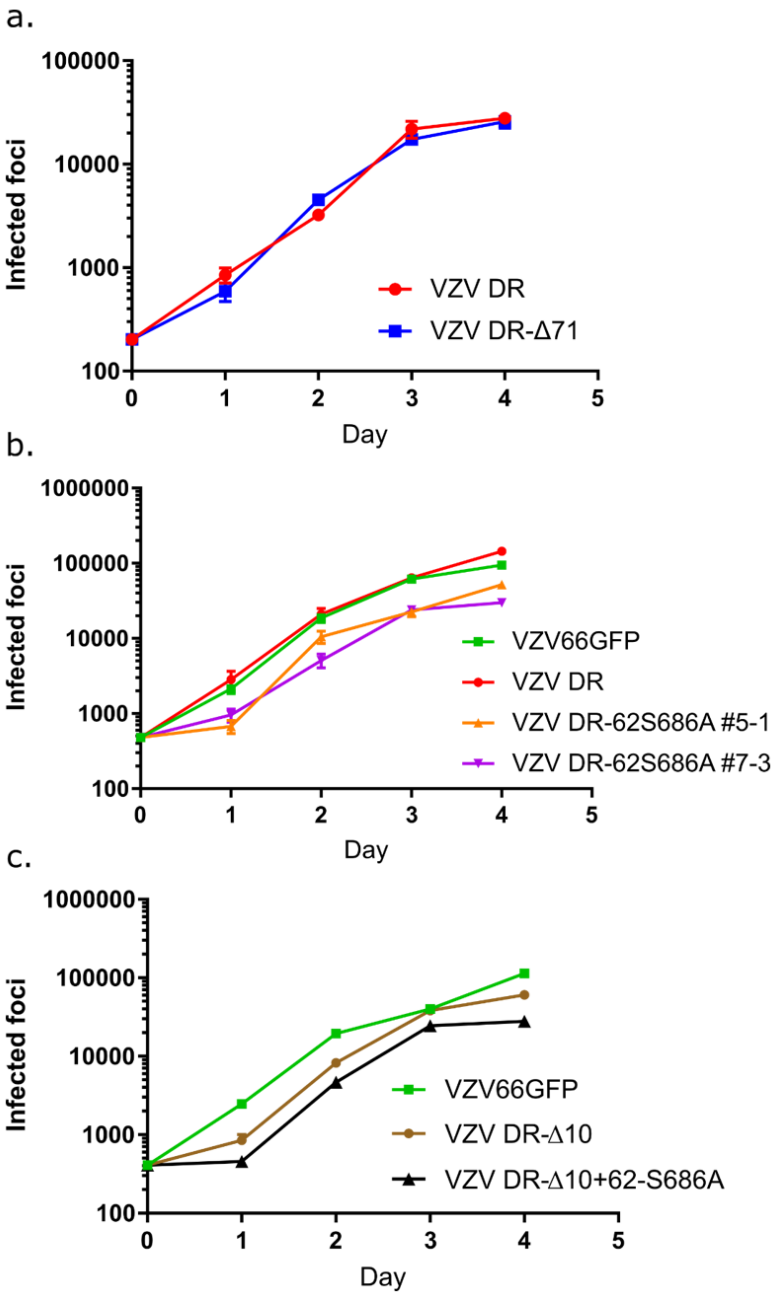

Figure 18 Growth rate comparisons of set B VZV in human epithelial ARPE-19 cells. Low-MOI initiated growth curves of recombinant VZV were assessed by plaque assay to enumerate the number of infectious centers over time, using conditions detailed in the methods and text. Viruses shown in each graph were assessed in parallel in triplicate from two replicates per time point. Graphs represent experiments with recombinant constructs made in the set B background, compared to the growth of WT-like control VZV (VZV DR or VZV 66GFP, VZV DR-Δ71). Growth curves were initiated with pre-frozen, pre-titrated cell associated stocks and then were normalized to the WT-like VZV66GFP input (parts (b) and (c), or VZV DR input (a) after the titration of virus at day 0. Each graph represents at one of least four independent experiments. Error bars represent standard error from the mean.

Set A viruses largely echoed these results, in that the growth of VZV mCherry-Δ10Turq replicated at rates similar to that of VZV66GFP (Fig 19a) and VZV that had been derived from BACs deleted for ORF71 ("VZV EYFP-Δ71"). VZV EYFP-62S686A showed a reduced replication by 0.5-0.8 log at each timepoint after day 0, with values at days 2 and 3 being significant (Fig 19b). Again, this reflected growth patterns reported previously [87]. Intriguingly, VZV EYFP-Δ10Turq+62S686A did not show the same growth reduction, but replicated at rates similar to VZV66GFP (Fig 19b). Taken together, the results indicate that deletion of ORF10, the insertion of 62-S686A, or combining both mutations together resulted in efficiently replicating VZV in epithelial cell cultures. The surprising observation of a marginal but significant loss of growth in VZV with 62-S686A mutation, which was not maintained when ORF10 was subsequently deleted, could not at this point be explained, but could have been the consequence of undefined compensations in tegument composition, which have been previously documented in HSV-1 and PRV [39], [44], [87], [368]–[370].

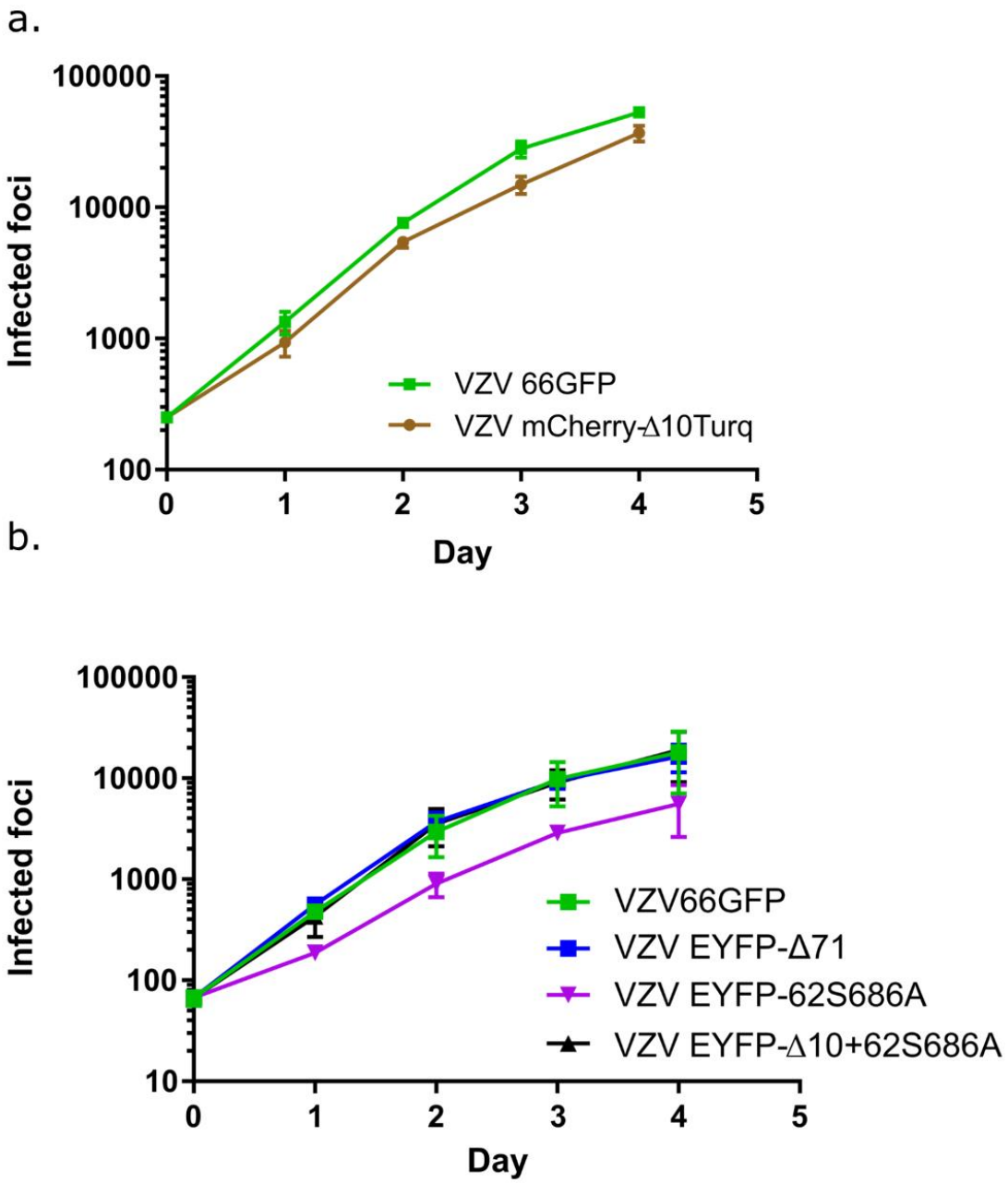

Figure 19 Growth of set A VZV in human epithelial ARPE-19 cells. Low-MOI initiated growth curves were initiated in duplicate per time point with select set A recombinant VZV, and the number of infectious centers forming infected cells were then quantified by trypsinization and infectious focus formation plaque assay. (a) A comparison of the set A background VZV containing deletion of ORF10 in comparison to the WT-like VZV 66GFP control. (b) A comparison of VZV EYFP- Δ 71, VZV containing a point mutation in S686 and VZV containing both mutation of ORF62 S686A and deletion of ORF10 in comparison to VZV 66GFP. Each graph represents at least four replicates (two technical replicates of two biological replicates per time point) and is representative of two independent experiments. Error bars represent standard error from the mean.

4.5.3 Replication of VZV lacking virion trans activator proteins in hESC-derived neuron cultures.

The role of the virion transactivator VP16 in HSV-1 neuronal infection and reactivation [102], [371]–[373] stimulated a hypothesis that one or both of the VZV virion transactivators could be important in VZV neuronal infections. We have previously detailed an hESC-derived neuron platform that can harbor VZV lytic infections when infected directly at the soma [182], [183], [318]. The growth and spread of different recombinant VZV with virion transactivator mutations were next assessed in this platform following an initial infection with 200 pfu per 12-well neuron culture, using pretitrated cell-associated mitomycin C-treated infected ARPE19 cells that were washed before addition to remove inhibitors and freezing media. The pretreatment of cell-associated virus stocks with mitomycin C before freezing prevents the replication and division of any residual uninfected cells, and since all cultures were greater than 95% fluorescence positive, there are few uninfected epithelial cells added to the monolayers. Real time microscopy for the development of fluorescent spread in neuronal cultures at the same points using positional memory software were used to gauge growth of each virus (representative times are shown in Fig. 20a and b; the full time course is shown in Fig 23a and b). Similar results were seen with recombinant VZV derived from the pretreated alternative set of BACs (Fig 23c), and representative images shown reflect those seen at multiple regions of cultures. Comparison of the development of fluorescence for VZV DR, VZV DR-Δ71, and VZV66GFP showed that all three viruses demonstrated expanding fluorescent foci in neurons, indicating cell-to-cell spread over time (Fig 20a). Fixation and staining of the infected neurons at day 21 for βIII tubulin confirmed that VZV fluorescent-positive cells were βIII tubulin positive, indicating they were predominantly neurons. The parallel study of neurons infected with VZV DR-Δ10 also indicated efficient replication in human neuron

cultures, as seen by expanding foci of fluorescence involving multiple neurons in 17 of 20 positions over the time frame of 20 days. However, neuron cultures infected with VZV DR62-S686A showed foci of infection at only a few positions early in infection (4 foci of 20 monitored that demonstrated a potential seeding infection) and the initial foci had only involved one or a few neurons by day 20 (Fig 20b). Similar results were also observed with viruses derived from the alternative set A BACs (Fig 23c), in that VZV with the ORF62-S686A mutation was greatly impaired for spread to neurons as compared to WT like VZV and VZV lacking ORF10. A surprising result was that while VZV 62-S686A appeared to be severely replication-impaired in neurons, VZV from the BAC that was subsequently deleted for ORF10 Showed the efficient formation of fluorescent foci that were not dissimilar to that seen for VZVDRΔ10, and developed for the majority (17 of 20) of positions monitored. This unexpected result was also seen for the double mutant virus derived from the set A BACs (Fig 23c), with VZV containing 62-S686A showing considerable impairment in replication while VZV with mutations to prevent both transactivators from virion incorporation grew and spread in neuronal cultures with high efficiency. Taken together, these results suggested that the virion incorporation of IE62 is required for the efficient growth of VZV in neuron cultures, while the subsequent deletion of ORF10 in the background of the 62-S686A mutation resulted in a compensatory effect that led to a more robust growth phenotype.

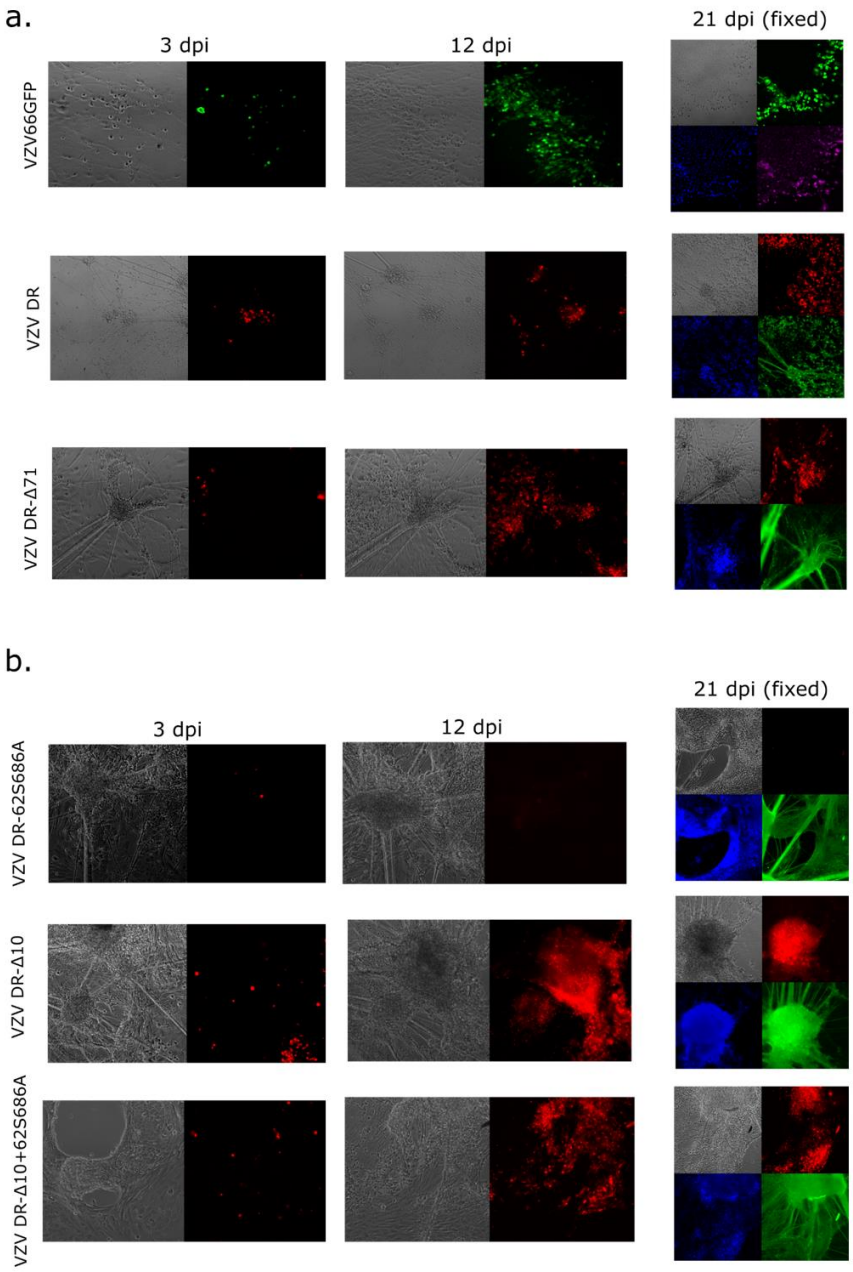

Figure 20 (a-b) Lytic infection and spread of Set B recombinant VZV in hESC-derived human neuron cultures. Infection of 14-day matured hESC-derived neurons were initiated with 200PFU of various viruses WT-like control viruses (a) or trans activator mutants (b). VZV-infected ARPE-19 cells were inoculated onto neuronal cultures in glass-bottom 12-well plates, and live-cell imaged at multiple positions over 21 days using a microscope with positional stage location memory. The figures show representative timepoints of a given position in the plate, and is representative of what we see in multiple positions over multiple experiments. At Day 21 infected neuron cultures were fixed and stained for DAPI (dark blue) and beta-III tubulin (green; or magenta in VZV66GFP infected samples). Fluorescently tagged viruses were pseudo-colored to match their fluorescent tags (green=GFP-tagged VZV, red=mCherry-tagged VZV, Gray=phase contrast), and images were taken at 10x magnification. The full range of timepoints in the growth analyses are shown in supplemental Figure 3.

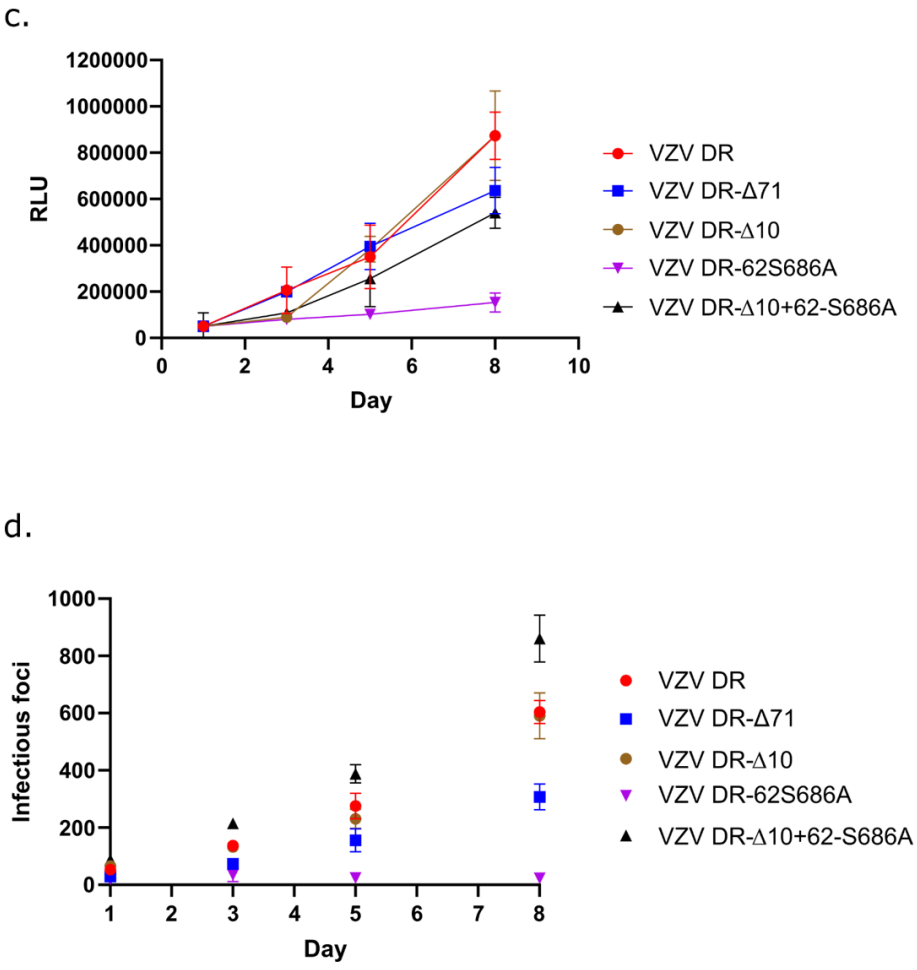

Figure 20 (c-d) Lytic infection and spread of Set B recombinant VZV in hESC-derived human neuron cultures. (c) For growth curve on neurons by luciferase activity, 12-wells of heavily seeded neurons were infected with 200 PFU of mutant VZV as shown, and then at days 1, 3, 5, and 8 post infection, neurons were scraped and triturated. Half of each well was then added to a tube of reporter lysis buffer (Promega, E3971) and then assessed for relative light units to assess luciferase-based growth curves. All graphs were normalized to the WT-like VZV DR starting VZV input at day 1. (d) Plaque counts over time were assessed by taking the same infected neuron culture samples at specific times indicated and then titrating 1/3rd and 1/30th of the triturated neurons onto confluent wells of ARPE-19 cells in duplicate. Plaques were then counted after 4 days using a fluorescent microscope. The number of infectious plaques forming foci were then quantified. Error bars represent mean with standard error.

The hESC-derived neuron cultures are three-dimensional, quite heterogeneous, and often do not form a uniform monolayer in culture dishes. To further support the qualitative microscopy

studies of growth in neurons, triplicate neuron cultures per virus and per timepoint were established in parallel, and after a 14-day maturation /differentiation period, parallel infections were established with 200 pfu/well with VZV derived from the set B BACs, which contain a VZV ORF57 promoter-driven luciferase reporter. At days 1, 3, 5, and 8 post infection, infected neuron cultures were manually dislodged, triturated, and a portion was titrated onto confluent monolayers of ARPE-19 cells. The number of plaques that form after four days were then back-calculated to give the number of infectious centers per neuron culture (Fig 20c). In addition, half of the neuron cultures from each timepoint were lysed and assessed for the expression of the luciferase reporter. This approach provided two readouts for growth kinetics of the viruses in neuron cultures (Fig 20d). VZV containing both functional ORF62 and ORF10 and those deleted for ORF10 alone or ORF10 in the background of the 62-S686A mutation were clearly capable of producing increasing numbers of infectious foci on ARPE-19 cells over the 8-day period, with luciferase expression reflecting the increasing yield of VZV over time. However, VZV DR 62S686A showed virtually no increase in the formation of plaques over time, and the increase in luciferase reporter expression was significantly reduced in comparison to the other viruses, reaching significance by day 8 compared to all other VZV evaluated. Taken together with the failure to initiate foci with multiple fluorescent infected neurons, this data strongly suggest that virion IE62 is important for neuronal lytic replication and spread of VZV, but the subsequent deletion of ORF10 results in a compensatory effect that restores the growth defect.

We further assessed the ability of these VZV to initiate a lytic infection following cell-associated infection of axons, using a compartmentalized microfluidic channel separated neuron cultures previously detailed [182], [185]. It was possible that the lack of a tegument protein transactivator could have impaired the ability of the virus to initiate a lytic infection in the soma.

In these cultures, axons from neurosphere soma seeded on one side of the chambers are driven to migrate through 12×10×150μm microfluidic channels using an NGF gradient, which takes 14-21 days. A hydrostatic pressure gradient is maintained of the axon and soma compartments to prevent virus leakage from the axon to soma compartment. Infections were initiated with cell-associated VZV, which was shown to initiate lytic infections as previously described [182]. Infections in the soma were initially monitored by live cell microscopy and cells were fixed at day 21 post-infection, when signs of mCherry expression were apparent, and immunostained for β-III tubulin to identify neuronal axons. High-resolution confocal imaging revealed the presence of mCherry positive nuclei in the soma of cultures infected by each set B virus (Fig. 21). The development of mCherry signals were seen in all virus infections on the soma side, but for some viruses, notably VZV DR, the infection resulted in large spreading infections in neurons in the clusters that tend to form. These three-dimensional compartmentalized bodies did not efficiently stain with the BIII tubulin antibody. As such, it was not practical to quantify the extent of the infections beyond the observation that all viruses were able to be axonally transported in a retrograde manner to the soma and could initiate the expression of a late gene (ORF23), as indicated by the development of mCherry-positivity in this platform.

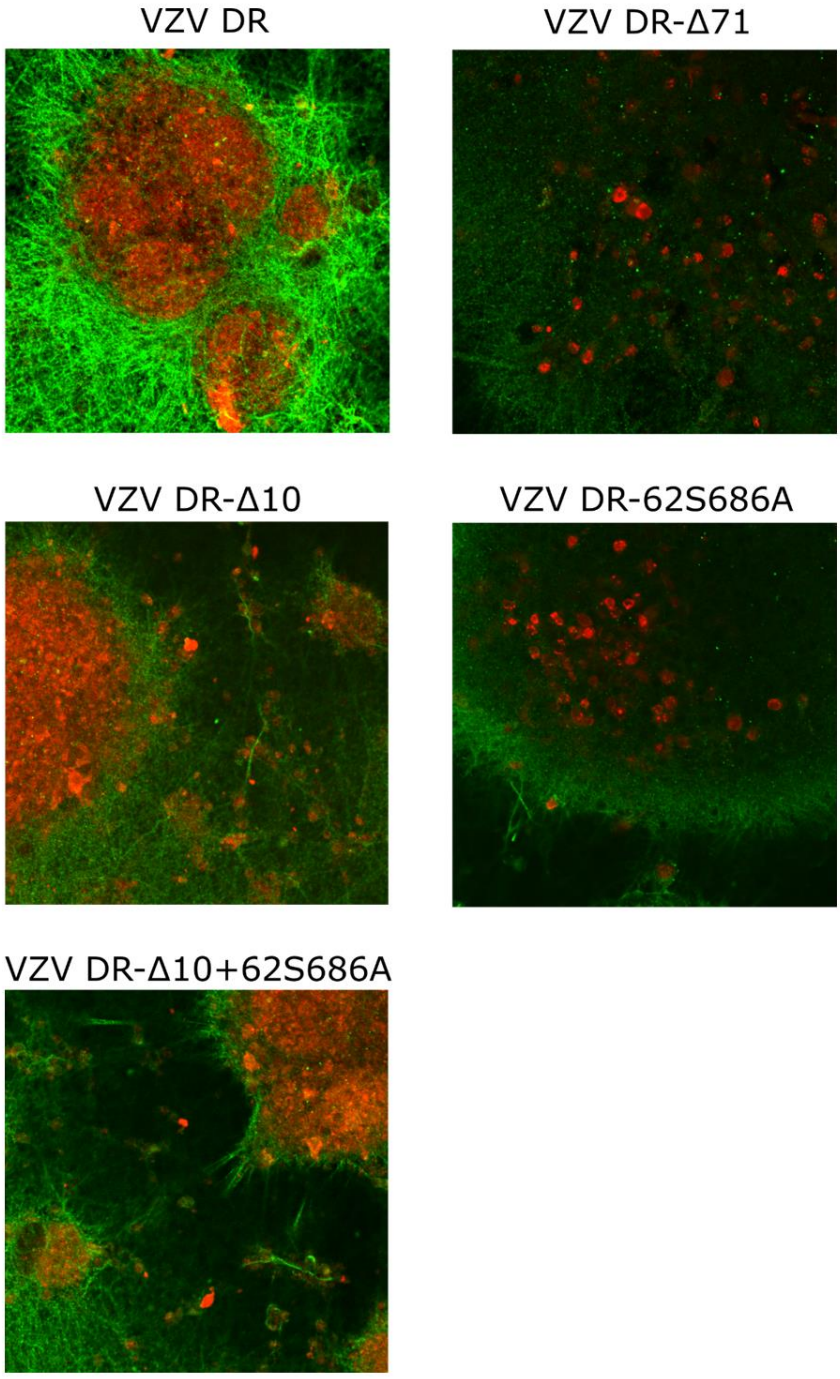

Figure 21 Infection of neurons by VZV via the axonal route in compartmentalized chamber neuron cultures. Compartmentalized chambers were established as detailed in methods and at 14 days post differentiation, 1000 PFU of mitomycin C treated ARPE19 cell-associated, mCherry-expressing VZV were inoculated into the axon chamber of microfluidic compartmentalized neuron chambers. After 21 days, neuronal soma was fixed and stained for beta-III tubulin (green) and then imaged for BIII tubulin and mCherry, using confocal microscopy. Images are projections of mCherry positive regions detected in some compartment after infection with the various viruses. All recombinant VZV were able to initiate some lytic soma infections from axons and express mCherry in neuronal nuclei.

4.5.4 Virion analyses suggest an ORF10 deletion-dependent compensatory mechanism to packaged virion IE62 that is independent of the accumulation of IE62 in the cytoplasm.

The deletion of ORF10 was found to have minimal effects on lytic replication of VZV in both epithelial cell cultures and in hESC-derived neurons, while VZV with the 62-S686A mutation were modestly impaired in epithelial cells and highly impaired in neurons. This suggests the virion form of IE62 has cell type-specific importance for VZV replication in neuron cultures. Surprisingly, the subsequent deletion of ORF10 in this background restored a major portion of the impaired neuron growth phenotype. In VZV with 62-S686A mutations with and without the ORF10 gene intact, IE62 consistently showed a complete nuclear localization. We have previously reported that virion incorporation required cytoplasmic distribution of ORF62, which is mediated by the ORF66 protein kinase [83]. To address the possible mechanisms for this surprising result, we examined the protein profile of virions purified from these VZV recombinants. Unlike HSV, the purification of virions has proven to be considerably more difficult than for HSV-1, since insufficient levels are usually released from cells to allow virion band visualization by light scattering. We optimized a previously used virion purification procedure by doing parallel side by side purifications of VZV with HSV virions released from infected MeWo or ARPE-19 cells to identify the regions of gradients expected to contain virions. Viruses were purified by a two-step gradient process from approximately 10^8 infected ARPE-19 cells for each virus (VZV DR, DR-Δ10, DR-62S686A, and two VZV DR Δ10+62-S686A viruses derived from independently isolated BACs). Cells were harvested at complete cytopathic effect from both media and cytoplasmic extracts, and sedimented first on 5-15% Ficoll gradients and then on 5-50% sucrose gradients as detailed previously, using parallel sedimentation of HSV released into infected cell media [87].

This strategy was required because virus yields of the recombinant VZV were low and not sufficient to obtain sufficient banding for light scattering in gradients. We then conducted an analysis for the presence of the gE protein, for candidate tegument proteins and for the absence of the nuclear and non-structural ssDNA binding protein encoded by ORF29. Antibodies to gE detected proteins in each virus preparation, including infected cells, while antibodies to ORF29 only detected the 130KDa species in infected cells and not in the virion preparations, indicating that the virions were not contaminated by nuclear proteins from nuclear lysis or leakage. The expression of the ORF10 protein could not be established by immunoblot analyses, since all recombinant viruses were based on the Japanese pOka strain, and we have previously reported that our rabbit antipeptide antibody to ORF10 does not efficiently recognize the protein from Japanese strains, due to clade-specific SNPs [360]. However, all virion samples showed presence of the tegument proteins expressed from the adjacent ORF9 and ORF11 genes, and for Set A viruses, by sequencing to ensure the ORF10 replacing kanamycin resistance cassette was present. ORF9 shows multiple forms, which are expected and caused by its phosphorylation [56], [178]. When extracts of virions were probed for the presence of virion IE62, a species of 160 kDa was detected in virions of the parental virus VZV DR, as well as VZV virions purified from cells infected with VZV containing ORF10 deletion. It was also seen in virions obtained from cells infected with VZV DRΔ71 (data not shown). As expected, virtually no IE62 was detected in virions obtained from cells infected with VZV DR-62S686A, in good agreement with previously published results using a different recombinant virus [87]. An unexpected result was that forms of IE62 was readily detected in virion extracts obtained from cells infected with two different independently derived VZV with simultaneous deletion ORF10 and the 62-S686A mutation (Fig.22). Full genome sequencing of the viral nucleocapsid DNA did not reveal the presence of mutations in either VZV

DR or VZV DR-Δ10+62S686A virus #2. This unexpected result indicates that simultaneous mutation/deletion to prevent both transactivators from virion incorporation results in a compensatory pathway of virion assembly that results in virions still retaining forms of IE62. Given that this virus still expresses an only nuclear form of IE62 (Fig 16 and 17), this data suggests that the compensatory mechanism circumvents the previous indicated mechanisms governing IE62 virion incorporation, which rely on cytoplasmic accumulation of the IE62 protein.

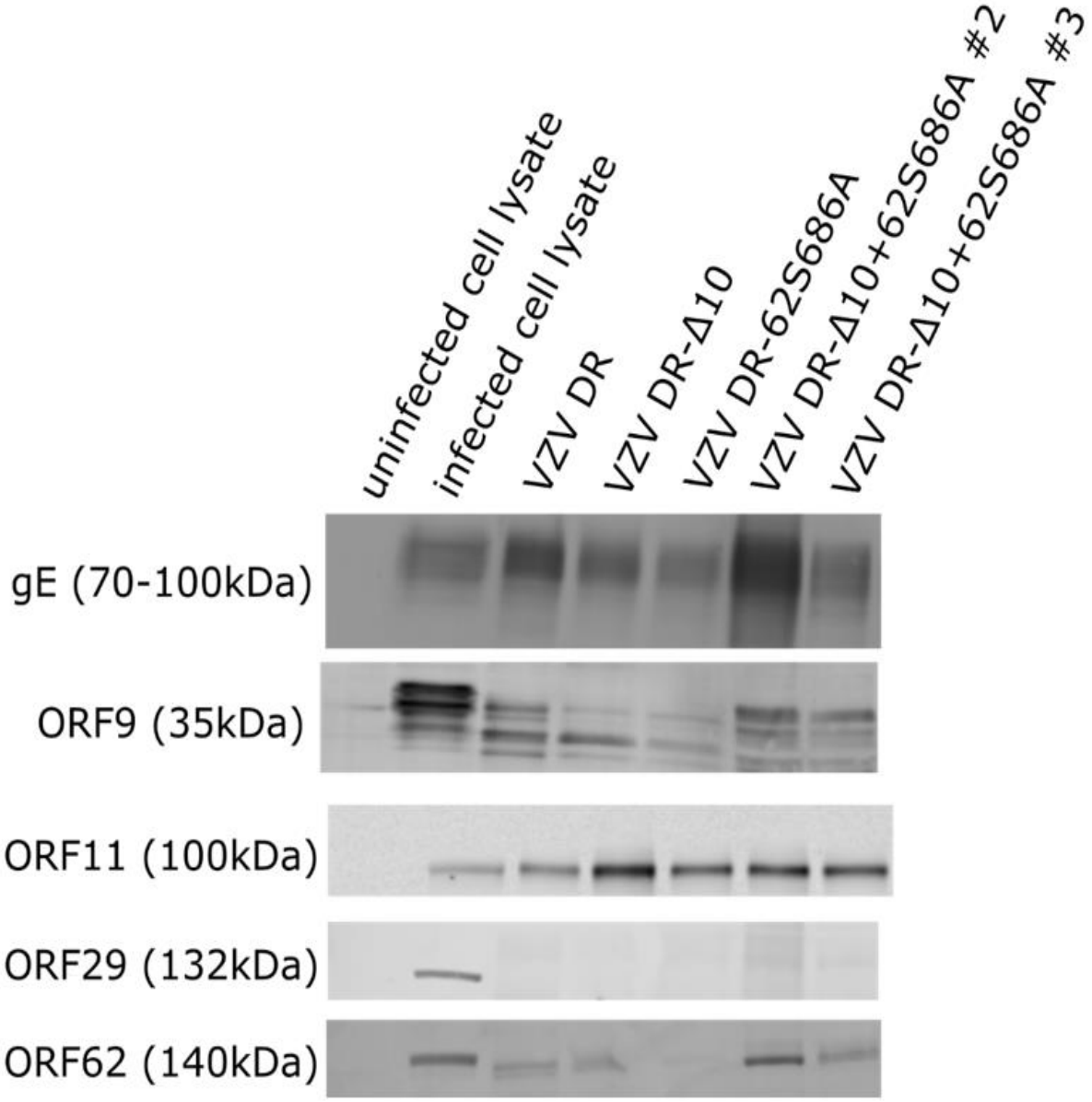

Figure 22 Immunoblotting of relevant tegument proteins in purified VZV virion preparations. (a) Immunoblotting of proteins obtained from uninfected and infected cell and virion preparations purified by sequential Ficoll and sucrose gradient fractionated virion preparations, using antibodies to the structural proteins from ORF 9 (essential tegument protein), ORF 11 (tegument protein), and ORF 68 (glycoprotein E); to the nonstructural nuclear ORF 29 ssDNA binding protein and to the ORF62 encoded protein. Both IE62 and ORF9 showed multiple forms that represent different phosphorylation species as previously described [54], [56]. Reactivity to IE62 was observed in virion preparations of VZV DR, VZV DRD10, but was barely detected in extracts of VZV virions containing ORF62 S686A mutation. However, virions prepared from two recombinant VZV containing the VZV ORF62 S686A mutations and simultaneous deletion of ORF10 showed the presence of virion forms of IE62. ORF10 could not be detected due to the exclusion of the reactivity of our ORF10 specific antibody with that derived from Japanese specific strains that include POka.

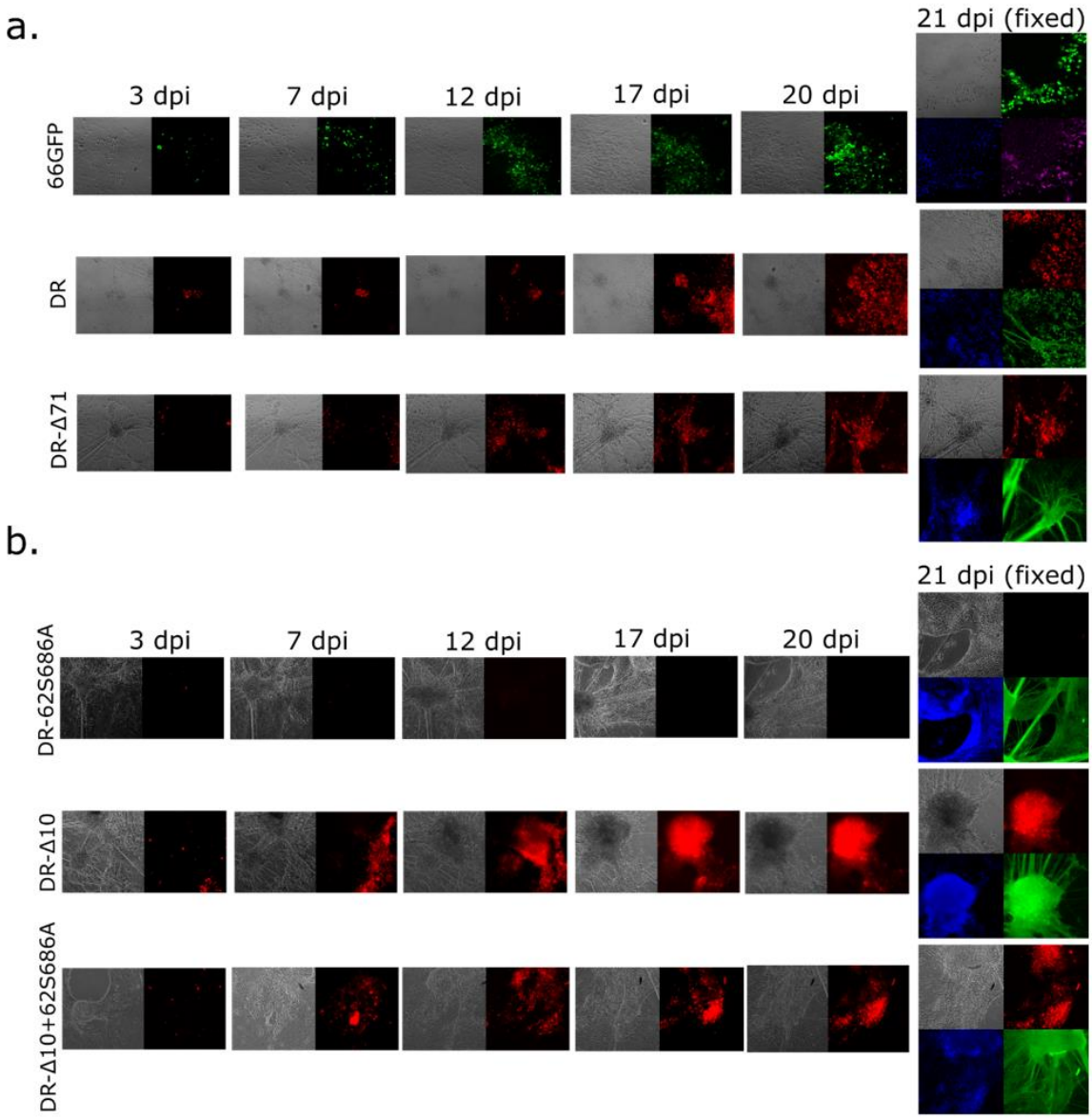

Figure 23 (a-b) Full time course of Lytic infection and spread of recombinant VZV in embryonic stem cell-derived human neuron cultures imaged by repetitive live cell microscopy at the same points. These images represent the full-time course of growth and spread. (a) shows a comparison of expanding fluorescent foci for three WT like VZV analyses in parallel, (b) shows a comparison of VZV containing mutations in ORF62 and/or a deletion of ORF10. Cultures were live-cell imaged for 20 days. Shown are representative locations over different times of a single position in the plate, but are representative of that seen at multiple positions. After the last day of live cell imaging, neurons were fixed and stained for DAPI (dark blue) a gray phase contrast image, beta-III tubulin (green). Fluorescently tagged viruses were pseudo-colored to match their fluorescent tags (red=mCherry-tagged VZV); gray=phase contrast. Images were taken at 10x magnification.

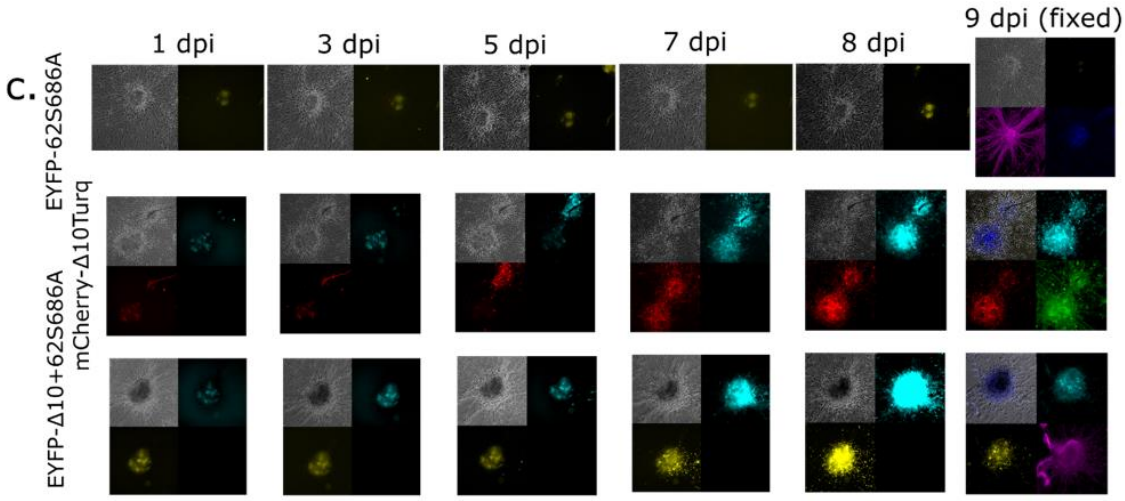

Figure 23 (c) Full time course of Lytic infection and spread of recombinant VZV in embryonic stem cell-derived human neuron cultures imaged by repetitive live cell microscopy at the same points. These images represent the full-time course of growth and spread. (c) shows lytic infection and spread of the Set A VZV on neurons after initiating with 200PFU of mitomycin treated VZV-infected ARPE-19 cells inoculated onto neuronal cultures in glass-bottom 12-well plates. Cultures were live-cell imaged for 9 days. Shown are representative locations over different times of a single position in the plate, but are representative of that seen at multiple positions. After the last day of live cell imaging, neurons were fixed and stained for DAPI (dark blue) a gray phase contrast image, beta-III tubulin (magenta (or green in mCherry-Δ10Turq VZV). Fluorescently tagged viruses were pseudo-colored to match their fluorescent tags (red=mCherry-tagged VZV, Turquoise=Turq2-tagged ORF10 in VZV, yellow=EYFP-tagged VZV. Gray=phase contrast), and images were taken at 10x magnification.

4.6 Discussion

These studies addressed the contribution of two abundant virion-associated transcriptional activators to human neuronal and epithelial cell models of VZV lytic infection and replication. Prior to this work, the role of virion forms of IE62 and the ORF10 protein had been partially dissected, but had not, to our knowledge, been assessed in human neuron cultures. VZV that were designed to lack both ORF10 and ORF62 transactivators had not been reported. VZV with the ORF10 deleted was shown early on in VZV genetic studies to be fully viable in epithelial cell

culture [88], although subsequent work by the Arvin group showed that VZV with ORF10 gene deletion, or disruption of a USF element in the ORF10 promoter, greatly impaired VZV growth in human fetal organized skin housed in SCID-hu mice [55], [89], [374]. While VZV with ORF62 fully deleted is not viable because IE62 is essential to VZV gene expression, VZV with the 62-S686A mutation was shown by our group to be only slightly growth impaired in epithelial cells [87]. The 62-S686A mutation resulted in IE62 showing completely nuclear forms throughout infection, and this correlated precisely with the loss of IE62 in purified virions. We concluded that IE62 virion tegument association occurred in the cytoplasm, consistent with the virion incorporation of the majority of herpesvirus tegument proteins [375]. The slight growth impairment in epithelial cell cultures compared to wild type virus suggested that virion IE62 was only marginally pro-viral. Since these studies, human neuron culture systems have undergone considerable development for VZV [157], [173], [179], [181]–[183], [318], [376]. Identifying those proteins that are important for neuronal infection could set a basis for the development of improved vaccines that are, perhaps, unable to infect ganglia, establish latency, or reactivate from it [179], [182], [183]. In this regard, we report here three novel findings. (1) The ORF10 protein is not required for VZV neuronal lytic infection or neuronal infection initiating from the axon; in contrast (2), the introduction of a 62-S686A mutation into ORF62 that abrogates virion forms of IE62, results in VZV severely impaired for growth and spread in neuron cultures. Finally, (3) subsequent deletion of ORF10 in the background of a VZV with the 62 S686A mutation (which was expected to abrogate the incorporation of both transactivators) had the unexpected consequence that this VZV was viable, and that the ORF10 deletion rescued the growth defect in VZV exerted by 62-S686A mutation in neurons. Virion analyses suggested an unexpected

compensatory mechanism to incorporate IE62 into the virion that did not depend on IE62 localization and accumulation into the cytoplasm.

In neuron cultures infected with VZV mutants, deletion of ORF10 had minimal effect on lytic growth, while the introduction of the 62-S686A mutation in ORF62 had a profound consequence to viral growth. This is the first report of a role for virion forms of IE62 in VZV replication. Growth was measured by multiple means, because neuron cultures are heterogenous, three-dimensional, and do not form monolayers, making a typical plaque-based growth curve considerably more difficult and variable. However, we incorporated reporter expression into our viruses, making neuronal growth assessment over time more feasible. Impairment of the VZV 62-S686A virus and near-parental growth of ORF10-deleted VZV was consistent from multiple methods, including fluorescent reporter expression in live-cell studies, by luciferase assay over time for the set B virus recombinants, and by determining the infectious nature of dislodged neurons in initiating infectious center formation on epithelial cell monolayers. This data suggests that the ORF10 protein does not have a significant role in human neuronal lytic infection. While VZV lacking ORF10 can efficiently replicate in epithelial cells, the lack of a role in neurons was perhaps a little surprising, since much evidence suggests that HSV VP16 transactivation has roles in neuronal replication and in particular, reactivation. HSV VP16 transactivation has been shown to be not absolutely required for lytic replication at higher multiplicities, but is more important at low multiplicity. VP16 has been found to be important for neuronal reactivation in the murine *in vivo* model of latency and reactivation [106], as well as in a two-phase embryonic rat neuronal culture model of reactivation [102], [377]. VP16 is also essential and required for virion assembly of HSV [91], but mutants of VP16 that retain the virus assembly functions have been examined, particularly HSV expressing VP16 with an insertion in the transactivation domain termed in1814.

Such mutants do not efficiently reactivate in neurons. The ORF10 protein lacks the C-terminal strong transactivator domain of HSV VP16, but it can nevertheless transactivate through a weaker N terminal domain found through structural analyses [356]. Given that ORF10 is not needed for growth, it is obviously not required for VZV virion assembly, so the functions attributed to VP16 must have evolved to be in other proteins. The essential ORF9 is a strong candidate as a focal point of tegument assembly, through multiple protein interactions that have been partly defined [126], [188], [378], [379]. What the exact important role is of the ORF10 protein for VZV replication in human organized skin is not clear. It is possible that it may have interactions with organized skin cell-specific factors. VZV gene expression is known to be tightly associated with skin cell differentiation [380], and we hypothesize that ORF10 may contribute to this process. It does, however, seem that this does not apply to neurons.

In contrast to ORF10, the virion forms of IE62 appear critical for efficient neuronal lytic infection. Such VZV barely replicate and spread in neuron cultures as measured by multiple methods. The introduction of the 62-S686A mutation into the genes encoding IE62 in order to prevent its virion incorporation was established previously by our group [87]. The virion incorporation was shown not to be responsible for the deficient growth of ORF66-negative VZV in primary corneal fibroblast cell cultures. ORF66-deficient VZV also do not incorporate VZV IE62 into virions, as ORF66 has a key role in phosphorylating IE62 at serine 686, which is adjacent to the IE62 NLS that mediates its cytoplasmic accumulation [83]. We thus speculate that studies to evaluate ORF66-deficient virus in the human neuron system would also reveal little virus growth. However, ORF66 is known to affect multiple host and viral genes and cellular processes, including type 1 histone deacetylases, actin homeostasis, the nuclear matrix protein matrin 3, and multiple host innate, intrinsic, and adaptive processes, so the role of vIE62 could not be dissected

out in such viruses [60], [358], [381]. The VZV 62-S686A has a much more defined effect and consequence. We have previously speculated that presence of other transactivators, such as the ORF10 protein, might have some overlapping functions and/or interact with some of the same cellular factors in aiding neuronal viral replication [60]. Clearly, such overlap may not occur as efficiently in human neuron cultures, which appear more reliant on the virion form of IE62. It thus seems that the initiation and regulation of VZV gene expression is cell type-specific, and virion IE62 is important for gene expression in neurons. Alternatively, we have not ruled out the possibility that virion-delivered IE62 is important in counteracting innate antiviral activities that might be more effective in neurons. VZV IE62 inhibits IRF3- and TBK-1-mediated signaling from pathogen-associated molecular patterns (PAMPs), which activate pattern-recognition receptors (PRRs) [52]. There is also known cross-talk between IE62 and types I and II interferon (IFN) signaling [382], [383]. An investigation of gene activation and PAMP-directed signaling is currently underway.

The third intriguing finding was that while VZV with the 62 S686A mutation was unable to efficiently replicate in neurons, the replication defect of VZV was almost fully restored when ORF10 was subsequently deleted, in the two independent BACs used to generate this 62 S686A background. Partially purified virion preparation analyses of the virions revealed that while VZV 62-S686A virions had little to no detectable IE62, which was expected and observed in previous studies [87], we saw comparatively abundant levels of IE62 in virions of VZV isolated from such double mutant viruses. This was despite the maintenance of a consistent completely nuclear localization of the IE62 protein in plaques and in infected cells, with no signs of any cytoplasmic accumulation. This observation suggested that the deletion of both transactivators unmasks a compensatory mechanism that influences the virion tegument composition and the incorporation

of IE62 that is not dependent upon its cytoplasmic accumulation. Compensatory changes resulting from tegument protein deletions have been well documented in HSV-1, PRV, as well as VZV [39], [44], [87], [368]–[370]. We are confident in detecting the presence or absence of IE62 in our Δ10+62-S686A double mutant virions (versus absence in 62-S686A-only VZV), although we do acknowledge that the cell-associated nature of VZV and the difficulty in purifying VZV virions is demanding and quite challenging, and that we cannot obtain virions to homogeneity. Nevertheless, the compensation would be consistent with the unexpected growth rates of VZV containing the 62-S686A and ORF10 deletions. At present, we can only speculate on how compensatory mechanisms might work to account for this unexpected observation. One mechanism to be tested is based on the fact that both ORF10 protein and IE62 show both nuclear and cytoplasmic forms in wildtype VZV infected cells. We speculate that nuclear forms of the ORF10 protein prevent the incorporation of nuclear IE62 into newly forming and aggregating virions in the nucleus, so that normal VZV incorporates only cytoplasmic IE62 to form the outer tegument in the cytoplasm. It has been shown that the predominantly cytoplasmic ORF9 can co-interact physically with IE62 [57], [384], and that ORF9 has been suggested to be a focal point of tegument formation in the cytoplasm [57]. It is also possible that the compensation is not ORF10-specific: deletion of additional VZV tegument proteins could trigger an alternative compensatory mechanism to mediate the incorporation of nuclear IE62 into virions. Of note is that ORF10 belongs to a conserved gene cluster which includes ORF11 and ORF12, that also encode abundant tegument proteins in the herpesviruses. Deletion of these has been shown to affect virus growth in skin like that seen for ORF10 [55]. We are currently addressing this by deleting combinations of genes in the ORFs 10-12 gene cluster, in a 62-S686A background.

Finally, one of the remaining challenges that was not done in this work was to assess the role of these virion transactivators in reactivation from latency. As just indicated, HSV VP16 has been shown to possess roles in promoting reactivation, and may be a key step in the mediation of the so called "animation/phase I" stage of reactivation, versus the full expression of the viral genome in "phase II," which leads to renewed virus production [102]. However, we have not been able to efficiently reactivate hESC-neuron cultures that were latently infected with these VZV recombinants, even for the parent virus. This is not a unique problem in the field, and other groups using similar neuron-based in vitro models have reported quite inefficient reactivation rates for recombinant VZV [157]. Our viruses contain reporter genes that may subtly impair reactivation efficiency that result in very low rates that do not allow quantitative assessment. A rate of 25-60% of neuron culture reactivations was also seen for parent and attenuated Oka virus, but vaccine Oka rates were significantly lower [179]. We are currently also exploring the ability to establish VZV latency without use of antivirals, and the use of additional multiple reactivation stimuli to reactivate VZV from model latent states.

To summarize, we report on the importance of the inclusion of IE62 into VZV virions for lytic replication in neuron cultures, but also report that recombinant viruses lacking ORF10 in the background of a 62-S686A point mutation restores a severe growth impairment seen in 62-S686A only viruses. This contrasts to VZV lacking ORF10, which replicates efficiently in neurons. This is the first data to suggest the importance of virion forms of IE62, and is intriguing, given that the levels of IE62 in virions are relatively very high compared to the HSV-1 ICP4 protein. We speculate that the neuronal environment is such that presence of vIE62 is needed to either augment the initiation of gene expression, or alternatively, counteract innate and/or intrinsic immune responses that develop in response to VZV neuronal infection.

4.7 Role of ORFs 10-12 in VZV replication

Following our study on the role of ORFs 10 and 62 in neuronal replication (which is about to be submitted for publication), we also performed some follow-up experiments to extend the deletion studies to ORFs 11 and 12 in addressing their roles in VZV neuronal replication. ORFs 11 and 12 are "dispensable" tegument proteins that are known to be involved in skin pathogenesis [55]. Indeed, recombinant VZV had been previously generated that lack pair wise and even all three of the 10-11-12 gene cluster [55]. Given the surprising finding that deletion of ORF10 restored the defective replication of VZV 62-S686A, the additional goal was to determine if the deletion of ORFs 11 and 12 had the same effect of restoring the 62-S686A defect. Their HSV homologs (UL 46 and 47) have been shown to bind both STING and TBK1 and counteract accumulation of IFI16 in the nucleus (by UL46), and early studies suggested they regulate VP16 activity (UL46 and UL47) [58], [59], [385]. The functions of the VZV 11 and 12 proteins are not well studied. Since VZV ORF10 is homologous to HSV VP16, it has been speculated that ORFs 11 and 12 might also regulate ORF10 functions, or contribute to transactivation upon infection of a new cell. To assess the role of these products in neuronal replication, we constructed various recombinant mutants lacking ORFs 11, 12 and combinations of the 10-12 cluster using the recombineering methods [188], [189]. They were developed in a VZV that had an mCherry-tagged ORF23 capsid protein. We made VZV with deletions of ORF10 (VZV Δ10), ORF11 (VZV Δ11), ORF12 (VZV Δ12); both 10 and 11 (VZV Δ10-11); both 11 and 12 (VZV Δ11-12), and all three of the genes (VZV Δ10-12). Deleted genes were engineered by replacing them with a turquoise2 fluorescent cassette. Following construction of these viruses, we initially assessed their replication kinetics in ARPE-19 epithelial cells by performing plaque assay-based low-MOI growth curves,

as previously described. Compared to WT-like VZV, we found that all recombinant VZV replicated with no drastic growth impartment (Fig 24).

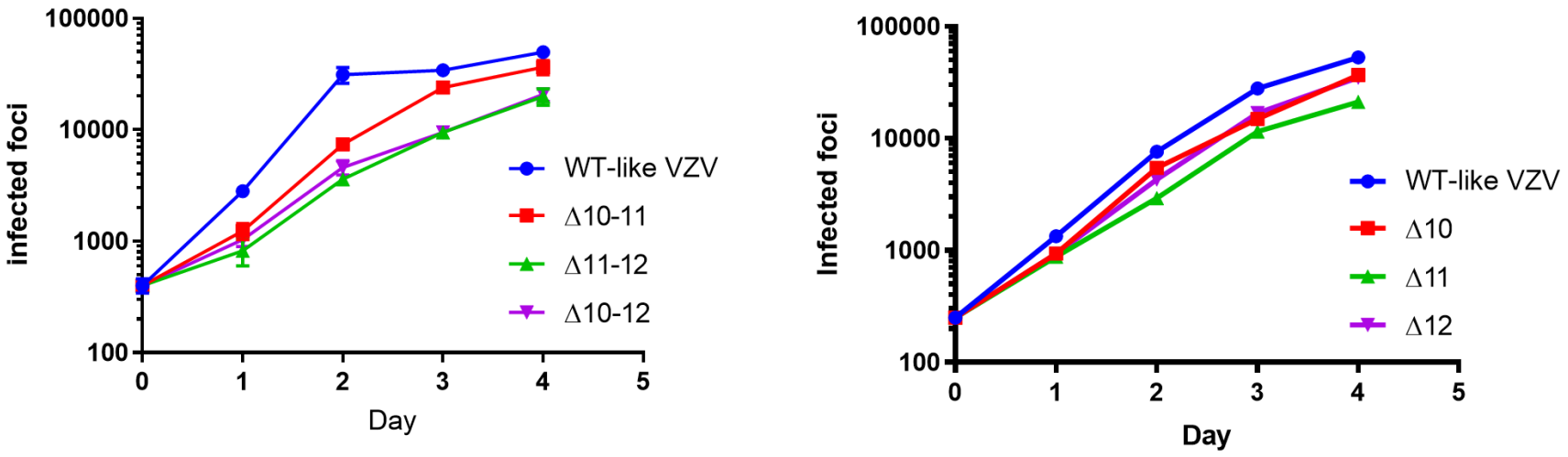

Figure 24 Growth rate comparisons of Δ10, 11, 12, Δ10-11, Δ11-12, and Δ10-12 VZV mutants in ARPE-19 cells. Low-MOI growth curves of recombinant VZV were assessed by plaque assay to enumerate the number of infectious centers over time, using conditions detailed previously. Viruses shown in each graph were assessed in parallel in triplicate from two replicates per time point, and compared to the growth of WT-like control VZV (VZV 66GFP). Growth curves were initiated with pre-frozen, pre-titrated cell associated stocks and then were normalized to the WT-like VZV66GFP input after the titration of virus at day 0. Each graph represents at one of least two independent experiments. Error bars represent standard error from the mean.

We next assessed growth and spread of these different recombinant VZV in hESC-derived neurons, using pretitrated and prewashed cell-associated and mitomycin C-treated infected ARPE-19 cells, to initiate an infection with 200 pfu per 12-well neuron culture. For single gene deletion viruses, we visualized evidence of growth and spread after four days (Fig 25a). For VZV with combinations of gene deletions, live cell microscopy using positional memory software was employed to gauge growth over 18 days, in a similar manner as we previously described (Fig 25b). After day 18, samples were fixed with 4% PFA, permeabilized, and stained for DAPI (nucleus) and βIII tubulin (neurons). The data show that VZV Δ10-11 replicated and spread much like the WT virus in neurons. However, VZV Δ11-12 did not replicate or spread to any significant degree in any of the neuron cultures tested, despite showing efficient replication in epithelial cell culture. Interestingly, a VZV in which the entire Δ10-12 cassette was deleted, was still able to replicate and spread in neuronal cells, although it showed a marked 4-5 day delay in the initiation of growth when compared to WT-like controls, and no red fluorescence was seen until later times in the infected neuron cultures. We conclude from these early preliminary studies that there are unresolved interactions between these proteins that may manifest in neurons. Future studies will aim to determine if the deletion of the 11, 12 and combination of the 10-12 cluster can restore the loss of the virion IE62 transactivator in influencing neuronal growth.

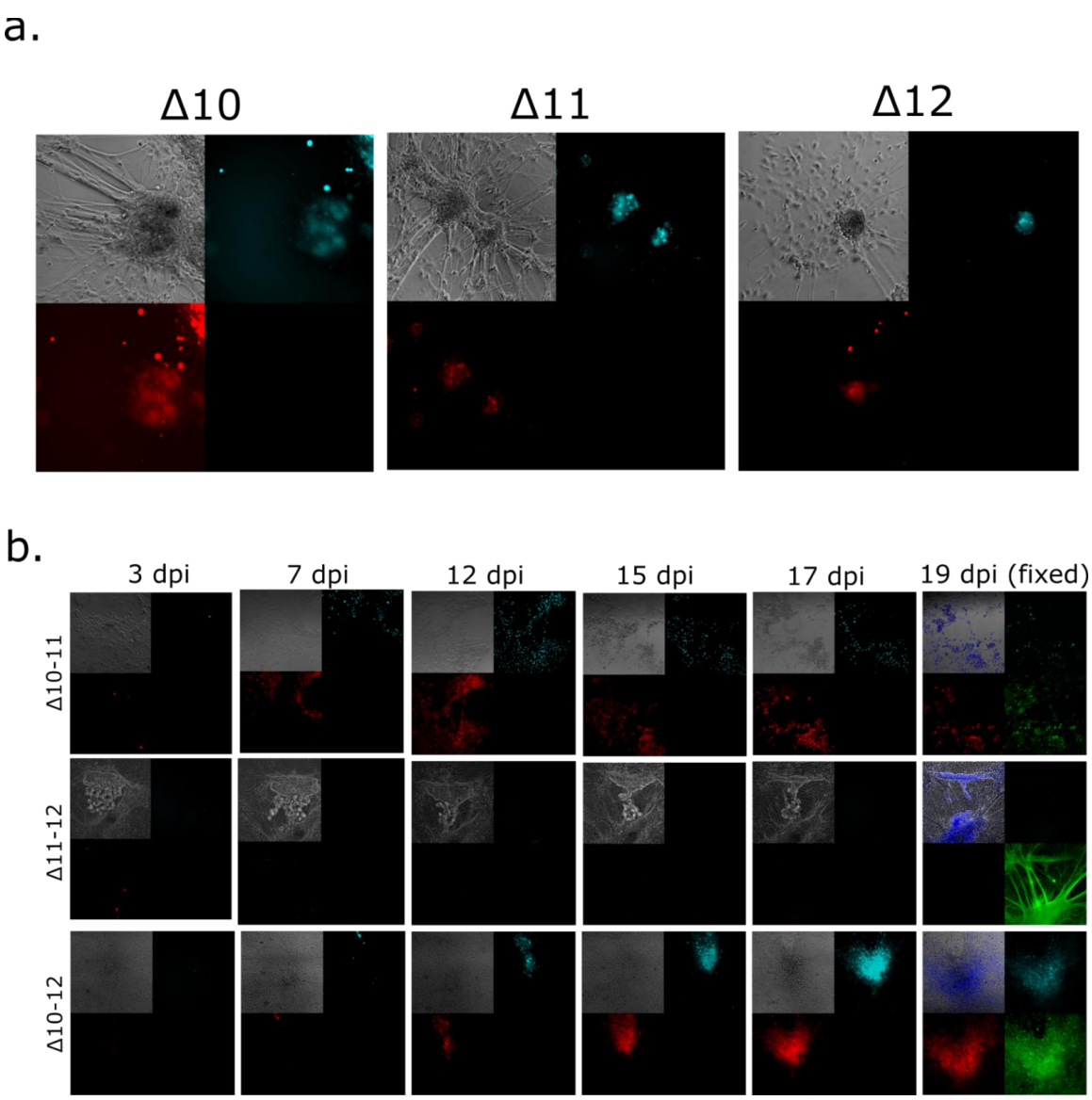

Figure 25 Time course of lytic infection and spread of recombinant VZV in hESC-derived neuron cultures imaged by live cell microscopy. (a) shows evidence of spread in neuron cultures infected with 200 PFU of mitomycin C treated, cell-associated VZV, after four days. Upper left of each image=phase contrast image, upper right=Turq2-tagged gene deletions, lower left=mCherry tagged VZV capsids. (b) shows a comparison of expanding fluorescent foci for the three combinational VZV mutants in parallel, after initiating with 200PFU of mitomycin treated, VZV-infected ARPE-19 cells inoculated onto neuronal cultures in glass-bottom 12-well plates. Cultures were live-cell imaged for 18 days. Shown are representative locations over different times of a single position in the plate, but are representative of that seen at multiple positions. After day 18, neurons were fixed, permeabilized, and stained for DAPI (dark blue, overlayed onto phasae contrast images at 19dpi fixed images) and beta-III tubulin (green; lower right in 19dpi fixed images). Fluorescently tagged viruses were pseudo-colored to match their fluorescent tags (red=mCherry-tagged VZV capsid (lower left), Turquoise=Turq2-tagged gene deletions in VZV (upper right). Gray=phase contrast (upper left)), and images were taken at 10x magnification.

5.0 Summary and Future Perspectives

We determined that VZV IE62 plays an important role in neuronal lytic infection and spread, and that in virions lacking both ORF10 protein and containing the 62-S686A point mutation (which typically prevents canonical packaging of IE62 into progeny virions), a yet unknown mechanism allows for completely IE62 to appear to associate with the virion tegument, presumably due to its importance in infection. We have also presented a novel method for the targeting of ORF62/71 for VZV genome inactivation using AAV-delivered CRISPR/Cas9, which is a potential promising antiviral strategy for targeting VZV genomes in both epithelial and neuronal tissue types.

Our data indicates that virion IE62 is critical for neuronal lytic infection, as absence of this protein in virions severely curtails neuronal spread, although it doesn't completely eradicate it. This is presumably because presence of other transactivators such as ORF10 protein might serve limited overlapping functions and/or interact with some of the same cellular factors, in aiding neuronal viral replication. In further examining which combination of transactivators is critical for neuronal replication, we have also generated mutant VZV lacking ORFs 11, 12, and combinations of 10-12 (i.e. 10-11, 1-12and 10-12) deleted in a WT-like background, since 11 and 12 encode additional tegument proteins [55], and there is some evidence suggesting that their HSV homologs (UL 46 and 47) regulate VP16 activity and contribute to IE gene expression [58], [59]. We have shown that all mutants (except VZV 62-S686A and Δ11-12) grow similar to WT-like kinetics, and while 62-S686A VZV had quite impaired neuronal spread and VZV, Δ11-12 failed to even grow in neuron cultures. All other mutants in the study were able to replicate and spread relatively efficiently in neurons. Interestingly, although these two VZV was unable to undergo efficient

neuronal replication, both VZV Δ10+62-S686A and VZV Δ10-12 containing additional deletions were able to replicate with increased efficiency, albeit the latter virus did demonstrate an apparent delayed spread compared to WT VZV. Perhaps one explanation for this is that deletion of certain gene combinations triggers yet unknown compensatory changes in the tegument, resulting in changes in the relative amounts or functions of other tegument components. Future studies could focus on starting to uncover the mechanism by which such compensatory or overlapping functions could restore neuronal spread, perhaps by initially generating all these ORFs 10-12 deletion mutants in an ORF62-S686A background to assess whether various combinations of these deletions with the 62-S686A mutation affects replication or reactivation from latency in neurons, or the presence of compensatory IE62 packaging into virion teguments.

The surprising result that loss of growth with the introduction of the 62-S686A mutation that is not maintained when ORF10 is subsequently deleted in this background could suggest that the sequential deletion of both transactivators resulted in compensatory changes that may influence the virion tegument. Certainly, such changes have been previously documented in HSV-1, PRV, as well as VZV [39], [44], [87], [368]–[370]. Though we were confident in detecting significant presence of IE62 in our Δ10/62-S686A double mutant virions (vs absence in 62-S686A-only VZV), we do acknowledge that investigating virion tegument changes in our study has been extremely challenging due to the difficulty in completely purifying VZV virions, which made mass spectroscopy analysis not ideal. One idea to circumvent this problem would be to utilize electron microscopy and immunogold labeling to visualize IE62 (as well as other tegument proteins of interest) in our virion particles, to both confirm our observation that there is compensatory IE62 in the tegument of double mutant virions, as well as to identify and assess any changes in the relative quantities of other tegument proteins in response to the various deletions of our mutant

viruses. Obviously, this would require the appropriate facilities, as well as further training and expertise in electron microscopy techniques and data analysis. We could also re-examine the previously published and described ORF66 kinase-deleted virus, and see if deletion of ORF66 in conjunction with ORF 10 triggers a similar compensatory response in regards to IE62 accumulation in double mutant virions, as our previous studies have demonstrated that ORF66 deletion leads to absence of S686 phosphorylated (cytoplasmic) IE62, and thus, absence of virion IE62 [87]. Another idea is that since HSV ICP4 and VZV IE62 share over 50% homology and VZV IE62 is able to transactivate HSV genomes, one could identify the NLS region in ICP4 and make a similar "S686A"-like mutation to affect the charges adjacent to the ICP4 NLS signal, effectively making an HSV version of the VZV 62-S686A packaging mutant. If this works, HSV virions are much more efficient to purify than VZV virions [16], [289], [292], [386]. Downstream quantification and mass spectroscopy analyses might be more feasible with these HSV preps, allowing us to assess virion tegument contents more readily and without the need for electron microscopy. Future studies should focus on investigating potential pathways by which nuclear IE62 can be incorporated into these Δ10+62-S686A virions, since our studies have shown that no cytoplasmic IE62 is present in such infected cells, implying there is a novel pathway by which this is occurring.

We determined the importance of VZV IE62 in neuronal lytic infection and spread, but one of the remaining challenges is assessing the role of such virion transactivators in reactivation from latency. This is largely due to difficulty in efficiently reactivating the hESC-neuron cultures. Unfortunately, this is not a unique problem in the field, as other groups using similar neuron-based *in vitro* models have reported similarly inefficient reactivation rates [157]. With our current protocol, we have optimized neuron culture reactivation rates to an estimated 1 in 4 culture wells,

but future work could focus on further optimizing latency and reactivation, perhaps using both a more effective strategy for establishing latency as well as more optimized concentrations and combinations of reactivation stimuli, including less well-characterized ones.

For more effective methods of establishing latency, we have been exploring the use of 5uM brivudine (BVDU), which is more efficient than acyclovir at establishing latent infections. However, since both these drugs are chain-terminating nucleoside analogs that incorporate into viral genomes, a concern with their use is that viral genomes will inefficiently reactivate due to some of them being damaged by the drug. For this reason, we have also been exploring cell-free axonal infections in the absence of ACV or BVDU, in our previously characterized compartmentalized chambers that separate neuronal soma from the axon termini [183]. Since the site for HSV-1 entry into neurons is crucial in determining whether sufficient transactivation of IE genes occurs to support lytic replication versus latent infection, it is very plausible that initiating cell-free infections from the axon termini will strongly encourage a latent infection [104]–[106].

In terms of optimizing reactivation from latency, further optimizing various concentrations and combinations of reactivation stimuli might be worthwhile. For example, we are currently investigating less well-characterized reactivation stimuli such as 42^{o}C heat shock treatment, arsenic trioxide, and TPA, the latter two of which that have not been extensively used for VZV reactivation, but has shown promise in reactivating other herpesviruses [387]–[394]. Another promising method to optimize reactivation replies on the fact that reactivation in HSV is proposed to be a two-stage process, in which expression of the IE gene activator VP16 is a decision point [102], [106], [165], [166]. Since VZV shares a high degree of homology with HSV and in HSV, exogenous expression of HSV ICP0 (homolog to VZV ORF61) is known to reactivate latent VZV [395], we have generated multiple AAV2 vectors expressing HSV ICP0, VZV ORFs 10, 61, and

the N-terminal activation domain of ORF62 under tetracycline-inducible promoters, for delivery into neurons **(**the IE62 gene is too large to fully package into AAV, but we have found that IE62 residues 1-840 can stimulate promoter-reporter genes in co transfection assays). Future work could involve assessing if these constructs can aid in increasing reactivation efficiency in latently infected neuron cultures. Finally, we can look into using other types of neuronal model systems for our studies, this may include organoid systems or other types of neurons; most recently, we have examined SH-SY5Y and LUHMES neurons. SH-SY5Y neuron-like cells are derived from neuroblastoma bone marrow biopsies. Although these cells lack certain characteristics of mature human ganglionic neurons, VZV have been reported to lytically replicate and spread in differentiated SH-SY5Y cultures [282]. However, more work is needed to assess whether a reactivable latent infection can be established in these neurons. LUHMES CNS-derived neurons have previously been shown to successfully host both lytic as well as latent and reactivable HSV infections [396]. In VZV, ongoing work from our lab has provided evidence that these cells cans support both a productive VZV lytic infection, as well as a latent infection that can be experimentally reactivated. Furthermore, LUHMES neurons can also be grown in compartmentalized chambers which separate neuronal soma from axonal termini, much like the hESC-derived neurons. Future work on this front might reveal relative reactivation efficiency differences between latent LUHMES infections versus hESC-derived neuron infections.

VZV IE62 undoubtedly plays many important roles in viral pathogenesis, from IE gene transactivation [54], [77], to host immune system evasion [52], to neuronal replication and spread. As a proof-of-concept study, we have shown that targeting ORFs 62/71 using AAV2-delivered CRISPR/Cas9 successfully decreases VZV infectivity in both lytic infection of epithelial and neuronal cells, as well as latently infected and subsequently reactivated neuronal infections [265].

This can potentially be adapted in the future for use as an antiviral strategy to complement current available treatments. In our study, we have examined the on-targeting ability of our construct by noting its inability to reduce VZV replication in multiple experiments, when we mutated the Cas9 recognition site in our VZV DR-62gmut viruses. However, if we wanted to further pursue this idea as a potential antiviral therapeutic, we could employ additional methods to further verify that our Cas9 cleaved the intended target sites, perhaps by performing a T7 endonuclease assay to look for mutational mismatches, or deep sequencing to visualize indels at the cleavage sites. For added effect in targeting VZV genomes for inactivation, we could also encode for multiple gRNA sequences, focusing on targeting duplicated, essential, and/or IE VZV genes, since these would make the biggest impact in hindering VZV replication. ORFs 63/70 would be an excellent target here, especially since preliminary transfection studies of ORF63/70-targeting saCas9 constructs were able to decrease signal of the target gene. Since the packaging limit of AAV is less than 5kb and adding additional gRNAs would probably put the total transgene size at greater than this limit, dual AAV systems can also be considered, whereby the transgene is split into two (with appropriate recombination sequences, splice donor and/or acceptor sites) and recombined into a single product after successful co-transduction of both vectors. The gRNAs can also be placed into one AAV vector and the saCas9 in another, although a consideration with both these strategies is that transduction with extremely high levels of AAVs can cause cell toxicity and trigger host cellular immune responses, due to the large amounts of ssDNA and protein that would be introduced. Finally, we can consider the use of either a smaller Cas molecule such as CasPhi or CasMINI [397], [398], or a bigger delivery vector that can accommodate multiple transgenes at once, such as the most recent iteration of the HSV vector (JΔNI8), which is naturally neurotrophic, minimally toxic to human cells, and can accommodate huge transgene inserts and multiple genes [399]–[403].

In addition to on-targeting effects, it would be a good idea to consider the off-targeting effects of saCas9 as well, since long-term Cas9 expression increases the likelihood of off-targeting, which can cause large deletions and complex rearrangements in the host genome [404]–[407]. Currently, many different computational, single-molecule, and *in vitro* bulk assay approaches have been developed for assessing off-targeting in a variety of experimental settings [408]. These methods often require specialized training and bioinformatics knowledge, but include CHIP-seq and GUIDE-seq, digenome-seq, DISCOVER-seq, *in silico* predictions, etc.… If our saCas9 had an unacceptably high off-targeting rate for therapeutic use, we could also consider replacing our saCas9 with a higher fidelity version of Cas molecule, of which there are many variants available to choose from (such as SpCas9-HF1, HypaCas9, cvoCas9, or HiFi Cas9) [409]–[414]. These Cas9 variants are often derived from directed evolution experiments, and contain amino acid substitutions that further enhance specificity and target recognition [415], [416]. Another consideration with regards to on/off targeting and Cas9 cleavage is that the methylation status of DNA at CpG sites may impede binding and cleavage efficiency of Cas9 in cells, although the degree of genome accessibility to Cas depends on a variety of different factors [417].

For our studies, we used AAV2, which worked well in transducing our tissue types of interest (i.e. neurons and VZV-permissive epithelial cells). However, because AAV2 binds heparan sulfate proteoglycans on host cells and thus has an extremely broad tissue tropism [418], [419], it would not be ideal for use therapeutically in patients, since AAV2 could theoretically transduce and cause mutations in germline cells as well. For this reason, future studies should also focus on optimizing the delivery vehicle for our CRISPR/Cas9 construct. For more optimal AAV tissue specificity, one can consider modifying the transgene plasmid so that the Cas9 is expressed under a tissue-specific promotor, perhaps by using a system such as Cre/loxP. We can also consider

optimizing the AAV serotype, since recent advances in directed evolution of capsid proteins have uncovered many additional recombinant serotypes for therapeutic use. Finally, for more transient Cas9 expression, especially in low-turnover neuronal cells, it might be beneficial to utilize an inducible promotor such as the tet on/off system, or even consider an alternate system utilizing direct protein transduction, such as an integrase defective, replication deficient lentiviral system. In the latter system, on e could conjugate Cas9 protein with *Vpr* or *Gag* (*Vpr* naturally binds *gag* during virion assembly, so the proteins will get packaged this way), include the gRNA genes in the expression plasmid along with a reporter if desired, pseudotype the envelope plasmid to express the neurotropic rabies G protein for neuron targeting, and perform either a three plasmid or four plasmid (if using *Vpr*) co-transfection protocol on packaging cell lines to produce neurotrophic replication defective lentiviral particles that encode gRNA and package Cas9 RNP, but do not encode the actual Cas9 genes, resulting in only transient Cas expression in the tissue types of interest [420]–[422].

Bibliography

[1] A. J. Davison *et al.*, "The order Herpesvirales," *Arch. Virol.*, vol. 154, no. 1, pp. 171–177, Jan. 2009.

[2] C. M. Zmasek, D. M. Knipe, P. E. Pellett, and R. H. Scheuermann, "Classification of human Herpesviridae proteins using Domain-architecture Aware Inference of Orthologs (DAIO)," *Virology*, vol. 529, pp. 29–42, Mar. 2019.

[3] P. E. Pellett and B. Roizman, *Fields Virology*, 6th ed. Philadelphia: Lippincott Williams & Wilkins, 2014.

[4] A. W. Kolb, A. C. Lewin, R. Moeller Trane, G. J. McLellan, and C. R. Brandt, "Phylogenetic and recombination analysis of the herpesvirus genus varicellovirus," *BMC Genomics*, vol. 18, no. 1, pp. 1–17, Nov. 2017.

[5] J. I. Cohen, "The Varicella-Zoster Virus Genome," *Curr. Top. Microbiol. Immunol.*, vol. 342, p. 1, 2010.

[6] S. A. Jackson and N. A. DeLuca, "Relationship of herpes simplex virus genome configuration to productive and persistent infections," *Proc. Natl. Acad. Sci. U. S. A.*, vol. 100, no. 13, pp. 7871–7876, Jun. 2003.

[7] C. Grose *et al.*, "Complete DNA Sequence Analyses of the First Two Varicella-Zoster Virus Glycoprotein E (D150N) Mutant Viruses Found in North America: Evolution of Genotypes with an Accelerated Cell Spread Phenotype," *J. Virol.*, vol. 78, no. 13, p. 6799, Jul. 2004.

[8] P. R. Kinchington, W. C. Reinhold, T. A. Casey, S. E. Straus, J. Hay, and W. T. Ruyechan, "Inversion and circularization of the varicella-zoster virus genome," *J. Virol.*, vol. 56, no. 1, pp. 194–200, Oct. 1985.

[9] P. Sheldrick and N. Berthelot, "Inverted repetitions in the chromosome of herpes simplex virus," *Cold Spring Harb. Symp. Quant. Biol.*, vol. 39 Pt 2, no. 2, pp. 667–678, 1975.

[10] S. E. Straus *et al.*, "Structure of varicella-zoster virus DNA," *J. Virol.*, vol. 40, no. 2, pp. 516–525, Nov. 1981.

[11] C. Mahiet *et al.*, "Structural Variability of the Herpes Simplex Virus 1 Genome In Vitro and In Vivo," *J. Virol.*, vol. 86, no. 16, p. 8592, Aug. 2012.

[12] G. S. Hayward, R. J. Jacob, S. C. Wadsworth, and B. Roizman, "Anatomy of herpes simplex virus DNA: evidence for four populations of molecules that differ in the relative orientations of their long and short components," *Proc. Natl. Acad. Sci. U. S. A.*, vol. 72, no. 11, pp. 4243–4247, 1975.

[13] J. R. Ecker and R. W. Hyman, “Varicella zoster virus DNA exists as two isomers,” *Proc. Natl. Acad. Sci. U. S. A.*, vol. 79, no. 1, pp. 156–160, 1982.

[14] B. B. Kaufer, B. Smejkal, and N. Osterrieder, “The Varicella-Zoster Virus ORFS/L (ORF0) Gene Is Required for Efficient Viral Replication and Contains an Element Involved in DNA Cleavage,” *J. Virol.*, vol. 84, no. 22, p. 11661, Nov. 2010.

[15] E. Eshleman, A. Shahzad, and R. J. Cohrs, “Varicella zoster virus latency,” *Future Virol.*, vol. 6, no. 3, p. 341, Mar. 2011.

[16] A. J. Davison and J. E. Scott, “The complete DNA sequence of varicella-zoster virus,” *J. Gen. Virol.*, vol. 67 (Pt 9), no. 9, pp. 1759–1816, 1986.

[17] N. D. Stow and A. J. Davison, “Identification of a varicella-zoster virus origin of DNA replication and its activation by herpes simplex virus type 1 gene products,” *J. Gen. Virol.*, vol. 67, no. 8, pp. 1613–1623, Aug. 1986.

[18] N. D. Stow, “Localization of an origin of DNA replication within the TRS/IRS repeated region of the herpes simplex virus type 1 genome.,” *EMBO J.*, vol. 1, no. 7, p. 863, 1982.

[19] M. I. Khalil, M. H. Sommer, J. Hay, W. T. Ruyechan, and A. M. Arvin, “Varicella-zoster virus (VZV) origin of DNA replication oriS influences origin-dependent DNA replication and flanking gene transcription,” *Virology*, vol. 481, pp. 179–186, Jul. 2015.

[20] Z. Zhang *et al.*, “Genome-wide mutagenesis reveals that ORF7 is a novel VZV skin-tropic factor,” *PLoS Pathog.*, vol. 6, no. 7, pp. 1–9, Jul. 2010.

[21] A. M. Arvin and D. Gilden, *Fields Virology*, 6th ed. Philadelphia: Lippincott Williams & Wilkins, 2013.

[22] J. I. Cohen, “The varicella-zoster virus genome.,” *Curr. Top. Microbiol. Immunol.*, vol. 342, pp. 1–14, 2010.

[23] G. W. Kemble *et al.*, “Open Reading Frame S/L of Varicella-Zoster VirusEncodes a Cytoplasmic Protein Expressed in Infected Cells,” *J. Virol.*, vol. 74, no. 23, p. 11311, Dec. 2000.

[24] E. Cox, S. Reddy, I. Iofin, and J. I. Cohen, “Varicella-zoster virus ORF57, unlike its pseudorabies virus UL3.5 homolog, is dispensable for viral replication in cell culture,” *Virology*, vol. 250, no. 1, pp. 205–209, Oct. 1998.

[25] J. I. Cohen and K. E. Seidel, “Varicella-zoster virus open reading frame 1 encodes a membrane protein that is dispensable for growth of VZV in vitro,” *Virology*, vol. 206, no. 2, pp. 835–842, Feb. 1995.

[26] H. Sato, L. Pesnicak, and J. I. Cohen, “Varicella-Zoster Virus Open Reading Frame 2 Encodes a Membrane Phosphoprotein That Is Dispensable for Viral Replication and for Establishment of Latency,” *J. Virol.*, vol. 76, no. 7, pp. 3575–3578, Apr. 2002.

[27] J. I. Cohen and K. E. Seidel, “Generation of varicella-zoster virus (VZV) and viral mutants from cosmid DNAs: VZV thymidylate synthetase is not essential for replication in vitro.,” *Proc. Natl. Acad. Sci. U. S. A.*, vol. 90, no. 15, p. 7376, 1993.

[28] S. M. Reddy, E. Cox, I. Iofin, W. Soong, and J. I. Cohen, “Varicella-Zoster Virus (VZV) ORF32 Encodes a Phosphoprotein That Is Posttranslationally Modified by the VZV ORF47 Protein Kinase,” *J. Virol.*, vol. 72, no. 10, p. 8083, Oct. 1998.

[29] B. R. Bowman, M. L. Baker, F. J. Rixon, W. Chiu, and F. A. Quiocho, “Structure of the herpesvirus major capsid protein,” *EMBO J.*, vol. 22, no. 4, p. 757, Feb. 2003.

[30] Z. H. Zhou, M. Dougherty, J. Jakana, H. Jing, F. J. Rixon, and W. Chiu, “Seeing the herpesvirus capsid at 8.5 A,” *Science*, vol. 288, no. 5467, pp. 877–880, May 2000.

[31] N. H. Mueller, D. H. Gilden, R. J. Cohrs, R. Mahalingam, and M. A. Nagel, “Varicella Zoster Virus Infection: Clinical Features, Molecular Pathogenesis of Disease, and Latency,” *Neurol. Clin.*, vol. 26, no. 3, p. 675, Aug. 2008.

[32] E. Kut and D. Rasschaert, “Assembly of Marek’s disease virus (MDV) capsids using recombinant baculoviruses expressing MDV capsid proteins,” *J. Gen. Virol.*, vol. 85, no. Pt 4, pp. 769–774, Apr. 2004.

[33] T. del Rio, T. H. Ch’ng, E. A. Flood, S. P. Gross, and L. W. Enquist, “Heterogeneity of a fluorescent tegument component in single pseudorabies virus virions and enveloped axonal assemblies,” *J. Virol.*, vol. 79, no. 7, pp. 3903–3919, Apr. 2005.

[34] G. H. Cohen, M. Ponce de Leon, H. Diggelmann, W. C. Lawrence, S. K. Vernon, and R. J. Eisenberg, “Structural analysis of the capsid polypeptides of herpes simplex virus types 1 and 2,” *J. Virol.*, vol. 34, no. 2, pp. 521–531, May 1980.

[35] M. A. Visalli, B. L. House, A. Selariu, H. Zhu, and R. J. Visalli, “The varicella-zoster virus portal protein is essential for cleavage and packaging of viral DNA,” *J. Virol.*, vol. 88, no. 14, pp. 7973–7986, Jul. 2014.

[36] W. Gibson, “Structure and assembly of the virion,” *Intervirology*, vol. 39, no. 5–6, pp. 389–400, 1996.

[37] R. Lippé, “Characterization of Extracellular HSV-1 Virions by Proteomics,” *Methods Mol. Biol.*, vol. 1144, pp. 181–190, 2014.

[38] S. Loret, G. Guay, and R. Lippé, “Comprehensive characterization of extracellular herpes simplex virus type 1 virions,” *J. Virol.*, vol. 82, no. 17, pp. 8605–8618, Sep. 2008.

[39] G. W. G. Luxton, S. Haverlock, K. E. Coller, S. E. Antinone, A. Pincetic, and G. A. Smith, “From the Cover: Targeting of herpesvirus capsid transport in axons is coupled to association with specific sets of tegument proteins,” *Proc. Natl. Acad. Sci. U. S. A.*, vol. 102, no. 16, p. 5832, Apr. 2005.

[40] A. Wolfstein, C. H. Nagel, K. Radtke, K. Döhner, V. J. Allan, and B. Sodeik, “The inner tegument promotes herpes simplex virus capsid motility along microtubules in vitro,” *Traffic*, vol. 7, no. 2, pp. 227–237, Feb. 2006.

[41] K. E. Coller and G. A. Smith, “Two viral kinases are required for sustained long-distance axon transport of a neuroinvasive herpesvirus,” *Traffic*, vol. 9, no. 9, p. 1458, 2008.

[42] K. Radtke *et al.*, “Plus- and minus-end directed microtubule motors bind simultaneously to herpes simplex virus capsids using different inner tegument structures,” *PLoS Pathog.*, vol. 6, no. 7, pp. 1–20, Jul. 2010.

[43] M. Sandbaumhüter *et al.*, “Cytosolic herpes simplex virus capsids not only require binding inner tegument protein pUL36 but also pUL37 for active transport prior to secondary envelopment,” *Cell. Microbiol.*, vol. 15, no. 2, pp. 248–269, Feb. 2013.

[44] W. Wang, T. Cheng, H. Zhu, and N. Xia, “Insights into the function of tegument proteins from the varicella zoster virus.,” *Sci. China. Life Sci.*, vol. 58, no. 8, pp. 739–49, Aug. 2015.

[45] P. Defechereux, L. Melen, L. Baudoux, M. Merville-louis, B. Rentier, and J. Pie, “Characterization of the regulatory functions of varicella-zoster virus open reading frame 4 gene product,” *J. Virol.*, vol. 67, no. 7, pp. 4379–4385, Jul. 1993.

[46] H. Moriuchi, M. Moriuchi, H. A. Smith, and J. I. Cohen, “Varicella-zoster virus open reading frame 4 protein is functionally distinct from and does not complement its herpes simplex virus type 1 homolog, ICP27,” *J. Virol.*, vol. 68, no. 3, pp. 1987–1992, Mar. 1994.

[47] L. P. Perera, J. D. Mosca, M. Sadeghi-Zadeh, W. T. Ruyechan, and J. Hay, “The Varicella-Zoster virus immediate early protein, IE62, can positively regulate its cognate promoter,” *Virology*, vol. 191, no. 1, pp. 346–354, Nov. 1992.

[48] B. Sato, H. Ito, S. Hinchliffe, M. H. Sommer, L. Zerboni, and A. M. Arvin, “Mutational analysis of open reading frames 62 and 71, encoding the varicella-zoster virus immediate-early transactivating protein, IE62, and effects on replication in vitro and in skin xenografts in the SCID-hu mouse in vivo,” *J. Virol.*, vol. 77, no. 10, pp. 5607–5620, May 2003.

[49] B. Sato, M. Sommer, H. Ito, and A. M. Arvin, “Requirement of Varicella-Zoster Virus Immediate-Early 4 Protein for Viral Replication,” *J. Virol.*, vol. 77, no. 22, p. 12369, Nov. 2003.

[50] S. E. Hoover, R. J. Cohrs, Z. G. Rangel, D. H. Gilden, P. Munson, and J. I. Cohen, “Downregulation of varicella-zoster virus (VZV) immediate-early ORF62 transcription by VZV ORF63 correlates with virus replication in vitro and with latency,” *J. Virol.*, vol. 80, no. 7, pp. 3459–3468, Apr. 2006.

[51] L. Yang *et al.*, “Innate Immune Evasion of Alphaherpesvirus Tegument Proteins,” *Front. Immunol.*, vol. 10, Sep. 2019.

[52] N. Sen, M. Sommer, X. Che, K. White, W. T. Ruyechan, and A. M. Arvin, “Varicella-zoster

virus immediate-early protein 62 blocks interferon regulatory factor 3 (IRF3) phosphorylation at key serine residues: a novel mechanism of IRF3 inhibition among herpesviruses.," *J. Virol.*, vol. 84, no. 18, pp. 9240–53, Sep. 2010.

[53] A. P. N. Ambagala and J. I. Cohen, "Varicella-Zoster virus IE63, a major viral latency protein, is required to inhibit the alpha interferon-induced antiviral response.," *J. Virol.*, vol. 81, no. 15, pp. 7844–51, Aug. 2007.

[54] P. R. Kinchington, J. K. Hougland, A. M. Arvin, W. T. Ruyechan, and J. Hay, "The varicella-zoster virus immediate-early protein IE62 is a major component of virus particles.," *J. Virol.*, vol. 66, no. 1, pp. 359–366, 1992.

[55] X. Che, M. Reichelt, M. H. Sommer, J. Rajamani, L. Zerboni, and A. M. Arvin, "Functions of the ORF9-to-ORF12 gene cluster in varicella-zoster virus replication and in the pathogenesis of skin infection.," *J. Virol.*, vol. 82, no. 12, pp. 5825–34, 2008.

[56] L. Riva *et al.*, "ORF9p Phosphorylation by ORF47p Is Crucial for the Formation and Egress of Varicella-Zoster Virus Viral Particles," *J. Virol.*, vol. 87, no. 5, pp. 2868–2881, Mar. 2013.

[57] C. Cilloniz, W. Jackson, C. Grose, D. Czechowski, J. Hay, and W. T. Ruyechan, "The Varicella-Zoster Virus (VZV) ORF9 Protein Interacts with the IE62 Major VZV Transactivator," *J. Virol.*, vol. 81, no. 2, pp. 761–774, Jan. 2007.

[58] J. L. McKnight, P. E. Pellett, F. J. Jenkins, and B. Roizman, "Characterization and nucleotide sequence of two herpes simplex virus 1 genes whose products modulate alpha-trans-inducing factor-dependent activation of alpha genes.," *J. Virol.*, vol. 61, no. 4, pp. 992–1001, Apr. 1987.

[59] Y. Zhang, D. A. Sirko, and J. L. McKnight, "Role of herpes simplex virus type 1 UL46 and UL47 in alpha TIF-mediated transcriptional induction: characterization of three viral deletion mutants.," *J. Virol.*, vol. 65, no. 2, pp. 829–41, Feb. 1991.

[60] A. Erazo and P. R. Kinchington, "Varicella-zoster virus open reading frame 66 protein kinase and its relationship to alphaherpesvirus US3 kinases," *Curr. Top. Microbiol. Immunol.*, vol. 342, pp. 79–98, 2010.

[61] E. Gershburg and J. S. Pagano, "Conserved herpesvirus protein kinases," *Biochim. Biophys. Acta*, vol. 1784, no. 1, p. 203, Jan. 2008.

[62] J. Besser *et al.*, "Differentiation of varicella-zoster virus ORF47 protein kinase and IE62 protein binding domains and their contributions to replication in human skin xenografts in the SCID-hu mouse," *J. Virol.*, vol. 77, no. 10, pp. 5964–5974, May 2003.

[63] A. Selariu *et al.*, "ORF7 of Varicella-Zoster Virus Is a Neurotropic Factor," *J. Virol.*, vol. 86, no. 16, pp. 8614–8624, Aug. 2012.

[64] W. Wang *et al.*, "Development of a skin- and neuro-attenuated live vaccine for varicella,"

Nat. Commun., vol. 13, no. 1, Dec. 2022.

[65] S. L. Oliver, E. Yang, and A. M. Arvin, "Varicella-Zoster Virus Glycoproteins: Entry, Replication, and Pathogenesis," *Curr. Clin. Microbiol. reports*, vol. 3, no. 4, pp. 204–215, Dec. 2016.

[66] A. Jacquet *et al.*, "The varicella zoster virus glycoprotein B (gB) plays a role in virus binding to cell surface heparan sulfate proteoglycans," *Virus Res.*, vol. 53, no. 2, pp. 197–207, Feb. 1998.

[67] K. M. Haan, S. Kyeong Lee, and R. Longnecker, "Different functional domains in the cytoplasmic tail of glycoprotein B are involved in Epstein-Barr virus-induced membrane fusion," *Virology*, vol. 290, no. 1, pp. 106–114, Nov. 2001.

[68] M. I. Muggeridge, "Characterization of cell-cell fusion mediated by herpes simplex virus 2 glycoproteins gB, gD, gH and gL in transfected cells," *J. Gen. Virol.*, vol. 81, no. Pt 8, pp. 2017–2027, 2000.

[69] P. E. Pertel, "Human herpesvirus 8 glycoprotein B (gB), gH, and gL can mediate cell fusion," *J. Virol.*, vol. 76, no. 9, pp. 4390–4400, May 2002.

[70] P. E. Pertel, A. Fridberg, M. L. Parish, and P. G. Spear, "Cell fusion induced by herpes simplex virus glycoproteins gB, gD, and gH-gL requires a gD receptor but not necessarily heparan sulfate," *Virology*, vol. 279, no. 1, pp. 313–324, Jan. 2001.

[71] S. A. Connolly, J. O. Jackson, T. S. Jardetzky, and R. Longnecker, "Fusing structure and function: a structural view of the herpesvirus entry machinery," *Nat. Rev. Microbiol.*, vol. 9, no. 5, pp. 369–381, May 2011.

[72] S. E. Vleck *et al.*, "Structure-function analysis of varicella-zoster virus glycoprotein H identifies domain-specific roles for fusion and skin tropism," *Proc. Natl. Acad. Sci. U. S. A.*, vol. 108, no. 45, pp. 18412–18417, Nov. 2011.

[73] T. Suenaga, T. Satoh, P. Somboonthum, Y. Kawaguchi, Y. Mori, and H. Arase, "Myelin-associated glycoprotein mediates membrane fusion and entry of neurotropic herpesviruses," *Proc. Natl. Acad. Sci. U. S. A.*, vol. 107, no. 2, pp. 866–871, 2010.

[74] P. R. Kinchington, J. P. Vergnes, P. Defechereux, J. Piette, and S. E. Turse, "Transcriptional mapping of the varicella-zoster virus regulatory genes encoding open reading frames 4 and 63," *J. Virol.*, vol. 68, no. 6, pp. 3570–3581, Jun. 1994.

[75] I. Ote *et al.*, "Varicella-Zoster Virus IE4 Protein Interacts with SR Proteins and Exports mRNAs through the TAP/NXF1 Pathway," *PLoS One*, vol. 4, no. 11, Nov. 2009.

[76] C. Hood *et al.*, "Varicella-zoster virus ORF63 inhibits apoptosis of primary human neurons," *J. Virol.*, vol. 80, no. 2, pp. 1025–1031, Jan. 2006.

[77] M. Moriuchi, H. Moriuchi, S. E. Straus, and J. I. Cohen, "Varicella-Zoster Virus (VZV)

Virion-Associated Transactivator Open Reading Frame 62 Protein Enhances the Infectivity of VZV DNA," *Virology*, vol. 200, no. 1, pp. 297–300, Apr. 1994.

[78] L. M. Wagner, A. Bayer, and N. A. DeLuca, "Requirement of the N-Terminal Activation Domain of Herpes Simplex Virus ICP4 for Viral Gene Expression," *J. Virol.*, vol. 87, no. 2, pp. 1010–1018, Jan. 2013.

[79] M. I. Khalil, M. Sommer, A. Arvin, J. Hay, and W. T. Ruyechan, "Cellular transcription factor YY1 mediates the varicella-zoster virus (VZV) IE62 transcriptional activation," *Virology*, vol. 449, pp. 244–253, Jan. 2014.

[80] W. T. Ruyechan, "Roles of cellular transcription factors in VZV replication," *Curr. Top. Microbiol. Immunol.*, vol. 342, pp. 43–65, 2010.

[81] S. Yamamoto, A. Eletsky, T. Szyperski, J. Hay, and W. T. Ruyechan, "Analysis of the varicella-zoster virus IE62 N-terminal acidic transactivating domain and its interaction with the human mediator complex," *J. Virol.*, vol. 83, no. 12, pp. 6300–6305, Jun. 2009.

[82] J. K. Tyler and R. D. Everett, "The DNA binding domains of the varicella-zoster virus gene 62 and herpes simplex virus type 1 ICP4 transactivator proteins heterodimerize and bind to DNA," *Nucleic Acids Res.*, vol. 22, no. 5, pp. 711–721, Mar. 1994.

[83] A. J. Eisfeld, S. E. Turse, S. A. Jackson, E. C. Lerner, and P. R. Kinchington, "Phosphorylation of the varicella-zoster virus (VZV) major transcriptional regulatory protein IE62 by the VZV open reading frame 66 protein kinase.," *J. Virol.*, vol. 80, no. 4, pp. 1710–23, Feb. 2006.

[84] P. R. Kinchington and S. E. Turse, "Regulated Nuclear Localization of the Varicella-Zoster Virus Major Regulatory Protein, IE62," *J. Infect. Dis.*, vol. 178, no. Supplement_1, pp. S16–S21, Nov. 1998.

[85] P. R. Kinchington, K. Fite, and S. E. Turse, "Nuclear Accumulation of IE62, the Varicella-Zoster Virus (VZV) Major Transcriptional Regulatory Protein, Is Inhibited by Phosphorylation Mediated by the VZV Open Reading Frame 66 Protein Kinase," *J. Virol.*, vol. 74, no. 5, pp. 2265–2277, Mar. 2000.

[86] P. R. Kinchington, K. Fite, A. Seman, and S. E. Turse, "Virion Association of IE62, the Varicella-Zoster Virus (VZV) Major Transcriptional Regulatory Protein, Requires Expression of the VZV Open Reading Frame 66 Protein Kinase," *J. Virol.*, vol. 75, no. 19, pp. 9106–9113, Oct. 2001.

[87] A. Erazo, M. B. Yee, N. Osterrieder, and P. R. Kinchington, "Varicella-zoster virus open reading frame 66 protein kinase is required for efficient viral growth in primary human corneal stromal fibroblast cells.," *J. Virol.*, vol. 82, no. 15, pp. 7653–65, 2008.

[88] J. I. Cohen and K. Seidel, "Varicella-zoster virus (VZV) open reading frame 10 protein, the homolog of the essential herpes simplex virus protein VP16, is dispensable for VZV replication in vitro.," *J. Virol.*, vol. 68, no. 12, pp. 7850–8, Dec. 1994.

[89] X. Che, L. Zerboni, M. H. Sommer, and A. M. Arvin, “Varicella-zoster virus open reading frame 10 is a virulence determinant in skin cells but not in T cells in vivo.,” *J. Virol.*, vol. 80, no. 7, pp. 3238–48, Apr. 2006.

[90] H. Moriuchi, M. Moriuchi, S. E. Straus, and J. I. Cohen, “Varicella-zoster virus open reading frame 10 protein, the herpes simplex virus VP16 homolog, transactivates herpesvirus immediate-early gene promoters.,” *J. Virol.*, vol. 67, no. 5, pp. 2739–46, May 1993.

[91] K. L. Mossman, R. Sherburne, C. Lavery, J. Duncan, and J. R. Smiley, “Evidence that Herpes Simplex Virus VP16 Is Required for Viral Egress Downstream of the Initial Envelopment Event,” *J. Virol.*, vol. 74, no. 14, pp. 6287–6299, Jul. 2000.

[92] G. Werstuck and J. P. Capone, “Mutational analysis of the herpes simplex virus trans-inducing factor Vmw65,” *Gene*, vol. 75, no. 2, pp. 213–224, Feb. 1989.

[93] C. I. Ace, T. A. McKee, J. M. Ryan, J. M. Cameron, and C. M. Preston, “Construction and characterization of a herpes simplex virus type 1 mutant unable to transinduce immediate-early gene expression,” *J. Virol.*, vol. 63, no. 5, pp. 2260–2269, May 1989.

[94] J. R. Smiley and J. Duncan, “Truncation of the C-terminal acidic transcriptional activation domain of herpes simplex virus VP16 produces a phenotype similar to that of the in1814 linker insertion mutation.,” *J. Virol.*, vol. 71, no. 8, p. 6191, Aug. 1997.

[95] I. Steiner, J. G. Spivack, S. L. Deshmane, C. I. Ace, C. M. Preston, and N. W. Fraser, “A herpes simplex virus type 1 mutant containing a nontransinducing Vmw65 protein establishes latent infection in vivo in the absence of viral replication and reactivates efficiently from explanted trigeminal ganglia,” *J. Virol.*, vol. 64, no. 4, pp. 1630–1638, Apr. 1990.

[96] R. Tal-Singer *et al.*, “The Transcriptional Activation Domain of VP16 Is Required for Efficient Infection and Establishment of Latency by HSV-1 in the Murine Peripheral and Central Nervous Systems,” *Virology*, vol. 259, no. 1, pp. 20–33, Jun. 1999.

[97] S. P. Weinheimer, B. A. Boyd, S. K. Durham, J. L. Resnick, and D. R. O’Boyle, “Deletion of the VP16 open reading frame of herpes simplex virus type 1.,” *J. Virol.*, vol. 66, no. 1, pp. 258–69, Jan. 1992.

[98] J. S. Lai and W. Herr, “Interdigitated residues within a small region of VP16 interact with Oct-1, HCF, and DNA,” *Mol. Cell. Biol.*, vol. 17, no. 7, pp. 3937–3946, Jul. 1997.

[99] L. P. Perera, J. D. Mosca, W. T. Ruyechan, and J. Hay, “Regulation of varicella-zoster virus gene expression in human T lymphocytes,” *J. Virol.*, vol. 66, no. 9, pp. 5298–5304, Sep. 1992.

[100] G. Inchauspe, S. Nagpal, and J. M. Ostrove, “Mapping of two varicella-zoster virus-encoded genes that activate the expression of viral early and late genes,” *Virology*, vol. 173, no. 2, pp. 700–709, 1989.

[101] H. Moriuchi, M. Moriuchi, and J. I. Cohen, “Proteins and cis-acting elements associated with transactivation of the varicella-zoster virus (VZV) immediate-early gene 62 promoter by VZV open reading frame 10 protein,” *J.Virol.*, vol. 69, no. 0022-538X, pp. 4693–4701, 1995.

[102] J.-Y. Kim, A. Mandarino, M. V. Chao, I. Mohr, and A. C. Wilson, “Transient reversal of episome silencing precedes VP16-dependent transcription during reactivation of latent HSV-1 in neurons,” *PLoS Pathog.*, vol. 8, no. 2, 2012.

[103] R. L. Thompson, C. M. Preston, and N. M. Sawtell, “De novo synthesis of VP16 coordinates the exit from HSV latency in vivo.,” *PLoS Pathog.*, vol. 5, no. 3, p. e1000352, Mar. 2009.

[104] W. Hafezi *et al.*, “Entry of herpes simplex virus type 1 (HSV-1) into the distal axons of trigeminal neurons favors the onset of nonproductive, silent infection,” *PLoS Pathog.*, vol. 8, no. 5, 2012.

[105] B. Roizman and A. E. Sears, “An Inquiry into the Mechanisms of Herpes Simplex Virus Latency,” *Annu. Rev. Microbiol.*, vol. 41, no. 1, pp. 543–571, Oct. 1987.

[106] N. M. Sawtell and R. L. Thompson, “De Novo Herpes Simplex Virus VP16 Expression Gates a Dynamic Programmatic Transition and Sets the Latent/Lytic Balance during Acute Infection in Trigeminal Ganglia.,” *PLoS Pathog.*, vol. 12, no. 9, p. e1005877, Sep. 2016.

[107] A. F. Lentine and S. L. Bachenheimer, “Intracellular organization of herpes simplex virus type 1 DNA assayed by staphylococcal nuclease sensitivity,” *Virus Res.*, vol. 16, no. 3, pp. 275–292, 1990.

[108] A. R. Cliffe *et al.*, “Neuronal Stress Pathway Mediating a Histone Methyl/Phospho Switch Is Required for Herpes Simplex Virus Reactivation.,” *Cell Host Microbe*, vol. 18, no. 6, pp. 649–58, Dec. 2015.

[109] S. R. Cuddy *et al.*, “Neuronal hyperexcitability is a DLK-dependent trigger of herpes simplex virus reactivation that can be induced by IL-1,” *Elife*, vol. 9, pp. 1–31, Dec. 2020.

[110] P. G. E. Kennedy, M. W. Graner, D. Gunaydin, J. Bowlin, T. Pointon, and X. Yu, “Varicella-Zoster Virus infected human neurons are resistant to apoptosis,” *J. Neurovirol.*, vol. 26, no. 3, pp. 330–337, Jun. 2020.

[111] P. G. E. Kennedy and T. H. Mogensen, “Varicella-Zoster Virus Infection of Neurons Derived from Neural Stem Cells,” *Viruses*, vol. 13, no. 3, Mar. 2021.

[112] C. M. Preston, M. C. Frame, and M. E. M. Campbell, “A complex formed between cell components and an HSV structural polypeptide binds to a viral immediate early gene regulatory DNA sequence,” *Cell*, vol. 52, no. 3, pp. 425–434, Feb. 1988.

[113] J. L. McKnight, T. M. Kristie, and B. Roizman, “Binding of the virion protein mediating alpha gene induction in herpes simplex virus 1-infected cells to its cis site requires cellular proteins,” *Proc. Natl. Acad. Sci. U. S. A.*, vol. 84, no. 20, pp. 7061–7065, 1987.

[114] T. Gerster and R. G. Roeder, “A herpesvirus trans-activating protein interacts with transcription factor OTF-1 and other cellular proteins,” *Proc. Natl. Acad. Sci. U. S. A.*, vol. 85, no. 17, pp. 6347–6351, 1988.

[115] S. E. Braspenning, T. Sadaoka, J. Breuer, G. M. G. M. Verjans, W. J. D. Ouwendijk, and D. P. Depledge, “Decoding the architecture of the varicella-zoster virus transcriptome,” *MBio*, vol. 11, no. 5, pp. 1–19, Sep. 2020.

[116] G. G. Maul, A. M. Ishov, and R. D. Everett, “Nuclear Domain 10 as Preexisting Potential Replication Start Sites of Herpes Simplex Virus Type-1,” *Virology*, vol. 217, no. 1, pp. 67–75, Mar. 1996.

[117] N. Morishige *et al.*, “Herpes simplex virus type 1 ICP0 localizes in the stromal layer of infected rabbit corneas and resides predominantly in the cytoplasm and/or perinuclear region of rabbit keratocytes,” *J. Gen. Virol.*, vol. 87, no. 10, pp. 2817–2825, Oct. 2006.

[118] L. E. Pomeranz, A. E. Reynolds, and C. J. Hengartner, “Molecular Biology of Pseudorabies Virus: Impact on Neurovirology and Veterinary Medicine,” *Microbiol. Mol. Biol. Rev.*, vol. 69, no. 3, p. 462, Sep. 2005.

[119] B. W. Wu, E. A. Engel, and L. W. Enquist, “Characterization of a Replication-Incompetent Pseudorabies Virus Mutant Lacking the Sole Immediate Early Gene IE180,” *MBio*, vol. 5, no. 6, Sep. 2014.

[120] J. I. Cohen, T. Krogmann, J. P. Ross, L. Pesnicak, and E. A. Prikhod’ko, “Varicella-Zoster Virus ORF4 Latency-Associated Protein Is Important for Establishment of Latency,” *J. Virol.*, vol. 79, no. 11, p. 6969, Jun. 2005.

[121] D. P, D. S, B. L, R. B, and P. J, “Varicella-zoster virus open reading frame 4 encodes an immediate-early protein with posttranscriptional regulatory properties,” *J. Virol.*, vol. 71, no. 9, pp. 7073–7079, Sep. 1997.

[122] L. Wang, M. Sommer, J. Rajamani, and A. M. Arvin, “Regulation of the ORF61 promoter and ORF61 functions in varicella-zoster virus replication and pathogenesis.,” *J. Virol.*, vol. 83, no. 15, pp. 7560–72, Aug. 2009.

[123] Y. Wu *et al.*, “Multifaceted Roles of ICP22/ORF63 Proteins in the Life Cycle of Human Herpesviruses,” *Front. Microbiol.*, vol. 12, Jun. 2021.

[124] S. E. Dremel and N. A. DeLuca, “Genome replication affects transcription factor binding mediating the cascade of herpes simplex virus transcription,” *Proc. Natl. Acad. Sci. U. S. A.*, vol. 116, no. 9, pp. 3734–3739, Feb. 2019.

[125] J. A. Dembowski, S. E. Dremel, and N. A. DeLuca, “Replication-Coupled Recruitment of Viral and Cellular Factors to Herpes Simplex Virus Type 1 Replication Forks for the Maintenance and Expression of Viral Genomes,” *PLoS Pathog.*, vol. 13, no. 1, p. e1006166, Jan. 2017.

[126] M. Lebrun *et al.*, “Varicella-zoster virus induces the formation of dynamic nuclear capsid aggregates,” *Virology*, vol. 454–455, no. 1, pp. 311–327, 2014.

[127] H. Granzow, B. G. Klupp, W. Fuchs, J. Veits, N. Osterrieder, and T. C. Mettenleiter, “Egress of alphaherpesviruses: comparative ultrastructural study,” *J. Virol.*, vol. 75, no. 8, pp. 3675–3684, Apr. 2001.

[128] J. N. Skepper, A. Whiteley, H. Browne, and A. Minson, “Herpes simplex virus nucleocapsids mature to progeny virions by an envelopment --> deenvelopment --> reenvelopment pathway,” *J. Virol.*, vol. 75, no. 12, pp. 5697–5702, Jun. 2001.

[129] R. Harson and C. Grose, “Egress of varicella-zoster virus from the melanoma cell: a tropism for the melanocyte,” *J. Virol.*, vol. 69, no. 8, pp. 4994–5010, Aug. 1995.

[130] H. Guo, S. Shen, L. Wang, and H. Deng, “Role of tegument proteins in herpesvirus assembly and egress,” *Protein Cell*, vol. 1, no. 11, pp. 987–998, 2010.

[131] T. C. Mettenleiter, “Intriguing interplay between viral proteins during herpesvirus assembly or: the herpesvirus assembly puzzle,” *Vet. Microbiol.*, vol. 113, no. 3–4, pp. 163–169, Mar. 2006.

[132] M. E. Padula, M. L. Sydnor, and D. W. Wilson, “Isolation and Preliminary Characterization of Herpes Simplex Virus 1 Primary Enveloped Virions from the Perinuclear Space,” *J. Virol.*, vol. 83, no. 10, pp. 4757–4765, May 2009.

[133] M. A. Bucks, K. J. O’Regan, M. A. Murphy, J. W. Wills, and R. J. Courtney, “Herpes simplex virus type 1 tegument proteins VP1/2 and UL37 are associated with intranuclear capsids,” *Virology*, vol. 361, no. 2, pp. 316–324, May 2007.

[134] R. Naldinho-Souto, H. Browne, and T. Minson, “Herpes simplex virus tegument protein VP16 is a component of primary enveloped virions,” *J. Virol.*, vol. 80, no. 5, pp. 2582–2584, Mar. 2006.

[135] M. Kopp, B. G. Klupp, H. Granzow, W. Fuchs, and T. C. Mettenleiter, “Identification and Characterization of the Pseudorabies Virus Tegument Proteins UL46 and UL47: Role for UL47 in Virion Morphogenesis in the Cytoplasm,” *J. Virol.*, vol. 76, no. 17, pp. 8820–8833, Sep. 2002.

[136] B. G. Klupp, W. Fuchs, H. Granzow, R. Nixdorf, and T. C. Mettenleiter, “Pseudorabies Virus UL36 Tegument Protein Physically Interacts with the UL37 Protein,” *J. Virol.*, vol. 76, no. 6, p. 3065, Mar. 2002.

[137] W. Fuchs, H. Granzow, B. G. Klupp, M. Kopp, and T. C. Mettenleiter, “The UL48 Tegument Protein of Pseudorabies Virus Is Critical for Intracytoplasmic Assembly of Infectious Virions,” *J. Virol.*, vol. 76, no. 13, pp. 6729–6742, Jul. 2002.

[138] T. C. Mettenleiter, “Budding events in herpesvirus morphogenesis,” *Virus Res.*, vol. 106, no. 2, pp. 167–180, 2004.

[139] T. C. Mettenleiter, "Herpesvirus Assembly and Egress," *J. Virol.*, vol. 76, no. 4, pp. 1537–1547, Feb. 2002.

[140] P. Wild *et al.*, "Exploring the Nuclear Envelope of Herpes Simplex Virus 1-Infected Cells by High-Resolution Microscopy," *J. Virol.*, vol. 83, no. 1, pp. 408–419, Jan. 2009.

[141] P. Wild *et al.*, "Impairment of nuclear pores in bovine herpesvirus 1-infected MDBK cells," *J. Virol.*, vol. 79, no. 2, pp. 1071–1083, Jan. 2005.

[142] H. Leuzinger *et al.*, "Herpes Simplex Virus 1 Envelopment Follows Two Diverse Pathways," *J. Virol.*, vol. 79, no. 20, pp. 13047–13059, Oct. 2005.

[143] P. Wild *et al.*, "The significance of the Golgi complex in envelopment of bovine herpesvirus 1 (BHV-1) as revealed by cryobased electron microscopy," *Micron*, vol. 33, no. 4, pp. 327–337, 2002.

[144] R. Kratchmarov, M. P. Taylor, and L. W. Enquist, "Making the case: married versus separate models of alphaherpes virus anterograde transport in axons.," *Rev. Med. Virol.*, vol. 22, no. 6, pp. 378–91, Nov. 2012.

[145] M. Reichelt, J. Brady, and A. M. Arvin, "The Replication Cycle of Varicella-Zoster Virus: Analysis of the Kinetics of Viral Protein Expression, Genome Synthesis, and Virion Assembly at the Single-Cell Level," *J. Virol.*, vol. 83, no. 8, pp. 3904–3918, Apr. 2009.

[146] L. Zerboni, N. Sen, S. L. Oliver, and A. M. Arvin, "Molecular mechanisms of varicella zoster virus pathogenesis," *Nat Rev Micro*, vol. 12, no. 3, pp. 197–210, Feb. 2014.

[147] N. Arnold, T. Girke, S. Sureshchandra, and I. Messaoudi, "Acute Simian Varicella Virus Infection Causes Robust and Sustained Changes in Gene Expression in the Sensory Ganglia," *J. Virol.*, vol. 90, no. 23, pp. 10823–10843, Dec. 2016.

[148] G. A. Smith, "Assembly and Egress of an Alphaherpesvirus Clockwork.," *Adv. Anat. Embryol. Cell Biol.*, vol. 223, pp. 171–193, 2017.

[149] H. Sato, L. Pesnicak, and J. I. Cohen, "Varicella-zoster virus ORF47 protein kinase, which is required for replication in human T cells, and ORF66 protein kinase, which is expressed during latency, are dispensable for establishment of latency.," *J. Virol.*, vol. 77, no. 20, pp. 11180–5, Oct. 2003.

[150] R. S. Goldstein and P. R. Kinchington, "Varicella Zoster Virus Neuronal Latency and Reactivation Modeled in Vitro," pp. 1–32, 2021.

[151] L. Zerboni, B. Berarducci, J. Rajamani, C. D. Jones, J. L. Zehnder, and A. Arvin, "Varicella-Zoster Virus Glycoprotein E Is a Critical Determinant of Virulence in the SCID Mouse-Human Model of Neuropathogenesis," *J. Virol.*, vol. 85, no. 1, pp. 98–111, Jan. 2011.

[152] W. J. D. Ouwendijk *et al.*, "Immunohistochemical detection of intra-neuronal VZV proteins in snap-frozen human ganglia is confounded by antibodies directed against blood group A1-

associated antigens," *J. Neurovirol.*, vol. 18, no. 3, pp. 172–180, 2012.

[153] L. Zerboni *et al.*, "Apparent expression of varicella-zoster virus proteins in latency resulting from reactivity of murine and rabbit antibodies with human blood group a determinants in sensory neurons.," *J. Virol.*, vol. 86, no. 1, pp. 578–83, 2012.

[154] R. J. Cohrs and D. H. Gilden, "Varicella zoster virus transcription in latently-infected human ganglia.," *Anticancer Res.*, vol. 23, no. 3A, pp. 2063–2069, May 2003.

[155] W. J. D. Ouwendijk *et al.*, "Restricted Varicella-Zoster Virus Transcription in Human Trigeminal Ganglia Obtained Soon after Death," *J. Virol.*, vol. 86, no. 18, pp. 10203–10206, 2012.

[156] D. P. Depledge *et al.*, "A spliced latency-associated VZV transcript maps antisense to the viral transactivator gene 61," *Nat. Commun.*, vol. 9, no. 1, p. 1167, Dec. 2018.

[157] W. J. D. Ouwendijk *et al.*, "Varicella-zoster virus VLT-ORF63 fusion transcript induces broad viral gene expression during reactivation from neuronal latency," *Nat. Commun.*, vol. 11, no. 1, Dec. 2020.

[158] C. A. Kyratsous and S. J. Silverstein, "Components of Nuclear Domain 10 Bodies Regulate Varicella-Zoster Virus Replication," *J. Virol.*, vol. 83, no. 9, pp. 4262–4274, May 2009.

[159] M. S. Walters, C. A. Kyratsous, and S. J. Silverstein, "The RING Finger Domain of Varicella-Zoster Virus ORF61p Has E3 Ubiquitin Ligase Activity That Is Essential for Efficient Autoubiquitination and Dispersion of Sp100-Containing Nuclear Bodies," *J. Virol.*, vol. 84, no. 13, pp. 6861–6865, Jul. 2010.

[160] M. Reichelt *et al.*, "Entrapment of viral capsids in nuclear PML cages is an intrinsic antiviral host defense against varicella-zoster virus.," *PLoS Pathog.*, vol. 7, no. 2, p. e1001266, Feb. 2011.

[161] L. Wang, S. L. Oliver, M. Sommer, J. Rajamani, M. Reichelt, and A. M. Arvin, "Disruption of PML Nuclear Bodies Is Mediated by ORF61 SUMO-Interacting Motifs and Required for Varicella-Zoster Virus Pathogenesis in Skin," *PLOS Pathog.*, vol. 7, no. 8, p. e1002157, Aug. 2011.

[162] R. Bernardi and P. P. Pandolfi, "Structure, dynamics and functions of promyelocytic leukaemia nuclear bodies," *Nat. Rev. Mol. Cell Biol.*, vol. 8, no. 12, pp. 1006–1016, Dec. 2007.

[163] S. Zhong, P. Salomoni, and P. P. Pandolfi, "The transcriptional role of PML and the nuclear body," *Nat. Cell Biol.*, vol. 2, no. 5, 2000.

[164] S. Kurapati *et al.*, "Role of the JNK Pathway in Varicella-Zoster Virus Lytic Infection and Reactivation," *J. Virol.*, vol. 91, no. 17, pp. 640–657, Sep. 2017.

[165] W. Cai, T. L. Astor, L. M. Liptak, C. Cho, D. M. Coen, and P. A. Schaffer, "The herpes

simplex virus type 1 regulatory protein ICP0 enhances virus replication during acute infection and reactivation from latency.," *J. Virol.*, vol. 67, no. 12, pp. 7501–12, Dec. 1993.

[166] D. A. Leib *et al.*, "Immediate-early regulatory gene mutants define different stages in the establishment and reactivation of herpes simplex virus latency.," *J. Virol.*, vol. 63, no. 2, pp. 759–68, Feb. 1989.

[167] A. R. Cliffe and A. C. Wilson, "Restarting Lytic Gene Transcription at the Onset of Herpes Simplex Virus Reactivation," *J. Virol.*, vol. 91, no. 2, Jan. 2017.

[168] C. A. Gabel, L. Dubey, S. P. Steinberg, D. Sherman, M. D. Gershon, and A. A. Gershon, "Varicella-zoster virus glycoprotein oligosaccharides are phosphorylated during posttranslational maturation.," *J. Virol.*, vol. 63, no. 10, p. 4264, Oct. 1989.

[169] J. J. Chen, A. A. Gershon, Z. S. Li, O. Lungu, and M. D. Gershon, "Latent and lytic infection of isolated guinea pig enteric ganglia by varicella zoster virus," *J. Med. Virol.*, vol. 70 Suppl 1, no. SUPPL. 1, May 2003.

[170] A. A. Gershon, J. Chen, and M. D. Gershon, "A model of lytic, latent, and reactivating varicella-zoster virus infections in isolated enteric neurons," *J. Infect. Dis.*, vol. 197 Suppl 2, no. SUPPL. 2, Mar. 2008.

[171] R. Mahalingam *et al.*, "Current In Vivo Models of Varicella-Zoster Virus Neurotropism," *Viruses*, vol. 11, no. 6, Jun. 2019.

[172] J. Besser *et al.*, "Differential requirement for cell fusion and virion formation in the pathogenesis of varicella-zoster virus infection in skin and T cells," *J. Virol.*, vol. 78, no. 23, pp. 13293–13305, Dec. 2004.

[173] T. Sadaoka *et al.*, "Human stem cell derived sensory neurons are positioned to support varicella zoster virus latency," *bioRxiv*, p. 2020.01.24.919290, Jan. 2020.

[174] C.-C. Ku, J. Besser, A. Abendroth, C. Grose, and A. M. Arvin, "Varicella-Zoster virus pathogenesis and immunobiology: new concepts emerging from investigations with the SCIDhu mouse model," *J. Virol.*, vol. 79, no. 5, pp. 2651–2658, Mar. 2005.

[175] C.-C. Ku, J. A. Padilla, C. Grose, E. C. Butcher, and A. M. Arvin, "Tropism of varicella-zoster virus for human tonsillar CD4(+) T lymphocytes that express activation, memory, and skin homing markers," *J. Virol.*, vol. 76, no. 22, pp. 11425–11433, Nov. 2002.

[176] S. M. Fleetwood-Walker *et al.*, "Behavioural changes in the rat following infection with varicella-zoster virus," *J. Gen. Virol.*, vol. 80 (Pt 9), no. 9, pp. 2433–2436, 1999.

[177] B. E. Warner, W. F. Goins, P. R. Kramer, and P. R. Kinchington, "A Guide to Preclinical Models of Zoster-Associated Pain and Postherpetic Neuralgia," *Curr. Top. Microbiol. Immunol.*, 2021.

[178] B. E. Warner *et al.*, "Varicella-zoster virus early infection but not complete replication is

required for the induction of chronic hypersensitivity in rat models of postherpetic neuralgia," *PLoS Pathog.*, vol. 17, no. 7, Jul. 2021.

[179] T. Sadaoka, D. P. Depledge, L. Rajbhandari, A. Venkatesan, J. Breuer, and J. I. Cohen, "In vitro system using human neurons demonstrates that varicella-zoster vaccine virus is impaired for reactivation, but not latency," *Proc. Natl. Acad. Sci. U. S. A.*, vol. 113, no. 17, pp. E2403–E2412, Apr. 2016.

[180] T. Sadaoka, C. L. Schwartz, L. Rajbhandari, A. Venkatesan, and J. I. Cohen, "Human Embryonic Stem Cell-Derived Neurons Are Highly Permissive for Varicella-Zoster Virus Lytic Infection.," *J. Virol.*, vol. 92, no. 1, pp. e01108-17, Jan. 2018.

[181] O. Pomp *et al.*, "PA6-induced human embryonic stem cell-derived neurospheres: a new source of human peripheral sensory neurons and neural crest cells," *Brain Res.*, vol. 1230, pp. 50–60, Sep. 2008.

[182] A. Markus *et al.*, "Varicella-zoster virus (VZV) infection of neurons derived from human embryonic stem cells: direct demonstration of axonal infection, transport of VZV, and productive neuronal infection.," *J. Virol.*, vol. 85, no. 13, pp. 6220–33, Jul. 2011.

[183] A. Markus, I. Lebenthal-Loinger, I. H. Yang, P. R. Kinchington, and R. S. Goldstein, "An In Vitro Model of Latency and Reactivation of Varicella Zoster Virus in Human Stem Cell-Derived NeuronsA," *PLoS Pathog.*, vol. 11, no. 6, pp. 1–22, 2015.

[184] R. Birenboim, A. Markus, and R. S. Goldstein, "Simple generation of neurons from human embryonic stem cells using agarose multiwell dishes," *J. Neurosci. Methods*, vol. 214, no. 1, pp. 9–14, Mar. 2013.

[185] I. H. Yang, R. Siddique, S. Hosmane, N. Thakor, and A. Höke, "Compartmentalized microfluidic culture platform to study mechanism of paclitaxel-induced axonal degeneration.," *Exp. Neurol.*, vol. 218, no. 1, pp. 124–8, Jul. 2009.

[186] K. Nagaike *et al.*, "Cloning of the varicella-zoster virus genome as an infectious bacterial artificial chromosome in Escherichia coli," *Vaccine*, vol. 22, no. 29–30, pp. 4069–4074, Sep. 2004.

[187] H. Yoshii, P. Somboonthum, M. Takahashi, K. Yamanishi, and Y. Mori, "Cloning of full length genome of varicella-zoster virus vaccine strain into a bacterial artificial chromosome and reconstitution of infectious virus," *Vaccine*, vol. 25, no. 27, pp. 5006–5012, Jun. 2007.

[188] B. K. Tischer, B. B. Kaufer, M. H. Sommer, F. Wussow, A. M. Arvin, and N. Osterrieder, "A self-excisable infectious bacterial artificial chromosome clone of varicella-zoster virus allows analysis of the essential tegument protein encoded by ORF9.," *J. Virol.*, vol. 81, no. 23, pp. 13200–8, Dec. 2007.

[189] B. K. Tischer, J. Von Einem, B. B. Kaufer, and N. Osterrieder, "Two-step Red-mediated recombination for versatile high-efficiency markerless DNA manipulation in Escherichia coli," *Biotechniques*, vol. 40, no. 2, pp. 191–197, 2006.

[190] Z. Zhang *et al.*, "Genetic analysis of varicella-zoster virus ORF0 to ORF4 by use of a novel luciferase bacterial artificial chromosome system," *J. Virol.*, vol. 81, no. 17, pp. 9024–9033, Sep. 2007.

[191] M. Tsolia, A. A. Gershon, S. P. Steiberg, and L. Gelb, "Live attenuated varicella vaccine: evidence that the virus is attenuated and the importance of skin lesions in transmission of varicella-zoster virus. National Institute of Allergy and Infectious Diseases Varicella Vaccine Collaborative Study Group," *J. Pediatr.*, vol. 116, no. 2, pp. 184–189, 1990.

[192] A. M. Arvin *et al.*, *Varicella-zoster Virus*. New York: Springer, 2010.

[193] J. F. Moffat *et al.*, "The ORF47 and ORF66 putative protein kinases of varicella-zoster virus determine tropism for human T cells and skin in the SCID-hu mouse," *Proc. Natl. Acad. Sci. U. S. A.*, vol. 95, no. 20, pp. 11969–11974, Sep. 1998.

[194] L. Zerboni, C. C. Ku, C. D. Jones, J. L. Zehnder, and A. M. Arvin, "Varicella-zoster virus infection of human dorsal root ganglia in vivo," *Proc. Natl. Acad. Sci. U. S. A.*, vol. 102, no. 18, pp. 6490–6495, May 2005.

[195] M. Reichelt, L. Zerboni, and A. M. Arvin, "Mechanisms of Varicella-Zoster Virus Neuropathogenesis in Human Dorsal Root Ganglia," *J. Virol.*, vol. 82, no. 8, pp. 3971–3983, Apr. 2008.

[196] M. Riera-Montes *et al.*, "Estimation of the burden of varicella in Europe before the introduction of universal childhood immunization," *BMC Infect. Dis.*, vol. 17, no. 1, pp. 1–16, May 2017.

[197] R. Finger, J. P. Hughes, B. J. Meade, A. R. Pelletier, and C. T. Palmer, "Age-specific incidence of chickenpox.," *Public Health Rep.*, vol. 109, no. 6, p. 750, 1994.

[198] A. A. Gershon *et al.*, "Varicella zoster virus infection.," *Nat. Rev. Dis. Prim.*, vol. 1, p. 15016, 2015.

[199] P. G. E. Kennedy and A. A. Gershon, "Clinical Features of Varicella-Zoster Virus Infection," *Viruses*, vol. 10, no. 11, Nov. 2018.

[200] B. K. Mandal, P. P. Mukherjee, C. Murphy, R. Mukherjee, and T. Naik, "Adult susceptibility to varicella in the tropics is a rural phenomenon due to the lack of previous exposure," *J. Infect. Dis.*, vol. 178 Suppl 1, no. 5 SUPPL., 1998.

[201] S. R. Preblud, "Varicella: Complications and Costs," *Pediatrics*, vol. 78, no. 4, pp. 728–735, Oct. 1986.

[202] L. Gregorakos, P. Myrianthefs, N. Markou, D. Chroni, and E. Sakagianni, "Severity of illness and outcome in adult patients with primary varicella pneumonia," *Respiration.*, vol. 69, no. 4, pp. 330–334, 2002.

[203] R. M. Joesoef, R. Harpaz, J. Leung, and S. R. Bialek, "Chronic Medical Conditions as Risk

Factors for Herpes Zoster," *Mayo Clin. Proc.*, vol. 87, no. 10, p. 961, 2012.

[204] B. P. Yawn and D. Gilden, "The global epidemiology of herpes zoster," *Neurology*, vol. 81, no. 10, pp. 928–930, Sep. 2013.

[205] R. W. Johnson *et al.*, "Herpes zoster epidemiology, management, and disease and economic burden in Europe: a multidisciplinary perspective," *Ther. Adv. Vaccines*, vol. 3, no. 4, p. 109, Jul. 2015.

[206] M. Marin, R. Harpaz, J. Zhang, P. C. Wollan, S. R. Bialek, and B. P. Yawn, "Risk Factors for Herpes Zoster Among Adults," *Open forum Infect. Dis.*, vol. 3, no. 3, May 2016.

[207] F. Marra, K. Parhar, B. Huang, and N. Vadlamudi, "Risk Factors for Herpes Zoster Infection: A Meta-Analysis," *Open Forum Infect. Dis.*, vol. 7, no. 1, Jan. 2020.

[208] H. J. Forbes, K. Bhaskaran, S. L. Thomas, L. Smeeth, T. Clayton, and S. M. Langan, "Quantification of risk factors for herpes zoster: population based case-control study," *BMJ*, vol. 348, May 2014.

[209] D. Weiskopf, B. Weinberger, and B. Grubeck-Loebenstein, "The aging of the immune system," *Transpl. Int.*, vol. 22, no. 11, pp. 1041–1050, Nov. 2009.

[210] E. Zorzoli, F. Pica, G. Masetti, E. Franco, A. Volpi, and G. Gabutti, "Herpes zoster in frail elderly patients: prevalence, impact, management, and preventive strategies," *Aging Clin. Exp. Res.*, vol. 30, no. 7, pp. 693–702, Jul. 2018.

[211] G. M. G. M. Verjans *et al.*, "Selective retention of herpes simplex virus-specific T cells in latently infected human trigeminal ganglia," *Proc. Natl. Acad. Sci. U. S. A.*, vol. 104, no. 9, pp. 3496–3501, Feb. 2007.

[212] A. Weinberg and M. J. Levin, "VZV T cell-mediated immunity," *Curr. Top. Microbiol. Immunol.*, vol. 342, pp. 341–357, 2010.

[213] M. Vukmanovic-Stejic *et al.*, "The Characterization of Varicella Zoster Virus-Specific T Cells in Skin and Blood during Aging," *J. Invest. Dermatol.*, vol. 135, no. 7, pp. 1752–1762, Jul. 2015.

[214] R. Harpaz, J. W. Leung, C. J. Brown, and F. J. Zhou, "Psychological stress as a trigger for herpes zoster: might the conventional wisdom be wrong?," *Clin. Infect. Dis.*, vol. 60, no. 5, pp. 781–785, Mar. 2015.

[215] H. Soh *et al.*, "Increased Risk of Herpes Zoster in Young and Metabolically Healthy Patients with Inflammatory Bowel Disease: A Nationwide Population-Based Study," *Gut Liver*, vol. 13, no. 3, pp. 333–341, 2019.

[216] B. V. Rooney, B. E. Crucian, D. L. Pierson, M. L. Laudenslager, and S. K. Mehta, "Herpes Virus Reactivation in Astronauts During Spaceflight and Its Application on Earth," *Front. Microbiol.*, vol. 10, no. feburay, p. 16, 2019.

[217] M. van Velzen *et al.*, "Longitudinal Study on Oral Shedding of Herpes Simplex Virus 1 and Varicella-Zoster Virus in Individuals Infected with HIV," *J. Med. Virol.*, vol. 85, no. 9, p. 1669, Sep. 2013.

[218] S. K. Mehta, R. J. Cohrs, B. Forghani, G. Zerbe, D. H. Gilden, and D. L. Pierson, "Stress-induced subclinical reactivation of varicella zoster virus in astronauts," *J. Med. Virol.*, vol. 72, no. 1, pp. 174–179, Jan. 2004.

[219] A. A. Gershon, J. Chen, and M. D. Gershon, "Use of Saliva to Identify Varicella Zoster Virus Infection of the Gut," *Clin. Infect. Dis.*, vol. 61, no. 4, pp. 536–544, Aug. 2015.

[220] M. Gershon and A. Gershon, "Varicella-Zoster Virus and the Enteric Nervous System," *J. Infect. Dis.*, vol. 218, no. Suppl 2, p. S113, Sep. 2018.

[221] S. E. Talbird, E. M. La, J. Mauskopf, A. Altland, V. Daniels, and L. J. Wolfson, "Understanding the role of exogenous boosting in modeling varicella vaccination," *Expert Rev. Vaccines*, vol. 17, no. 11, pp. 1021–1035, Nov. 2018.

[222] M. N. Oxman *et al.*, "A vaccine to prevent herpes zoster and postherpetic neuralgia in older adults.," *N. Engl. J. Med.*, vol. 352, no. 22, pp. 2271–84, Jun. 2005.

[223] S. A. Pergam and A. P. Limaye, "Varicella zoster virus in solid organ transplantation: Guidelines from the American Society of Transplantation Infectious Diseases Community of Practice," *Clin. Transplant.*, vol. 33, no. 9, Sep. 2019.

[224] D. E. Kwon, H. S. Lee, K. H. Lee, Y. La, S. H. Han, and Y. G. Song, "Incidence of herpes zoster in adult solid organ transplant recipients: A meta-analysis and comprehensive review," *Transpl. Infect. Dis.*, vol. 23, no. 4, Aug. 2021.

[225] M. M. L. Kho *et al.*, "Herpes Zoster in Solid Organ Transplantation: Incidence and Risk Factors," *Front. Immunol.*, vol. 12, Mar. 2021.

[226] T. F. Leung *et al.*, "Incidence, risk factors and outcome of varicella-zoster virus infection in children after haematopoietic stem cell transplantation," *Bone Marrow Transplant.*, vol. 25, no. 2, pp. 167–172, 2000.

[227] C. L. Vermont *et al.*, "Varicella zoster reactivation after hematopoietic stem cell transplant in children is strongly correlated with leukemia treatment and suppression of host T-lymphocyte immunity," *Transpl. Infect. Dis.*, vol. 16, no. 2, pp. 188–194, 2014.

[228] O. Blennow, G. Fjaertoft, J. Winiarski, P. Ljungman, J. Mattsson, and M. Remberger, "Varicella-zoster reactivation after allogeneic stem cell transplantation without routine prophylaxis--the incidence remains high," *Biol. Blood Marrow Transplant.*, vol. 20, no. 10, pp. 1646–1649, Oct. 2014.

[229] S. L. Thomas, J. G. Wheeler, and A. J. Hall, "Case-control study of the effect of mechanical trauma on the risk of herpes zoster," *BMJ Br. Med. J.*, vol. 328, no. 7437, p. 439, Feb. 2004.

[230] M. Zak-Prelich, J. L. Borkowski, F. Alexander, and M. Norval, “The role of solar ultraviolet irradiation in zoster,” *Epidemiol. Infect.*, vol. 129, no. 3, pp. 593–597, 2002.

[231] P. G. E. Kennedy, T. H. Mogensen, and R. J. Cohrs, “Recent Issues in Varicella-Zoster Virus Latency,” *Viruses*, vol. 13, no. 10, Oct. 2021.

[232] M. M. Esiri and A. H. Tomlinson, “Herpes Zoster. Demonstration of virus in trigeminal nerve and ganglion by immunofluorescence and electron microscopy,” *J. Neurol. Sci.*, vol. 15, no. 1, pp. 35–48, 1972.

[233] K. Gowrishankar *et al.*, “Characterization of the host immune response in human Ganglia after herpes zoster,” *J. Virol.*, vol. 84, no. 17, pp. 8861–8870, Sep. 2010.

[234] H. J. Forbes *et al.*, “Quantification of risk factors for postherpetic neuralgia in herpes zoster patients: A cohort study,” *Neurology*, vol. 87, no. 1, p. 94, Jul. 2016.

[235] H. J. Forbes *et al.*, “A systematic review and meta-analysis of risk factors for postherpetic neuralgia,” *Pain*, vol. 157, no. 1, pp. 30–54, Jan. 2016.

[236] D. H. Gilden, A. N. Dueland, M. E. Devlin, R. Mahalingam, and R. Cohrs, “Varicella-zoster virus reactivation without rash,” *J. Infect. Dis.*, vol. 166 Suppl 1, pp. S30–S34, 1992.

[237] M. A. Nagel and D. Gilden, “Complications of varicella zoster virus reactivation,” *Curr. Treat. Options Neurol.*, vol. 15, no. 4, pp. 439–453, Aug. 2013.

[238] M. Woodward, A. Marko, S. Galea, B. Eagel, and W. Straus, “Varicella Virus Vaccine Live: A 22-Year Review of Postmarketing Safety Data,” *Open forum Infect. Dis.*, vol. 6, no. 8, Jun. 2019.

[239] H. F. Tseng *et al.*, “Declining Effectiveness of Herpes Zoster Vaccine in Adults Aged ≥60 Years,” *J. Infect. Dis.*, vol. 213, no. 12, pp. 1872–1875, Jun. 2016.

[240] H. Lal *et al.*, “Efficacy of an Adjuvanted Herpes Zoster Subunit Vaccine in Older Adults,” *N. Engl. J. Med.*, vol. 372, no. 22, pp. 2087–2096, 2015.

[241] K. L. Dooling *et al.*, “Recommendations of the Advisory Committee on Immunization Practices for Use of Herpes Zoster Vaccines,” *MMWR. Morb. Mortal. Wkly. Rep.*, vol. 67, no. 3, pp. 103–108, Jan. 2019.

[242] T. Bharucha, D. Ming, and J. Breuer, “A critical appraisal of ‘Shingrix’, a novel Herpes Zoster Subunit (HZ/Su or GSK1437173A) vaccine for Varicella Zoster Virus,” *Hum. Vaccin. Immunother.*, pp. 00–00, Apr. 2017.

[243] A. L. Cunningham and T. Heineman, “Vaccine profile of herpes zoster (HZ/su) subunit vaccine,” *Expert Rev. Vaccines*, vol. 16, no. 7, pp. 661–670, Jul. 2017.

[244] B. J. Patterson, C. C. Chen, C. B. McGuiness, L. I. Glasser, K. Sun, and P. O. Buck, “Early examination of real-world uptake and second-dose completion of recombinant zoster

vaccine in the United States from October 2017 to September 2019," *Hum. Vaccin. Immunother.*, vol. 17, no. 8, pp. 2482–2487, 2021.

[245] K. Kawai, B. G. Gebremeskel, and C. J. Acosta, "Systematic review of incidence and complications of herpes zoster: towards a global perspective," *BMJ Open*, vol. 4, no. 6, pp. e004833–e004833, Jun. 2014.

[246] S. Esposito *et al.*, "The public health value of vaccination for seniors in Europe," *Vaccine*, vol. 36, no. 19, pp. 2523–2528, May 2018.

[247] A. Flatt and J. Breuer, "Varicella vaccines," *Br. Med. Bull.*, vol. 103, no. 1, pp. 115–127, Sep. 2012.

[248] G. B. Elion, "The biochemistry and mechanism of action of acyclovir," *J. Antimicrob. Chemother.*, vol. 12 Suppl B, no. SUPPL. B, pp. 9–17, 1983.

[249] S. D. Shafran *et al.*, "Once, twice, or three times daily famciclovir compared with aciclovir for the oral treatment of herpes zoster in immunocompetent adults: A randomized, multicenter, double-blind clinical trial," *J. Clin. Virol.*, vol. 29, no. 4, pp. 248–253, 2004.

[250] S. Tyring *et al.*, "Famciclovir for the treatment of acute herpes zoster: effects on acute disease and postherpetic neuralgia. A randomized, double-blind, placebo-controlled trial. Collaborative Famciclovir Herpes Zoster Study Group," *Ann. Intern. Med.*, vol. 123, no. 2, pp. 89–96, 1995.

[251] E. Saint-Leéger *et al.*, "Clinical and virologic characterization of acyclovir-resistant varicella-zoster viruses isolated from 11 patients with acquired immunodeficiency syndrome," *Clin. Infect. Dis.*, vol. 33, no. 12, pp. 2061–2067, Dec. 2001.

[252] J. Piret and G. Boivin, "Antiviral resistance in herpes simplex virus and varicella-zoster virus infections: diagnosis and management," *Curr. Opin. Infect. Dis.*, vol. 29, no. 6, pp. 654–662, Nov. 2016.

[253] K. J. Smith, D. C. Kahlter, C. Davis, W. D. James, H. G. Skelton, and P. Angritt, "Acyclovir-Resistant Varicella Zoster Responsive to Foscarnet," *Arch. Dermatol.*, vol. 127, no. 7, pp. 1069–1071, Jul. 1991.

[254] I. T. Hagag *et al.*, "Abrogation of Marek's disease virus replication using CRISPR/Cas9," *Sci. Rep.*, vol. 10, no. 1, Dec. 2020.

[255] M. Aubert *et al.*, "In vitro Inactivation of Latent HSV by Targeted Mutagenesis Using an HSV-specific Homing Endonuclease," *Mol. Ther. - Nucleic Acids*, vol. 3, no. December 2013, p. e146, 2014.

[256] F. R. van Diemen *et al.*, "CRISPR/Cas9-Mediated Genome Editing of Herpesviruses Limits Productive and Latent Infections," *PLoS Pathog.*, vol. 12, no. 6, pp. 1–29, 2016.

[257] J. Wang and S. R. Quake, "RNA-guided endonuclease provides a therapeutic strategy to

cure latent herpesviridae infection," *Proc. Natl. Acad. Sci.*, vol. 111, no. 36, pp. 13157–13162, 2014.

[258] M. Aubert *et al.*, "In vivo disruption of latent HSV by designer endonuclease therapy," *JCI Insight*, vol. 1, no. 14, Sep. 2016.

[259] C. H. Dang *et al.*, "In vivo dynamics of AAV-mediated gene delivery to sensory neurons of the trigeminal ganglia.," *Sci. Rep.*, vol. 7, no. 1, p. 927, 2017.

[260] R. H. Dworkin *et al.*, "Recommendations for the management of herpes zoster," *Clin. Infect. Dis.*, vol. 44 Suppl 1, no. SUPPL. 1, Jan. 2007.

[261] N. Chen, Q. Li, J. Yang, M. Zhou, D. Zhou, and L. He, "Antiviral treatment for preventing postherpetic neuralgia," *Cochrane Database of Systematic Reviews*, vol. 2014, no. 2. 2014.

[262] L. Feller, R. A. G. Khammissa, J. Fourie, M. Bouckaert, and J. Lemmer, "Postherpetic Neuralgia and Trigeminal Neuralgia," *Pain Res. Treat.*, vol. 2017, 2017.

[263] I. Ducic and J. M. Felder, "Peripheral nerve surgery for the treatment of postherpetic neuralgia," *Ann. Plast. Surg.*, vol. 71, no. 4, pp. 384–385, Oct. 2013.

[264] J. Schutzer-Weissmann and P. Farquhar-Smith, "Post-herpetic neuralgia – A review of current management and future directions," *Expert Opin. Pharmacother.*, vol. 18, no. 16, pp. 1739–1750, 2017.

[265] B. W. Wu, M. B. Yee, R. S. Goldstein, and P. R. Kinchington, "Antiviral Targeting of Varicella Zoster Virus Replication and Neuronal Reactivation Using CRISPR/Cas9 Cleavage of the Duplicated Open Reading Frames 62/71," *Viruses*, vol. 14, no. 2, Feb. 2022.

[266] R. W. Johnson, "Herpes Zoster and Postherpetic Neuralgia," *Expert Rev. Vaccines*, vol. 9, no. sup3, pp. 21–26, 2014.

[267] A. A. Gershon and M. D. Gershon, "Pathogenesis and current approaches to control of varicella-zoster virus infections.," *Clin. Microbiol. Rev.*, vol. 26, no. 4, pp. 728–43, Oct. 2013.

[268] A. R. P. Edell and E. J. Cohen, "Herpes Simplex and Herpes Zoster Eye Disease," *Eye Contact Lens Sci. Clin. Pract.*, vol. 39, no. 4, pp. 311–314, Jul. 2013.

[269] D. Pavan-Langston, "Herpes Zoster. Antivirals and Pain Management," *Ophthalmology*, vol. 115, no. 2 SUPPL., pp. 13–20, 2008.

[270] C. Chun *et al.*, "Laboratory Characteristics of Suspected Herpes Zoster in Vaccinated Children," *Pediatr. Infect. Dis. J.*, vol. 30, no. 8, pp. 721–723, Aug. 2011.

[271] H. F. Tseng *et al.*, "Herpes zoster caused by vaccine-strain varicella zoster virus in an immunocompetent recipient of zoster vaccine.," *Clin. Infect. Dis.*, vol. 58, no. 8, pp. 1125–8, Apr. 2014.

[272] A. L. Cunningham *et al.*, "Efficacy of the Herpes Zoster Subunit Vaccine in Adults 70 Years of Age or Older," *N. Engl. J. Med.*, vol. 375, no. 11, pp. 1019–1032, 2016.

[273] H. Lal *et al.*, "Immunogenicity, reactogenicity and safety of 2 doses of an adjuvanted herpes zoster subunit vaccine administered 2, 6 or 12 months apart in older adults: Results of a phase III, randomized, open-label, multicenter study," *Vaccine*, vol. 36, no. 1, pp. 148–154, Jan. 2018.

[274] E. Koshy, L. Mengting, H. Kumar, and W. Jianbo, "Epidemiology, treatment and prevention of herpes zoster: A comprehensive review," *Indian J. Dermatol. Venereol. Leprol.*, vol. 84, no. 3, pp. 251–262, May 2018.

[275] A. Sauerbrei, "Diagnosis, antiviral therapy, and prophylaxis of varicella-zoster virus infections," *Eur. J. Clin. Microbiol. Infect. Dis.*, vol. 35, no. 5, pp. 723–734, May 2016.

[276] J. M. G. Guedon, M. B. Yee, M. Zhang, S. A. K. Harvey, W. F. Goins, and P. R. Kinchington, "Neuronal changes induced by Varicella Zoster Virus in a rat model of postherpetic neuralgia," *Virology*, vol. 482, pp. 167–180, Aug. 2015.

[277] R. J. Cohrs, H. Badani, N. L. Baird, T. M. White, B. Sanford, and D. Gilden, "Induction of varicella zoster virus DNA replication in dissociated human trigeminal ganglia," *J. Neurovirol.*, vol. 23, no. 1, p. 152, Feb. 2017.

[278] J. Rowe, R. J. Greenblatt, D. Liu, and J. F. Moffat, "Compounds that target host cell proteins prevent varicella-zoster virus replication in culture, ex vivo, and in SCID-Hu mice," *Antiviral Res.*, vol. 86, no. 3, pp. 276–285, Jun. 2010.

[279] L. Zerboni and A. Arvin, "Neuronal Subtype and Satellite Cell Tropism Are Determinants of Varicella-Zoster Virus Virulence in Human Dorsal Root Ganglia Xenografts In Vivo," *PLoS Pathog.*, vol. 11, no. 6, Jun. 2015.

[280] C. De *et al.*, "β-l-1-[5-(E-2-bromovinyl)-2-(hydroxymethyl)-1,3-(dioxolan-4-yl)] uracil (l-BHDU) prevents varicella-zoster virus replication in a SCID-Hu mouse model and does not interfere with 5-fluorouracil catabolism," *Antiviral Res.*, vol. 110, no. 1, pp. 10–19, 2014.

[281] A. Sloutskin, P. R. Kinchington, and R. S. Goldstein, "Productive vs non-productive infection by cell-free varicella zoster virus of human neurons derived from embryonic stem cells is dependent upon infectious viral dose," *Virology*, vol. 443, no. 2, pp. 285–293, Sep. 2013.

[282] J. Christensen, M. Steain, B. Slobedman, and A. Abendroth, "Differentiated neuroblastoma cells provide a highly efficient model for studies of productive varicella-zoster virus infection of neuronal cells," *J. Virol.*, vol. 85, no. 16, pp. 8436–8442, Aug. 2011.

[283] N. L. Baird, J. L. Bowlin, R. J. Cohrs, D. Gilden, and K. L. Jones, "Comparison of varicella-zoster virus RNA sequences in human neurons and fibroblasts," *J. Virol.*, vol. 88, no. 10, pp. 5877–5880, May 2014.

[284] N. L. Baird, S. Zhu, C. M. Pearce, and A. Viejo-Borbolla, “Current In Vitro Models to Study Varicella Zoster Virus Latency and Reactivation,” *Viruses*, vol. 11, no. 2, Jan. 2019.

[285] L. Laemmle, R. S. Goldstein, and P. R. Kinchington, “Modeling Varicella Zoster Virus Persistence and Reactivation – Closer to Resolving a Perplexing Persistent State,” *Front. Microbiol.*, vol. 10, Jul. 2019.

[286] M. Aubert *et al.*, “Gene editing and elimination of latent herpes simplex virus in vivo,” *Nat. Commun.*, vol. 11, no. 1, Dec. 2020.

[287] F. A. Ran *et al.*, “In vivo genome editing using Staphylococcus aureus Cas9.,” *Nature*, vol. 520, no. 7546, pp. 186–91, Apr. 2015.

[288] Z. Wu, H. Yang, and P. Colosi, “Effect of Genome Size on AAV Vector Packaging,” *Mol. Ther.*, vol. 18, no. 1, p. 80, Jan. 2010.

[289] A. J. Davison and J. E. Scott, “DNA sequence of the major inverted repeat in the varicella-zoster virus genome,” *J. Gen. Virol.*, vol. 66 (Pt 2), no. 2, pp. 207–220, 1985.

[290] M. H. Sommer *et al.*, “Mutational analysis of the repeated open reading frames, ORFs 63 and 70 and ORFs 64 and 69, of varicella-zoster virus,” *J. Virol.*, vol. 75, no. 17, pp. 8224–8239, Sep. 2001.

[291] S. E. Dremel and N. A. Deluca, “Herpes simplex viral nucleoprotein creates a competitive transcriptional environment facilitating robust viral transcription and host shut off,” *Elife*, vol. 8, Oct. 2019.

[292] J. M. Felser, P. R. Kinchington, G. Inchauspe, S. E. Straus, and J. M. Ostrove, “Cell lines containing varicella-zoster virus open reading frame 62 and expressing the ‘IE’ 175 protein complement ICP4 mutants of herpes simplex virus type 1.,” *J. Virol.*, vol. 62, no. 6, pp. 2076–82, Jun. 1988.

[293] G. H. Disney and R. D. Everett, “A herpes simplex virus type 1 recombinant with both copies of the Vmw175 coding sequences replaced by the homologous varicella-zoster virus open reading frame,” *J. Gen. Virol.*, vol. 71 (Pt 11), no. 11, pp. 2681–2689, 1990.

[294] G. P. Niemeyer *et al.*, “Long-term correction of inhibitor-prone hemophilia B dogs treated with liver-directed AAV2-mediated factor IX gene therapy,” *Blood*, vol. 113, no. 4, pp. 797–806, Jan. 2009.

[295] T. Harding *et al.*, “Intravenous administration of an AAV-2 vector for the expression of factor IX in mice and a dog model of hemophilia B,” *Gene Ther.*, vol. 11, no. 2, pp. 204–213, Jan. 2004.

[296] J. D. Mount *et al.*, “Sustained phenotypic correction of hemophilia B dogs with a factor IX null mutation by liver-directed gene therapy,” *Blood*, vol. 99, no. 8, pp. 2670–2676, Apr. 2002.

[297] A. C. Nathwani *et al.*, "Adenovirus-associated virus vector-mediated gene transfer in hemophilia B," *N. Engl. J. Med.*, vol. 365, no. 25, pp. 2357–2365, Dec. 2011.

[298] C. S. Manno *et al.*, "Successful transduction of liver in hemophilia by AAV-Factor IX and limitations imposed by the host immune response," *Nat. Med.*, vol. 12, no. 3, pp. 342–347, Mar. 2006.

[299] J.-M. Guedon, M. Zhang, J. Glorioso, W. Goins, and P. Kinchington, "Relief of pain induced by varicella-zoster virus in a rat model of post-herpetic neuralgia using a herpes simplex virus vector expressing enkephalin," *Gene Ther.*, vol. 21, no. 7, p. 694, 2014.

[300] A. Sloutskin and R. S. Goldstein, "Laboratory preparation of Varicella-Zoster Virus: Concentration of virus-containing supernatant, use of a debris fraction and magnetofection for consistent cell-free VZV infections," *J. Virol. Methods*, vol. 206, pp. 128–132, 2014.

[301] L. Cong *et al.*, "Multiplex genome engineering using CRISPR/Cas systems," *Science*, vol. 339, no. 6121, pp. 819–823, Feb. 2013.

[302] T. A. Russell, T. Stefanovic, and D. C. Tscharke, "Engineering herpes simplex viruses by infection-transfection methods including recombination site targeting by CRISPR/Cas9 nucleases," *J. Virol. Methods*, vol. 213, pp. 18–25, Mar. 2015.

[303] V. W. Choi, A. Asokan, R. A. Haberman, and R. J. Samulski, "Production of recombinant adeno-associated viral vectors for in vitro and in vivo use," *Curr. Protoc. Mol. Biol.*, vol. Chapter 16, no. 1, Apr. 2007.

[304] S. Zolotukhin *et al.*, "Recombinant adeno-associated virus purification using novel methods improves infectious titer and yield," *Gene Ther.*, vol. 6, no. 6, pp. 973–985, Jun. 1999.

[305] C. Aurnhammer *et al.*, "Universal real-time PCR for the detection and quantification of adeno-associated virus serotype 2-derived inverted terminal repeat sequences," *Hum. Gene Ther. Methods*, vol. 23, no. 1, pp. 18–28, Feb. 2012.

[306] M. G. Lloyd *et al.*, "A Novel Human Skin Tissue Model To Study Varicella-Zoster Virus and Human Cytomegalovirus," *J. Virol.*, vol. 94, no. 22, pp. 1082–1102, Oct. 2020.

[307] O. Pomp, I. Brokhman, I. Ben-Dor, B. Reubinoff, and R. S. Goldstein, "Generation of peripheral sensory and sympathetic neurons and neural crest cells from human embryonic stem cells," *Stem Cells*, vol. 23, no. 7, pp. 923–930, Aug. 2005.

[308] T. Velusamy, A. Gowripalan, and D. C. Tscharke, "CRISPR/Cas9-Based Genome Editing of HSV," *Methods Mol. Biol.*, vol. 2060, pp. 169–183, 2020.

[309] J. O. Jones, M. Sommer, S. Stamatis, and A. M. Arvin, "Mutational analysis of the varicella-zoster virus ORF62/63 intergenic region," *J. Virol.*, vol. 80, no. 6, pp. 3116–3121, Mar. 2006.

[310] A. P. N. Ambagala, T. Krogmann, J. Qin, L. Pesnicak, and J. I. Cohen, "A varicella-zoster

virus mutant impaired for latency in rodents, but not impaired for replication in cell culture," *Virology*, vol. 399, no. 2, p. 194, Apr. 2010.

[311] J. M. Taymans *et al.*, "Comparative analysis of adeno-associated viral vector serotypes 1, 2, 5, 7, and 8 in mouse brain," *Hum. Gene Ther.*, vol. 18, no. 3, pp. 195–206, Mar. 2007.

[312] G. Gao, L. Vandenberghe, and J. Wilson, "New recombinant serotypes of AAV vectors," *Curr. Gene Ther.*, vol. 5, no. 3, pp. 285–297, Jun. 2005.

[313] C. N. Cearley and J. H. Wolfe, "Transduction characteristics of adeno-associated virus vectors expressing cap serotypes 7, 8, 9, and Rh10 in the mouse brain," *Mol. Ther.*, vol. 13, no. 3, pp. 528–537, Mar. 2006.

[314] C. N. Cearley and J. H. Wolfe, "A single injection of an adeno-associated virus vector into nuclei with divergent connections results in widespread vector distribution in the brain and global correction of a neurogenetic disease," *J. Neurosci.*, vol. 27, no. 37, pp. 9928–9940, Sep. 2007.

[315] L. Haery *et al.*, "Adeno-Associated Virus Technologies and Methods for Targeted Neuronal Manipulation," *Front. Neuroanat.*, vol. 13, p. 93, Nov. 2019.

[316] A. Auricchio *et al.*, "Exchange of surface proteins impacts on viral vector cellular specificity and transduction characteristics: the retina as a model," *Hum. Mol. Genet.*, vol. 10, no. 26, pp. 3075–3081, Dec. 2001.

[317] B. L. Davidson *et al.*, "Recombinant adeno-associated virus type 2, 4, and 5 vectors: Transduction of variant cell types and regions in the mammalian central nervous system," *Proc. Natl. Acad. Sci.*, vol. 97, no. 7, pp. 3428–3432, Mar. 2000.

[318] A. Dukhovny, A. Sloutskin, A. Markus, M. B. Yee, P. R. Kinchington, and R. S. Goldstein, "Varicella-zoster virus infects human embryonic stem cell-derived neurons and neurospheres but not pluripotent embryonic stem cells or early progenitors.," *J. Virol.*, vol. 86, no. 6, pp. 3211–8, Mar. 2012.

[319] H. Lin *et al.*, "The Use of CRISPR/Cas9 as a Tool to Study Human Infectious Viruses," *Front. Cell. Infect. Microbiol.*, vol. 11, Aug. 2021.

[320] H. S. Oh *et al.*, "Herpesviral lytic gene functions render the viral genome susceptible to novel editing by CRISPR/Cas9," *Elife*, vol. 8, Dec. 2019.

[321] W. Neuhausser *et al.*, "Screening Method for CRISPR/Cas9 Inhibition of a Human DNA Virus: Herpes Simplex Virus," *Bio-protocol*, vol. 10, no. 17, 2020.

[322] D. Stone *et al.*, "CRISPR-Cas9 gene editing of hepatitis B virus in chronically infected humanized mice," *Mol. Ther. Methods Clin. Dev.*, vol. 20, p. 258, Mar. 2021.

[323] K. Yan *et al.*, "Inhibition of Hepatitis B Virus by AAV8-Derived CRISPR/SaCas9 Expressed From Liver-Specific Promoters," *Front. Microbiol.*, vol. 12, p. 665184, Jun.

2021.

[324] C. Kunze *et al.*, “Synthetic AAV/CRISPR vectors for blocking HIV-1 expression in persistently infected astrocytes,” *Glia*, vol. 66, no. 2, pp. 413–427, Feb. 2018.

[325] C. Yin *et al.*, “In Vivo Excision of HIV-1 Provirus by saCas9 and Multiplex Single-Guide RNAs in Animal Models,” *Mol. Ther.*, vol. 25, no. 5, pp. 1168–1186, May 2017.

[326] Y. C. Chen, J. Sheng, P. Trang, and F. Liu, “Potential Application of the CRISPR/Cas9 System against Herpesvirus Infections,” *Viruses*, vol. 10, no. 6, Jun. 2018.

[327] K. S. Yuen *et al.*, “CRISPR/Cas9-mediated genome editing of Epstein-Barr virus in human cells,” *J. Gen. Virol.*, vol. 96, no. Pt 3, pp. 626–636, 2015.

[328] C. S. Adamson and M. M. Nevels, “Bright and Early: Inhibiting Human Cytomegalovirus by Targeting Major Immediate-Early Gene Expression or Protein Function,” *Viruses*, vol. 12, no. 1, 2020.

[329] K. Brackett, A. Mungale, M. Lopez-Isidro, D. A. Proctor, G. Najarro, and C. Arias, “CRISPR Interference Efficiently Silences Latent and Lytic Viral Genes in Kaposi’s Sarcoma-Associated Herpesvirus-Infected Cells,” *Viruses*, vol. 13, no. 5, May 2021.

[330] E. Akidil *et al.*, “Highly efficient CRISPR-Cas9-mediated gene knockout in primary human B cells for functional genetic studies of Epstein-Barr virus infection,” *PLoS Pathog.*, vol. 17, no. 4, Apr. 2021.

[331] S. E. Braspenning *et al.*, “Mutagenesis of the varicella-zoster virus genome demonstrates that vlt and vlt-orf63 proteins are dispensable for lytic infection,” *Viruses*, vol. 13, no. 11, Nov. 2021.

[332] J. R. Mendell *et al.*, “Current Clinical Applications of In Vivo Gene Therapy with AAVs,” *Mol. Ther.*, vol. 29, no. 2, pp. 464–488, Feb. 2021.

[333] M. Broeders, P. Herrero-Hernandez, M. P. T. Ernst, A. T. van der Ploeg, and W. W. M. P. Pijnappel, “Sharpening the Molecular Scissors: Advances in Gene-Editing Technology,” *iScience*, vol. 23, no. 1, p. 100789, Jan. 2020.

[334] K. T. McCullough *et al.*, “Somatic Gene Editing of GUCY2D by AAV-CRISPR/Cas9 Alters Retinal Structure and Function in Mouse and Macaque,” *Hum. Gene Ther.*, vol. 30, no. 5, pp. 571–589, May 2019.

[335] C. A. Ramlogan-Steel, A. Murali, S. Andrzejewski, B. Dhungel, J. C. Steel, and C. J. Layton, “Gene therapy and the adeno-associated virus in the treatment of genetic and acquired ophthalmic diseases in humans: Trials, future directions and safety considerations,” *Clin. Experiment. Ophthalmol.*, vol. 47, no. 4, pp. 521–536, May 2019.

[336] B. L. da Costa, S. R. Levi, E. Eulau, Y.-T. Tsai, and P. M. J. Quinn, “Prime Editing for Inherited Retinal Diseases,” *Front. genome Ed.*, vol. 3, Nov. 2021.

[337] S. Kedar, L. N. Jayagopal, and J. R. Berger, “Neurological and Ophthalmological Manifestations of Varicella Zoster Virus,” *J. Neuroophthalmol.*, vol. 39, no. 2, pp. 220–231, Jun. 2019.

[338] S. D. Schoenberger *et al.*, “Diagnosis and Treatment of Acute Retinal Necrosis: A Report by the American Academy of Ophthalmology,” *Ophthalmology*, vol. 124, no. 3, pp. 382–392, Mar. 2017.

[339] N. F. Nidetz *et al.*, “Adeno-associated viral vector-mediated immune responses: Understanding barriers to gene delivery,” *Pharmacol. Ther.*, vol. 207, Mar. 2020.

[340] G. S. Goldman and P. G. King, “Review of the United States universal varicella vaccination program: Herpes zoster incidence rates, cost-effectiveness, and vaccine efficacy based primarily on the Antelope Valley Varicella Active Surveillance Project data,” *Vaccine*, vol. 31, no. 13, pp. 1680–1694, Mar. 2013.

[341] D. S. Schmid and A. O. Jumaan, “Impact of varicella vaccine on varicella-zoster virus dynamics.,” *Clin. Microbiol. Rev.*, vol. 23, no. 1, pp. 202–17, Jan. 2010.

[342] I. Leroux-Roels *et al.*, “A Phase 1/2 Clinical Trial Evaluating Safety and Immunogenicity of a Varicella Zoster Glycoprotein E Subunit Vaccine Candidate in Young and Older Adults,” *J. Infect. Dis.*, vol. 206, no. 8, pp. 1280–1290, 2012.

[343] W. L. Gray, “Simian varicella: a model for human varicella-zoster virus infections,” *Rev. Med. Virol.*, vol. 14, no. 6, pp. 363–381, Nov. 2004.

[344] R. S. Goldstein and P. R. Kinchington, “Varicella Zoster Virus Neuronal Latency and Reactivation Modeled in Vitro,” *Curr. Top. Microbiol. Immunol.*, 2021.

[345] K. Döhner, A. Cornelius, M. C. Serrero, and B. Sodeik, “The journey of herpesvirus capsids and genomes to the host cell nucleus,” *Curr. Opin. Virol.*, vol. 50, pp. 147–158, Oct. 2021.

[346] G. A. Smith, “Navigating the Cytoplasm: Delivery of the Alphaherpesvirus Genome to the Nucleus,” *Curr. Issues Mol. Biol.*, vol. 41, pp. 171–220, 2021.

[347] G. S. Read, “Virus-encoded endonucleases: expected and novel functions,” *Wiley Interdiscip. Rev. RNA*, vol. 4, no. 6, pp. 693–708, Nov. 2013.

[348] E. B. Draganova, J. Valentin, and E. E. Heldwein, “The Ins and Outs of Herpesviral Capsids: Divergent Structures and Assembly Mechanisms across the Three Subfamilies,” *Viruses*, vol. 13, no. 10, Oct. 2021.

[349] T. M. Kristie and B. Roizman, “Host cell proteins bind to the cis-acting site required for virion-mediated induction of herpes simplex virus 1 alpha genes,” *Proc. Natl. Acad. Sci. U. S. A.*, vol. 84, no. 1, pp. 71–75, 1987.

[350] S. Stern, M. Tanaka, and W. Herr, “The Oct-1 homoeodomain directs formation of a multiprotein-DNA complex with the HSV transactivator VP16,” *Nature*, vol. 341, no. 6243,

pp. 624–630, 1989.

[351] J. P. Weir, “Regulation of herpes simplex virus gene expression,” *Gene*, vol. 271, no. 2, pp. 117–130, Jun. 2001.

[352] S. Svobodova, S. Bell, and C. M. Crump, “Analysis of the interaction between the essential herpes simplex virus 1 tegument proteins VP16 and VP1/2,” *J. Virol.*, vol. 86, no. 1, pp. 473–483, Jan. 2012.

[353] W. C. Yang, G. V. Devi-Rao, P. Ghazal, E. K. Wagner, and S. J. Triezenberg, “General and specific alterations in programming of global viral gene expression during infection by VP16 activation-deficient mutants of herpes simplex virus type 1,” *J. Virol.*, vol. 76, no. 24, pp. 12758–12774, Dec. 2002.

[354] R. L. Gibeault, K. L. Conn, M. D. Bildersheim, and L. M. Schang, “An Essential Viral Transcription Activator Modulates Chromatin Dynamics,” *PLoS Pathog.*, vol. 12, no. 8, Aug. 2016.

[355] M. A. Maroui *et al.*, “Latency Entry of Herpes Simplex Virus 1 Is Determined by the Interaction of Its Genome with the Nuclear Environment,” *PLoS Pathog.*, vol. 12, no. 9, Sep. 2016.

[356] H. Moriuchi, M. Moriuchi, R. Pichvangkura, S. J. Triezenberg, S. E. Straus, and J. I. Cohen, “Hydrophobic cluster analysis predicts an amino-terminal domain of varicella-zoster virus open reading frame 10 required for transcriptional activation,” *Proc. Natl. Acad. Sci. U. S. A.*, vol. 92, no. 20, pp. 9333–9337, Sep. 1995.

[357] F. Yao and R. J. Courtney, “A major transcriptional regulatory protein (ICP4) of herpes simplex virus type 1 is associated with purified virions.,” *J. Virol.*, vol. 63, no. 8, p. 3338, Aug. 1989.

[358] A. Erazo, M. B. Yee, B. W. Banfield, and P. R. Kinchington, “The Alphaherpesvirus US3/ORF66 Protein Kinases Direct Phosphorylation of the Nuclear Matrix Protein Matrin 3,” *J. Virol.*, vol. 85, no. 1, p. 568, Jan. 2011.

[359] M. L. Szpara, Y. R. Tafuri, and L. W. Enquist, “Preparation of Viral DNA from Nucleocapsids,” *J. Vis. Exp.*, no. 54, p. 3151, Aug. 2011.

[360] P. R. Kinchington and S. E. Turse, “Molecular basis for a geographic variation of varicella-zoster virus recognized by a peptide antibody.,” *Neurology*, vol. 45, no. 12 Suppl 8, pp. S13-4, Dec. 1995.

[361] P. R. Kinchington, G. Inchauspe, J. H. Subak-Sharpe, F. Robey, J. Hay, and W. T. Ruyechan, “Identification and characterization of a varicella-zoster virus DNA-binding protein by using antisera directed against a predicted synthetic oligopeptide.,” *J. Virol.*, vol. 62, no. 3, p. 802, Mar. 1988.

[362] P. M. Gerk, “Quantitative immunofluorescent blotting of the multidrug resistance-

associated protein 2 (MRP2)," *J. Pharmacol. Toxicol. Methods*, vol. 63, no. 3, pp. 279–282, 2011.

[363] P. Desai and S. Person, "Incorporation of the green fluorescent protein into the herpes simplex virus type 1 capsid.," *J. Virol.*, vol. 72, no. 9, pp. 7563–8, Sep. 1998.

[364] I. B. Hogue, J. Jean, A. D. Esteves, N. S. Tanneti, J. Scherer, and L. W. Enquist, "Functional Carboxy-Terminal Fluorescent Protein Fusion to Pseudorabies Virus Small Capsid Protein VP26," *J. Virol.*, vol. 92, no. 1, Oct. 2017.

[365] V. Chaudhuri, M. Sommer, J. Rajamani, L. Zerboni, and A. M. Arvin, "Functions of Varicella-zoster virus ORF23 capsid protein in viral replication and the pathogenesis of skin infection," *J. Virol.*, vol. 82, no. 20, pp. 10231–10246, Oct. 2008.

[366] S. Grigoryan *et al.*, "Retrograde axonal transport of VZV: kinetic studies in hESC-derived neurons," *J. Neurovirol.*, vol. 18, no. 6, pp. 462–470, Dec. 2012.

[367] M. G. Lloyd and J. F. Moffat, "Humanized Severe Combined Immunodeficient (SCID) Mouse Models for Varicella-Zoster Virus Pathogenesis," *Curr. Top. Microbiol. Immunol.*, 2022.

[368] T. del Rio, C. J. DeCoste, and L. W. Enquist, "Actin Is a Component of the Compensation Mechanism in Pseudorabies Virus Virions Lacking the Major Tegument Protein VP22," *J. Virol.*, vol. 79, no. 13, p. 8614, Jul. 2005.

[369] K. Michael, B. G. Klupp, T. C. Mettenleiter, and A. Karger, "Composition of Pseudorabies Virus Particles Lacking Tegument Protein US3, UL47, or UL49 or Envelope Glycoprotein E," *J. Virol.*, vol. 80, no. 3, pp. 1332–1339, Feb. 2006.

[370] J. L. McKnight, M. Doerr, and Y. Zhang, "An 85-kilodalton herpes simplex virus type 1 alpha trans-induction factor (VP16)-VP13/14 fusion protein retains the transactivation and structural properties of the wild-type molecule during virus infection.," *J. Virol.*, vol. 68, no. 3, pp. 1750–7, Mar. 1994.

[371] N. M. Sawtell and R. L. Thompson, "Alphaherpesvirus Latency and Reactivation with a Focus on Herpes Simplex Virus," *Curr. Issues Mol. Biol.*, vol. 41, pp. 267–356, 2021.

[372] D. Fan *et al.*, "The Role of VP16 in the Life Cycle of Alphaherpesviruses," *Front. Microbiol.*, vol. 11, Aug. 2020.

[373] R. L. Thompson and N. M. Sawtell, "Targeted Promoter Replacement Reveals That Herpes Simplex Virus Type-1 and 2 Specific VP16 Promoters Direct Distinct Rates of Entry Into the Lytic Program in Sensory Neurons in vivo," *Front. Microbiol.*, vol. 10, Jul. 2019.

[374] X. Che, B. Berarducci, M. Sommer, W. T. Ruyechan, and A. M. Arvin, "The ubiquitous cellular transcriptional factor USF targets the varicella-zoster virus open reading frame 10 promoter and determines virulence in human skin xenografts in SCIDhu mice in vivo," *J. Virol.*, vol. 81, no. 7, pp. 3229–3239, Apr. 2007.

[375] C. Crump, “Virus Assembly and Egress of HSV,” *Adv. Exp. Med. Biol.*, vol. 1045, pp. 23–44, 2018.

[376] D. P. Depledge *et al.*, “A unique, spliced varicella-zoster virus latency transcript represses expression of the viral transactivator gene 61,” *bioRxiv*, p. 174797, Oct. 2017.

[377] M. Kobayashi *et al.*, “A primary neuron culture system for the study of herpes simplex virus latency and reactivation.,” *J. Vis. Exp.*, no. 62, Apr. 2012.

[378] L. Riva, M. Thiry, M. Lebrun, L. L’homme, J. Piette, and C. Sadzot-Delvaux, “Deletion of the ORF9p acidic cluster impairs the nuclear egress of varicella-zoster virus capsids,” *J. Virol.*, vol. 89, no. 4, pp. 2436–2441, Feb. 2015.

[379] X. Che *et al.*, “ORF11 protein interacts with the ORF9 essential tegument protein in varicella-zoster virus infection.,” *J. Virol.*, vol. 87, no. 9, pp. 5106–17, May 2013.

[380] M. Jones *et al.*, “RNA-seq analysis of host and viral gene expression highlights interaction between varicella zoster virus and keratinocyte differentiation,” *PLoS Pathog.*, vol. 10, no. 1, Jan. 2014.

[381] M. S. Walters, A. Erazo, P. R. Kinchington, and S. Silverstein, “Histone deacetylases 1 and 2 are phosphorylated at novel sites during varicella-zoster virus infection,” *J. Virol.*, vol. 83, no. 22, pp. 11502–11513, Nov. 2009.

[382] A. K. Shakya, D. J. O’Callaghan, and S. K. Kim, “Interferon Gamma Inhibits Varicella-Zoster Virus Replication in a Cell Line-Dependent Manner,” *J. Virol.*, vol. 93, no. 12, Jun. 2019.

[383] C. C. Ku, Y. H. Chang, Y. Chien, and T. L. Lee, “Type I interferon inhibits varicella-zoster virus replication by interfering with the dynamic interaction between mediator and IE62 within replication compartments,” *Cell Biosci.*, vol. 6, no. 1, 2016.

[384] M. Spengler, N. Niesen, C. Grose, W. T. Ruyechan, and J. Hay, “Interactions among structural proteins of varicella zoster virus,” *Arch. Virol. Suppl.*, no. 17, pp. 71–79, 2001.

[385] T. Deschamps and M. Kalamvoki, “Evasion of the STING DNA-Sensing Pathway by VP11/12 of Herpes Simplex Virus 1.,” *J. Virol.*, vol. 91, no. 16, pp. e00535-17, Aug. 2017.

[386] J. M. Felser, S. E. Straus, and J. M. Ostrove, “Varicella-zoster virus complements herpes simplex virus type 1 temperature-sensitive mutants,” *J. Virol.*, vol. 61, no. 1, pp. 225–228, Jan. 1987.

[387] J. L. Glass *et al.*, “Arsenic trioxide therapy predisposes to herpes zoster reactivation despite minimally myelosuppressive therapy,” *Leuk. Res.*, vol. 106, Jul. 2021.

[388] M. Yamakura *et al.*, “High frequency of varicella zoster virus reactivation associated with the use of arsenic trioxide in patients with acute promyelocytic leukemia,” *Acta Haematol.*, vol. 131, no. 2, pp. 76–77, 2014.

[389] X. Li, J. Feng, and R. Sun, “Oxidative Stress Induces Reactivation of Kaposi’s Sarcoma-Associated Herpesvirus and Death of Primary Effusion Lymphoma Cells,” *J. Virol.*, vol. 85, no. 2, pp. 715–724, Jan. 2011.

[390] X. Gao, H. Wang, and T. Sairenji, “Inhibition of Epstein-Barr virus (EBV) reactivation by short interfering RNAs targeting p38 mitogen-activated protein kinase or c-myc in EBV-positive epithelial cells,” *J. Virol.*, vol. 78, no. 21, pp. 11798–11806, Nov. 2004.

[391] E. Flemington and S. H. Speck, “Autoregulation of Epstein-Barr virus putative lytic switch gene BZLF1,” *J. Virol.*, vol. 64, no. 3, pp. 1227–1232, Mar. 1990.

[392] X. Gao, K. Ikuta, M. Tajima, and T. Sairenji, “12-O-tetradecanoylphorbol-13-acetate induces Epstein-Barr virus reactivation via NF-kappaB and AP-1 as regulated by protein kinase C and mitogen-activated protein kinase,” *Virology*, vol. 286, no. 1, pp. 91–99, Jul. 2001.

[393] X. Gao, M. Tajima, and T. Sairenji, “Nitric oxide down-regulates Epstein-Barr virus reactivation in epithelial cell lines,” *Virology*, vol. 258, no. 2, pp. 375–381, Jun. 1999.

[394] H. Zur Hausen, F. J. O’Neill, U. K. Freese, and E. Hecker, “Persisting oncogenic herpesvirus induced by the tumour promotor TPA,” *Nature*, vol. 272, no. 5651, pp. 373–375, 1978.

[395] W. P. Halford, C. D. Kemp, J. A. Isler, D. J. Davido, and P. A. Schaffer, “ICP0, ICP4, or VP16 expressed from adenovirus vectors induces reactivation of latent herpes simplex virus type 1 in primary cultures of latently infected trigeminal ganglion cells.,” *J. Virol.*, vol. 75, no. 13, pp. 6143–53, Jul. 2001.

[396] T. G. Edwards and D. C. Bloom, “Lund Human Mesencephalic (LUHMES) Neuronal Cell Line Supports Herpes Simplex Virus 1 Latency In Vitro,” *J. Virol.*, vol. 93, no. 6, Mar. 2019.

[397] P. Pausch *et al.*, “CRISPR-CasΦ from huge phages is a hypercompact genome editor,” *Science*, vol. 369, no. 6501, pp. 333–337, Jul. 2020.

[398] X. Xu *et al.*, “Engineered miniature CRISPR-Cas system for mammalian genome regulation and editing,” *Mol. Cell*, vol. 81, no. 20, pp. 4333-4345.e4, Oct. 2021.

[399] D. M. Krisky *et al.*, “Deletion of multiple immediate-early genes from herpes simplex virus reduces cytotoxicity and permits long-term gene expression in neurons,” *Gene Ther.*, vol. 5, no. 12, pp. 1593–1603, 1998.

[400] F. Han *et al.*, “Cellular Antisilencing Elements Support Transgene Expression from Herpes Simplex Virus Vectors in the Absence of Immediate Early Gene Expression,” *J. Virol.*, vol. 92, no. 17, Sep. 2018.

[401] Y. Miyagawa *et al.*, “Deletion of the Virion Host Shut-off Gene Enhances Neuronal-Selective Transgene Expression from an HSV Vector Lacking Functional IE Genes,” *Mol.*

Ther. - Methods Clin. Dev., vol. 6, pp. 79–90, Sep. 2017.

[402] W. F. Goins, S. Huang, J. B. Cohen, and J. C. Glorioso, "Engineering HSV-1 vectors for gene therapy," *Methods Mol. Biol.*, vol. 1144, pp. 63–79, 2014.

[403] S. Artusi, Y. Miyagawa, W. F. Goins, J. B. Cohen, and J. C. Glorioso, "Herpes Simplex Virus Vectors for Gene Transfer to the Central Nervous System," *Diseases*, vol. 6, no. 3, p. 74, Aug. 2018.

[404] M. Naeem, S. Majeed, M. Z. Hoque, and I. Ahmad, "Latest Developed Strategies to Minimize the Off-Target Effects in CRISPR-Cas-Mediated Genome Editing," *Cells*, vol. 9, no. 7, Jul. 2020.

[405] M. Kosicki, K. Tomberg, and A. Bradley, "Repair of double-strand breaks induced by CRISPR-Cas9 leads to large deletions and complex rearrangements," *Nat. Biotechnol.*, vol. 36, no. 8, pp. 765–771, Sep. 2018.

[406] H.-X. Deng *et al.*, "Efficacy and long-term safety of CRISPR/Cas9 genome editing in the SOD1-linked mouse models of ALS," *Commun. Biol. 2021 41*, vol. 4, no. 1, pp. 1–11, Mar. 2021.

[407] H. Y. Shin *et al.*, "CRISPR/Cas9 targeting events cause complex deletions and insertions at 17 sites in the mouse genome," *Nat. Commun.*, vol. 8, May 2017.

[408] H. Manghwar *et al.*, "CRISPR/Cas Systems in Genome Editing: Methodologies and Tools for sgRNA Design, Off-Target Evaluation, and Strategies to Mitigate Off-Target Effects," *Adv. Sci.*, vol. 7, no. 6, p. 1902312, Mar. 2020.

[409] A. Ikeda, W. Fujii, K. Sugiura, and K. Naito, "High-fidelity endonuclease variant HypaCas9 facilitates accurate allele-specific gene modification in mouse zygotes," *Commun. Biol. 2019 21*, vol. 2, no. 1, pp. 1–7, Oct. 2019.

[410] B. P. Kleinstiver *et al.*, "High-fidelity CRISPR–Cas9 nucleases with no detectable genome-wide off-target effects," *Nat. 2015 5297587*, vol. 529, no. 7587, pp. 490–495, Jan. 2016.

[411] P. I. Kulcsár *et al.*, "Crossing enhanced and high fidelity SpCas9 nucleases to optimize specificity and cleavage," *Genome Biol.*, vol. 18, no. 1, pp. 1–17, Oct. 2017.

[412] A. Casini *et al.*, "A highly specific SpCas9 variant is identified by in vivo screening in yeast," *Nat. Biotechnol. 2018 363*, vol. 36, no. 3, pp. 265–271, Jan. 2018.

[413] C. A. Vakulskas *et al.*, "A high-fidelity Cas9 mutant delivered as a ribonucleoprotein complex enables efficient gene editing in human hematopoietic stem and progenitor cells," *Nat. Med. 2018 248*, vol. 24, no. 8, pp. 1216–1224, Aug. 2018.

[414] J. S. Chen *et al.*, "Enhanced proofreading governs CRISPR–Cas9 targeting accuracy," *Nat. 2017 5507676*, vol. 550, no. 7676, pp. 407–410, Sep. 2017.

[415] I. M. Slaymaker, L. Gao, B. Zetsche, D. A. Scott, W. X. Yan, and F. Zhang, "Rationally engineered Cas9 nucleases with improved specificity," *Science (80-.).*, vol. 351, no. 6268, pp. 84–88, Jan. 2016.

[416] J. K. Lee *et al.*, "Directed evolution of CRISPR-Cas9 to increase its specificity," *Nat. Commun. 2018 91*, vol. 9, no. 1, pp. 1–10, Aug. 2018.

[417] E. M. Kallimasioti-Pazi *et al.*, "Heterochromatin delays CRISPR-Cas9 mutagenesis but does not influence the outcome of mutagenic DNA repair," *PLOS Biol.*, vol. 16, no. 12, p. e2005595, Dec. 2018.

[418] A. Srivastava, "In vivo tissue-tropism of adeno-associated viral vectors," *Curr. Opin. Virol.*, vol. 21, p. 75, Dec. 2016.

[419] M. J. Castle, H. T. Turunen, L. H. Vandenberghe, and J. H. Wolfe, "Controlling AAV Tropism in the Nervous System with Natural and Engineered Capsids," *Methods Mol. Biol.*, vol. 1382, p. 133, 2016.

[420] T. Aoki, K. Miyauchi, E. Urano, R. Ichikawa, and J. Komano, "Protein transduction by pseudotyped lentivirus-like nanoparticles," *Gene Ther. 2011 189*, vol. 18, no. 9, pp. 936–941, Mar. 2011.

[421] M. Cavrois, C. De Noronha, and W. C. Greene, "A sensitive and specific enzyme-based assay detecting HIV-1 virion fusion in primary T lymphocytes," *Nat. Biotechnol. 2002 2011*, vol. 20, no. 11, pp. 1151–1154, Sep. 2002.

[422] O. W. Merten, M. Hebben, and C. Bovolenta, "Production of lentiviral vectors," *Mol. Ther. Methods Clin. Dev.*, vol. 3, p. 16017, Mar. 2016.